

1991

An acoustic emission study of structural steel columns used for offshore platforms

Robert W. Kowalik
Lehigh University

Follow this and additional works at: <https://preserve.lehigh.edu/etd>



Part of the [Materials Science and Engineering Commons](#)

Recommended Citation

Kowalik, Robert W., "An acoustic emission study of structural steel columns used for offshore platforms" (1991). *Theses and Dissertations*. 5510.
<https://preserve.lehigh.edu/etd/5510>

This Thesis is brought to you for free and open access by Lehigh Preserve. It has been accepted for inclusion in Theses and Dissertations by an authorized administrator of Lehigh Preserve. For more information, please contact preserve@lehigh.edu.

AN ACOUSTIC EMISSION STUDY OF STRUCTURAL STEEL
COLUMNS USED FOR OFFSHORE PLATFORMS

By

Robert W. Kowalik

A Thesis

Presented to the Graduate Committee
of Lehigh University
in Candidacy for the Degree of
Masters of Science

in

The Department of Materials Science and Engineering

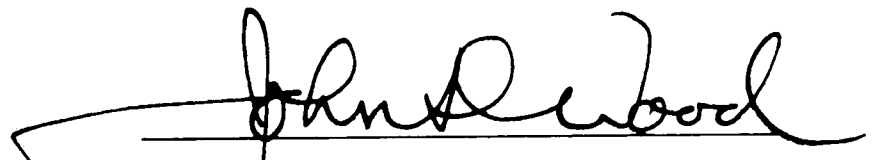
Lehigh University

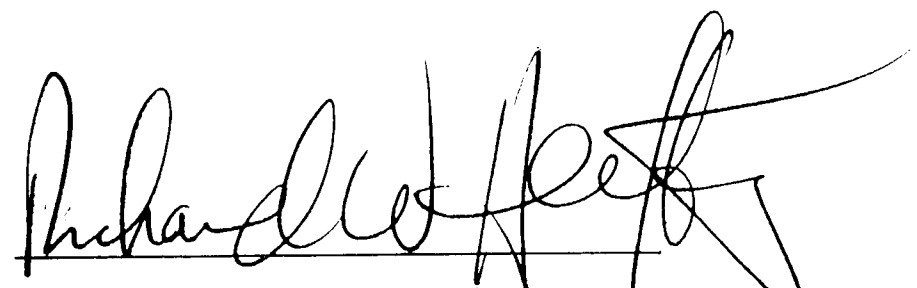
August 1991

CERTIFICATE OF APPROVAL

This thesis is accepted and approved in partial fulfillment of the requirements for the degree of Master of Science.

8/23/91
Date


Professor John D. Wood
Thesis Advisor


Richard W. Hertzberg
Department Chairman

ACKNOWLEDGEMENTS

The technical advise of Dr. John D. Wood was paramount in the completion of this thesis and is gratefully acknowledged. The insight gained from discussions with Dr. Adrian Pollock were greatly appreciated. Preparation and mechanical testing of the large structural columns could not have been completed without the aid of Brad Wood and his work is acknowledged.

Informal discussions with Daniel Henkel and Pat Estupinan were helpful with both this thesis and other technical topics.

This study could not have been undertaken without the financial support of Chevron, Exxon, Mobil, Shell, Texaco, U.S. Dept. of Interior, U.K. Dept. of Energy, and American Iron and Steel Institute. The technical support of Physical Acoustics Corp. is also appreciated.

Finally I wish to thank my parents and my brothers and sister, Thomas, Steven, and Janis for their support throughout my academic career.

TABLE OF CONTENTS

Certificate of Approval	ii
Acknowledgements	iii
Table of Contents	iv
List of Tables	vi
List of Figures	vii
Abstract	1
I Introduction	2
A. Defining The Problem	2
B. Background on Acoustic Emissions	4
C. Acoustic Emission sensing on offshore platforms	9
D. Surface conditions of structural columns	13
II Experimental Procedure	16
A. Overview	16
B. Specimen History	16
a) In Service Columns	16
b) Fabricated Columns	17
C. Equipment	18
D. Tensile Tests	21
E. Stub Column	22
F. Long Column	23
G. Four Point Bending	24

III	Results/Discussion	28
	A. Tensile Tests	28
	B. Stub Column	31
	C. Long Column	36
	D. Four Point Bending Tests	43
	E. Equipment Evaluation	49
IV	Conclusions	54
V	Suggestions for future work	56
VI	References	57
VII	Appendix	98
VIII	Vita	100

LIST OF TABLES

	<u>Page</u>
Table I - Relationship Between Gain and Amplification	8
Table II - Specimen Geometries and Sensitivities.	18
Table III - Surface Preparation and Environmental History of Four Point Bend Specimens.	26
Table IV - Surface Preparation and Environmental History of Four Point Bend Specimens Fabricated From a Salvaged Column.	27
Table V - Rockwell Hardness Measurements of The Specimens.	29
Table VI - A Representative Group of Data That Was Recorded For A Fabricated Long Column P1-LC.	49
Table VII - A Representative Group of Data from 4pt. Bend Specimen FNS1.	51

LIST OF FIGURES

Figure		<u>Page</u>
1.	Cumulative Emissions vs. Load Diagram Showing the Kaiser Effect.	62
2.	Schematic of a Typical Wave Form From a Burst Type Emission.	62
3.	Two R6I Acoustic Sensors With Built-in 40dB Preamplifiers.	63
4.	Three R6 Acoustic Sensors With One P.A.C. 1220-A Preamplifier.	63
5.	A Typical Frequency Response Plot for R6 & R6I Sensors.	64
6.	Physical Acoustic's 3000 Processor With a 3104 Amplifier.	64
7.	Stub Column P1-SC Being Compressed In A Baldwin.	65
8.	Schematic of A Stub Column Showing The Location of AE Sensors.	65
9.	Long column P2-LC Under Compressed In A 34.5 GPa Capacity Baldwin.	66
10.	Three AE Sensor Arrays Used For Long Column Tests.	66
11a.	Four Point Bending Set-up.	67
11b.	Schematic Of The Above Four Point Bend Set-up.	67
12.	AE Data Generated From Tensile Coupon Testing Of ASTM A36 Steel.	68
13.	Tensile Specimen Fabricated From A Salvaged Column With All Oxide Layers Removed Prior To Testing	68
14.	A Representative Correlation Plot Showing That Mechanical Noise (A) And EMI Noise (B) Were Not Recorded.	69
15.	Surface Condition of A Salvaged Column (E1).	70
16.	AE Data Generated From Stub Column E1-SC	70

LIST OF FIGURES (CONTINUED)

Figure		Page
17.	A Representative Load vs. Displacement Diagram For A Long Column.	71
18.	AE Data For Stub Column E3-SC.	71
19.	Surface Condition of Stub Column S2-SC.	72
20.	Surface Condition Inside Stub Column S2-SC.	72
21.	A Representative Photograph of The Surface Condition of The Fabricated Specimens.	73
22.	AE Data From Long Column E1-LC.	73
23.	A Linear Location Diagram of Long Column E1-LC.	74
24.	AE Data From Long Column E3-LC	74
25.	AE Data From Long Column B3-LC.	75
26.	Location of AE Sensors On Long Column P4-LC.	76
27a.	Planar Location Plots of Long Column P4-LC.	77
27b.	Planar Location Plot of Long Column P4-LC.	78
28.	Placement of AE Sensors On Long Column P2-LC.	79
29.	Linear Location Plot of Long Column P2-LC.	80
30.	Linear Location Plot of Long Column P2-LC In The Early Stages of Testing.	80
31.	Linear Location Plot of Long Column D3-LC	81
32.	Four Point Bend Specimen of Polished ASTM A572 Steel.	81
33.	Surface of As Received ASTM A572 Steel Plate With Mill Scale.	82
34.	Four Point Bend Data For A572 Steel With Mill Scale.	82
35.	Surface Condition of ASTM 572 Steel Plate With Mill Scale And A 600hr. Exposure To Salt Water.	83
36.	Four Point Bend Data For Specimen FE1.	83
37.	Surface Condition of ASTM A572 Steel Plate With Mill Scale And A 1200hr. Exposure To Salt Water.	84
38.	Four Point Bend Data For Specimen FE2.	84
39.	Surface Condition of ASTM A572 Steel Plate With Mill Scale And A 2400hr. Salt Water Exposure.	85

LIST OF FIGURES (CONTINUED)

Figure		Page
40.	Four Point Bend Data For Specimen FE3.	85
41.	Surface Condition of A ASTM A572 Steel Plate Without Mill Scale and Exposed For 600hr. In A Salt Water Environment.	86
42.	Four Point Bend Data For Specimen FNSE1.	86
43.	Surface Condition of A ASTM A572 Steel Plate Without Mill Scale And Exposed For 1800hr. In A Salt Water Environment.	87
44.	Four Point Bend Data For Specimen FNSE2.	87
45.	Surface Condition of A ASTM Steel Plate Without Mill Scale And Thermally Oxidized For 100hr. At 560 C.	88
46.	Four Point Bend Data For Specimen FS1.	88
47.	Surface Condition of A ASTM A572 Steel Plate Without Mill Scale And Thermally Oxidized For 300hrs. at 550 C.	89
48.	Four Point Bend Data For Specimen FS2.	89
49.	Surface Condition of A ASTM A572 Steel Plate Without Mill Scale And Thermally Oxidized For 10 hrs. at 960 C.	90
50.	Four Point Bend Data For Specimen FS3.	90
51.	Four Point Bend Data For A Polished Specimen That Was Fabricated From Long Column E1-LC.	91
52.	Surface Condition of A Four Point Bend Specimen That Was Fabricated From A Salvaged Column After All Oxides Were Removed, And Then Exposed To A Salt Water Environment For 600hr.	92
53.	Four Point Bend Data For Specimen IE1.	92
54.	Surface Condition of A Four Point Bend Specimen That Was Fabricated From A Salvaged Column After All Oxides Were Removed, And Then Exposed To A Salt Water Environment For 1200hr.	93
55.	Four Point Bend Data For Specimen IE2.	93

LIST OF FIGURES (CONTINUED)

Figure		Page
56.	Surface Condition of A Four Point Bend Specimen That Was Fabricated From A Salvaged Column After All Oxides Were Removed, And Then Exposed To A Salt Water Environment For 2400hr.	94
57.	Four Point Bend Data For Specimen IE3.	94
58.	Surface Condition of Four Point Bend Specimen Fabricated From A Salvaged Column.	95
59.	Four Point Bend Data For Specimen I1.	95
60.	AE Data Showing The Effects of Filtering.	96

ABSTRACT

The structural integrity of offshore oil platforms is of concern due to possible loss of life and ecological damage that may occur with a structural failure. Therefore, the platforms are nondestructively inspected on a periodic basis. Inspection of the platforms with conventional methods, such as ultrasonic and magnetic particle testing, is a very labor intensive and costly procedure.

Acoustic emission (AE) monitoring is a nondestructive test method that may curtail the cost of offshore evaluation of platforms. This report examines the AE characteristics of various stressed structural steels to determine the feasibility of utilizing the AE monitoring method for offshore applications.

Structural columns that were salvaged from offshore oil platforms as well as new fabricated columns were tested in this study. It has been shown with the aid of long column, stub column and four point bend specimens that structural steels used for offshore applications exhibit bursts of acoustic emissions from the spalling of the brittle surface layers at the initiation of yielding. Therefore, overloading of a damaged column may be identified with the AE technique. The location of the a damaged area on structural columns has also been successfully identified by utilizing time of arrival analysis and triangulation methods.

I INTRODUCTION

A) DEFINING THE PROBLEM

The structural integrity of offshore oil platforms is of paramount concern due to the possible loss of life and the severity of ecological damage that may occur from a catastrophic failure. Under the Construction and Survey Regulation of the OFFSHORE INSTALLATION ACT OF 1971¹, it is required that the structures are extensively inspected on a routine basis to keep a valid "Certificate of Fitness". The inspection includes underwater evaluation by divers and robots which is a very expensive and time consuming task and it has been shown that it is economically impractical to inspect the entire structure². These limitations are further intensified in some locations such as the North Sea where the ocean temperature and wave intensity are severe. Hence only critically stressed areas can be examined during the summer months. Furthermore, these areas are not continuously monitored, rather they are inspected on a periodical basis. The occurrence of inspection is dictated by weather and economic factors. To appreciate the magnitude of the time and expense, it cost more than 500,000 dollars and five years to inspect one structure in the North Sea (Costs are in 1979 dollars)³.

The splash zone of the structures have been determined to

be of greatest concern with respect to physical damage³. This is the result of accelerated general corrosion that occurs due to the oxygen gradient present between the water and the atmosphere. The result of this corrosion is a reduction of load carrying material with time. A more detrimental corrosive process in this area (splash zone) caused by the attachment of marine life such as barnacles⁴ to the column. Marine life is deleterious because it produces a galvanic cell on the structure in which the area under this organic material is anodic with respect to rest of the structure and this in turn results in localized corrosion called pitting. A third concern with the splash zone is with accidental mechanical damage by supply boats and other vessels that may collide with the structure. Once the column is dented, the load bearing capacity is no longer predictable and the safety of the structure is in question.

In summary, the splash zone is most likely to be accidentally damaged by vessels and corrosion occurs in this region at an accelerated rate. Therefore, it is of great importance to inspect this region of the structure on a routine basis. The mechanical properties of a dented column are not fully understood and a concurrent investigation was conducted at Lehigh University⁵ to determine the effects of denting.

An ultimate goal for offshore inspections would be to determine an economical way of continuously monitoring a

platform, and alerting an inspector when plastic deformation (overloading) is occurring in one or more of the structural members. Also location of the damaged area would be beneficial.

Acoustic emission (AE) technology appears to be a viable solution in achieving the ultimate goal mentioned above. Therefore, the remainder of this thesis is concerned with the feasibility of utilizing acoustic emission technology in determining the occurrence and location of plastic deformation on large structural columns. Two sets of specimens were investigated in this thesis. The first group of columns were salvaged from platforms in the Gulf of Mexico and the second set of columns, that were never in service, were fabricated specifically for this study. Both sets of columns were tested on land in a dry environment.

B) BACKGROUND ON ACOUSTIC EMISSIONS

Acoustic emissions (AE) monitoring is a passive nondestructive technique that can locate plastically deforming areas and propagating cracks. The technique relies on piezoelectric sensors that are excited by stress waves in the material. The piezoelectric sensor transforms the mechanical energy (stress wave) into an electrical potential which is then amplified and processed by a computer. These stress waves are generated by material imperfections such as inclusions cracking, cracks growing, oxides debonding, and can be as

small as dislocation movement which occurs during plastic deformation. For this technique to work, a stress has to be applied to the specimen otherwise it would not emit acoustic pressure waves.

A beneficial characteristic of acoustic emissions is called the Kaiser effect. Emissions will be generated only when the stress is increased, however if the stress is no longer applied, then no new emissions will be generated. In other words, emissions are present during the loading cycle and are absent during the unloading sequence. If the specimen is then reloaded, no new emissions will be generated until the previous maximum load was surpassed. This characteristic is called the Kaiser effect and is depicted in Figure 1. The Kaiser effect is beneficial because it can warn an operator if a new maximum stress level is being experienced on the monitored structure. Sometimes the Kaiser effect is not observed and new emissions can occur at lower stress levels. This breakdown of the Kaiser effect is called the Felicity effect⁶.

The acoustic emission technique can be utilized to simultaneously monitor large areas of a structure. In other words, the area to be examined does not have to be scanned for the damaged area, rather the entire structure can be monitored and data analysis can determine the location of the damaged area. The location capabilities is achieved by positioning an array of sensors on the specimen. If the exact location of

these sensors is known then triangulation methods can be utilized to determine the location of the damaged area. Hardware has been designed so that on-the-fly analysis is possible⁷, therefore allowing AE equipment to inform the inspector where and when overloading is occurring.

The following paragraph is a brief summary of the terminology used with acoustic emissions technology. When a stress wave is generated from a flaw in the material, it is called an event. Not all events are recorded by the equipment. The criteria for recording an event is dictated by the sensitivity parameters that the inspector selects and the type of equipment available. When an event is recorded, it is called a hit. A hit has many attributes that can be examined by the inspector. Each hit has a duration, rise time, amplitude, and energy (Figure 2). The rise time is the time required for the wave to reach its maximum amplitude from the point when it first surpassed the threshold. Duration is the amount of time when the signal first surpasses the threshold until it dampens below it. Amplitude is simply the maximum height of the pulse. Finally energy is the area under the curve generated by the signal with its lower bound dictated by the threshold setting (Figure 2). These parameters (hits, rise time, duration, amplitude, and energy) as well as parametrics (load, displacement etc.) can be plotted against each other and important information about the specimen and experimental set-up can be ascertained. For example, it has

been determined that unwanted electrical noise has the characteristic of zero rise time⁸. Thus, an inspector can determine if erroneous noise is being recorded by viewing a plot of rise time versus a parametric input.

Two types of acoustic emissions can occur in a specimen. First is burst type emissions, which are discrete individual events that occur in the specimen. Each individual burst type of emission can be analyzed by examining the parameters mentioned previously (rise time, duration, etc.). An example of a burst type emission would be generated from cracking of an inclusion under an applied stress. The second type of AE that can be generated is called continuous emissions. In essence the piezoelectric crystal is continuously excited. Hence, the burst emission parameters can not be used for analysis because individual events overlap each other. An example of continuous emissions would be the onset of yielding of steel. The emissions recorded would be from the unpinning and movement of dislocations which are too numerous to be resolved on an individual basis.

The energy generated by the piezoelectric crystal in the transducer is very low, therefore the signal has to be increased by a preamplifier. This preamplifier may be a separate unit or may be incorporated into the transducer housing. The preamplification is in the order of 20 to 60 decibels (dB) which correlates to a 10 to 1000 fold increase in signal as shown in Table I. The signal is then further

increased by the main amplifier. The gain and threshold

TABLE I
Relationship Between Gain and Amplification.

GAIN (dB)	Amplification
0	1.00 X
5	1.78 X
10	3.16 X
15	5.62 X
20	10.00 X
40	100.00 X
60	1000.00 X

settings can be selected on this main amplifier. The gain is essentially the dB level that the signal is increased and the threshold is the parameter that dictates the minimum magnitude of the signal that is recorded as a hit(Figure 2). The gain and threshold have to be determined prior to testing so that the proper type of data would be recorded. For example, detection of dislocation movement in a tensile specimen requires the maximum sensitivity. Maximum sensitivity of the equipment is achieved with a high gain (amplification) and a low threshold. While detection of an impact on a structure by a supply boat would require a low gain and high threshold.

The proper settings for these parameters are critical if meaningful data is to be obtained. For example, background noise, such as mechanical noise from the equipment on the platform, can be deleted from detection by a proper setting of these parameters (gain and threshold).

C) ACOUSTIC EMISSION SENSING ON OFFSHORE PLATFORMS

AE technology has advanced substantially in the past few years in that the sensors today can be permanently placed on structures and continuously monitor for a number of years. Permanently placed sensors have been successfully installed on Light-Water Reactor Systems by Hutton⁹. The ocean, however, is a more hostile environment, and it is of concern that the sensors may fall off the structure or lose sensitivity. Sensitivity or the efficiency of the sensor is partly determined by the interface between the sensor and the structure. If air pockets are present between the sensor and the structure, then some of the AE generated from the structure would not be transferred to the sensor. Sensors are now available for permanent installation and they apparently do not lose sensitivity with time. Parry completed a study indicating that underwater attachment techniques of sensors were possible for either temporary or permanent monitoring¹⁰. Another concern was with the large amount of ambient noise generated from the ocean such as impact of waves and sonar from marine life. Again this did not pose a problem with a

proper setting of the gain and threshold. Rogers et al.¹¹ successfully monitored the growth of a crack on a oil platform and did not record erroneous data from marine life and impact from waves. Another independent study by Parry support this claim and his conclusions were "This analysis showed that the noise generated by operating platform equipment was not of sufficient amplitude to mask the acquisition of acoustic signals on the platform legs. Noise created by waves breaking against the leg structure could be detected, but was also found to be of insufficient intensity to interfere with acoustic emission detection and analysis"¹⁰.

Three methods can be utilized to reduce the recording of background noise. First as previously mentioned is the proper setting of the gain and threshold. If there is a particularly noisy location of the structure, then alteration of the sensitivity parameters (gain and threshold) may not be the solution. An alternative would be to use the second method which utilizes guard sensors. A guard sensor would be placed near the location that is generating the unwanted noise, and if a signal interacts with this transducer first, then it will not allow any signals to be recorded. If this unwanted noise is continuous in nature then utilizing guard sensors would not be a viable solution because when a guard sensor is activated, then data acquisition would be suspended. Therefore, a continuous signal at the guard sensor would result in no data acquisition. If this is determined to be the case, then the

third method can be used which is frequency filtering.

Frequency filtering relies on the fact that the unwanted noise may lie in a specific regime of the frequency spectrum. Transducers that are not sensitive to this area of the spectrum and filters that cut out signals in the area of the spectrum may be selected, and this in turn reduces the amount of unwanted noise. As an example, assume that mechanical vibrations, from drilling, produce emissions at a frequency of 20 kHz. By using a 30kHz filter, (any signal below 30 kHz is filtered) this unwanted noise can be reduced. Successful results of determining changes in signals by studying their frequency spectrum was shown by Bassim et al¹². Work completed by Hartman et al.¹³ also conclude that frequency analysis may be a beneficial technique.

Frequency filtering is a debatable topic and some authors ¹⁴ believe that frequency analysis is a very limited technique and does not have a practical application. The difficulty associated with frequency filtering is that the frequency spectrum of an event is affected by the specimen geometry, microstructure, and temperature. Thus, the same event, for example inclusion cracking, would have a different frequency spectrum if it occurred at a different location in the same specimen. This makes event identification very difficult. In other words, the events can be detected, but determination if they were generated from inclusion cracking or by dislocation movement is not possible. It should be

noted, however, that frequency filtering can be successfully used in a limited fashion, for example, filtering out very low frequencies (mechanical vibrations) and very high frequencies (electro magnetic interference) is possible.

Acoustic emission characteristics vary for different types of materials. For example a 1020 type steel may emit more emissions than a 4340 steel. It should also be noted that the same material can have different AE characteristics if it was processed differently.¹⁵ For example, a different heat treatment or different amounts of cold working may change the amount of emissions generated. Thus, this poses a problem with the proposed application of the AE technique. It has been shown by various authors ^{15,16,17,18} that some steels are quiet while others are noisy. This would not be a problem if the standards for the construction of offshore structures dictated a specific steel to be used, but apparently the standards are not very specific. For instance, the standard only calls for A36 or a minimum yield strength of a 36ksi (248 MPa) structural steel to be utilized. Therefore, a wide range of steels can be used and to add to the confusion, different steels are sometimes welded together to form one column.

For the successful application of the AE technique on offshore platforms, it is imperative that the identification of a similar AE characteristic for all the structural steels used in construction of these structures be determined. With this characteristic identified, an in depth study can be

performed to determine if relevant information can be ascertained from this one universal attribute. Some authors in the past claimed that the steels used on these offshore rigs were acoustically quiet and the success of AE as a method of nondestructive evaluation would have very little chance of success¹⁹. These authors tested the intrinsic steel and did not consider the oxide layers that are present on the structures.

D) Surface Condition of Structural Columns

The structural columns for offshore structures are usually fabricated by rolling the plate into a cylinder followed by a longitudinal weld. The steel plate initially has a mill scale present on it which is usually composed of 40-95% FeO (wustite), 5-60% Fe₃O₄ (magnetite) and 0-10% Fe₂O₃ (haematite)²⁰. The thickness of the scale is dependent on the processing temperature and time. The mill scale is very coherent to the metal substrate (plate) and would require a process such as pickling to remove it. The scale is present after the fabrication of the columns and it generally is not removed from the structure before it is placed in service. It is usually removed only if the column is to be painted with a protective coating. Coatings may cause a problem if they are not uniformly applied resulting in uncoated parts of the column, or if they are damaged in service, because accelerated localized corrosion may occur. Corrosion is also a problem

when the mill scale is left on the structure because it is cathodic to the base material and again localized corrosion can occur. Generally the scale is left on the structure and corrosion is controlled by a sacrificial anode such as aluminum.

The structural member will still experience oxidization (pitting) with time even though sacrificial anodes are used. In essence the mill scale is replaced by different oxides, sulfides, and hydroxides. It has also been noticed that at the splash zone, marine life tends to grow. These barnacles attach themselves to the structures by secreting an adhesive that is polysacharide in nature²¹. In summary, the surface of these columns have a combination of mill scale, rust (oxides and hydrexides), and marine life. For realistic AE testing to be accomplished, this surface layer should not be removed. Drew et al.²² performed such a AE test on pipeline steels and noted that the debonding of mill scale occurred at the yield point of specimen which resulted in the generation of large amplitude hits.

It is postulated in this thesis that the universal AE characteristic sought for determination of gross deformation in offshore platforms is the spalling of the oxides and marine life. Since the modulus of elasticity is different for the base steel and the surface layers, the bonding between them will fail at large strains²³. This thesis investigates the effects of various surface layers (corrosion, marine life,

mill scale) on structural.

At present these oxides and marine life are a hinderance to routine inspections because damaged areas (dented regions) may become covered and difficult to locate. This does not pose a problem with AE technology. It has been determined that a simple one dimensional location scheme was adequate in locating flaws in an aircraft structure. Dunegan²⁴ has expanded this technique by using a planar location scheme by using an array of sensors. Both linear and planar location plots were used in this thesis to determine the feasibility of locating the damaged area with AE.

II EXPERIMENTAL PROCEDURE

A. Overview

This study was a sub-project of the Residual Strength of Damaged and Deteriorated Offshore Structures program undertaken at Lehigh University²⁵. The specimen geometries and mechanical test set-up was arranged by the Civil Engineer in charge of testing. The acoustic monitoring was included in the testing procedure and performed during most of their testing. Four types of specimens; long column, stub column, four point bend, and tensile coupon were fabricated for this project. More detail of each will be discussed below. The study included two sets of material to be examined. First, long columns were salvaged from one or more offshore structures in the Gulf of Mexico and were subsequently machined into the four specimen geometries mentioned above. The second material group was ordered from the steel mill specifically for this project and was also fabricated into the four specimen geometries.

B. Specimen History

a) Salvaged columns

Fifteen large structural columns (approx. 9 m. long) were selected from a group that was salvaged from one or more offshore oil platforms. It is believed that all of these columns originated from platforms located in the Gulf of

Mexico. The surface condition of the columns varied drastically. Some had a protective coating on them while others had a layer of marine life with various amounts of corrosion present. One column had a protective monel sheet around it (Monel sheathing is sometimes used to protect the steel from corrosion). Both general and localized corrosion were present on the columns. It is speculated that the platforms were cathodically protected in service with aluminum sacrificial anodes. This was deduced because an aluminum anode was included in the shipment.

The geometry of the tubes varied in size and thickness. It should also be noted that the types of steels also varied. This was determined by taking hardness readings of each column. The exact history of the steel or the columns was not available.

b) Fabricated Columns

Fabricated columns were ordered from L&M Fabrication & Machine, Inc. Various thicknesses and circumferences (Table II) were fabricated out of two steels ASTM A36 and ASTM A572. All the plates had a coherent mill scale on them. The plates were cold rolled into cylinders and then welded longitudinally. These cylinders were then circumferentially welded together to form a column. Four point bending specimens were fabricated from a flat ASTM A572 steel plate.

TABLE II
SPECIMEN GEOMETRIES AND SENSITIVITIES
STUB COLUMNS

	<u>Specimen</u>	<u>Length(m)</u>	<u>Diameter(cm)</u>	<u>Thickness(cm)</u>	<u>Sensitivity</u>
*	E1-SC	1.07	27.5	0.95	45
*	E3-SC	1.07	35.6	1.10	48
*	S2-SC	1.06	36.0	1.14	70
	P1-SC	1.23	38.1	0.64	70
	P2-SC	1.37	43.2	0.95	70
	P3-SC	1.91	62.2	0.79	70

LONG COLUMNS

	<u>Specimen</u>	<u>Length(m)</u>	<u>Diameter(cm)</u>	<u>Thickness(cm)</u>	<u>Sensitivity</u>
*	E1-LC	7.47	27.5	0.95	45
*	E3-LC	7.95	35.6	1.10	70
*	B3-LC	8.53	35.6	1.10	60
*	D3-LC	8.53	35.6	1.10	73
	P2-LC	10.67	43.2	0.95	63
	P4-LC	9.56	47.6	0.48	65

* Specimens that were fabricated from salvaged columns.

C. Equipment

The acoustic equipment utilized in this thesis was supplied by Physical Acoustic Corporation. Two types of transducers (sensors) were used in this study - R6I and R6. The R6I sensor has a 40 dB preamplifier built into the sensor housing while the R6 requires a separate preamplifier (Figures 3 & 4). The approximate resonant frequency of both types of transducers is 90 KHz while their typical operating frequency regime is 50 - 200 KHz. A representative frequency response curve for these transducers can be viewed in Figure 5. It can

be seen from this figure that the sensitivity of the sensor begins to decrease at frequencies above 200 KHz.

The varying voltage pulse from the AE sensor travels down a coaxial cable to a Physical Acoustic's 3104 amplifier (Figure 6). The amplification is set by a thumb wheel and can be varied from 0 to 100 dB. The threshold ranging from 0 to 9.9 volts is also controlled by a thumbwheel on this amplifier. Proper setting of both these parameters is critical and is dependent on the type of specimen being examined (This will be explained in the results/discussion).

The amplified signal is then processed and saved by a P.A.C. 3000 unit (Figure 6). The data can be analyzed after the testing by utilizing the 3000. The saved parameters are hits, time, duration, counts, energy, amplitude, rise time, and Parametrics. The Parametrics saved for the testing in this thesis were load and displacement.

Calibration of the acoustic equipment before testing is of paramount importance. Numerous sensors are used during a single test, and to obtain meaningful data, it is critical that all the sensors behave similarly. After each sensor was coated with a couplant (for this study Ultragell II²⁶ was used) and mounted on the specimen via ASTM standard E650-85²⁷, either with elastic bands or magnetic hold downs, the sensitivity of each had to be determined. This was achieved by a pencil lead break procedure as in ASTM E976 standards²⁸. A mechanical pencil with 0.5mm diameter lead and 3-4 mm. long is held at a

30° angle, with respect to the specimen, and broken on the specimen at a predetermined distance from the sensor. The standards do not specify the type of lead to be used, only that it should be the same for all measurements. The amplitude of the pressure wave generated from the lead break is displayed on the 3000. A pencil break for each sensor must be completed and the amplitude should not vary more than 10 percent between transducers. An average amplitude for this procedure using R6I sensors was 94 dB at a distance of 10cm.

Once the sensitivities of the sensors were determined to be similar, the proper gain and threshold of the amplifier had to be set. These settings varied for each test and will be noted in the appropriate sections. Initially the settings were set so that the sensor would be as sensitive as possible without recording extraneous noise such as mechanical vibrations from the loading apparatus or electromagnetic interference. As the loading started, the gain and threshold of the amplifier may have been adjusted so that only meaningful data would be recorded. Therefore, the first specimen of a set of tests usually determined the settings for the remaining specimens.

Before the long column specimens were tested, attenuation and the speed of sound in the structure had to be determined if location plots were desired. This was achieved by the breaking pencil lead breaks at various distances from the sensors. The attenuation was determined by noting the

decrease in dB recorded from the sensors as the distance from the lead break to the sensor increased. The determination of the speed of sound was achieved by a pencil break next to one sensor and noting the time delay before another sensor recorded the pulse. The distance between the sensors was noted and the velocity was then easily calculated.

D. Tensile tests

Tensile coupons were fabricated from two ASTM A36 steel plates. This material was not used elsewhere in this study. The coupons did not have any mill scale or corrosion products on the surface when tested. The specimens were tested in tensile in a 413.8 MPa. capacity hydraulically controlled universal testing apparatus (Baldwin). Ultragell II was used as the couplant material to ensure good sound transmission from the specimen to the transducer. The Ultragell II was placed on the sensor head which was then attached to the center of the gage section of the specimen with elastic bands.

A second set of tensile coupons were fabricated out of salvaged columns from the Gulf of Mexico. The surface of the specimens were machined cleaned of all oxides and corrosion products. All of the tensile specimens in this thesis were flat. The tensile specimens from the salvaged columns had to be machined flat since they initially had a curvature. One R6I sensor with Ultragell II couplant on its face was placed above the gage section of the tensile coupon with elastic bands. An

extensometer was attached in the gage section of these specimens. The specimens were tested at a constant crosshead extension rate on a Tinius Olsen screw driven tensile machine.

E. Stub Columns

A select group of salvaged columns were selected to be tested. Some of the criteria for selection were, severity of corrosion, and uniform hardness readings along the column. Since the majority of the columns had transverse welds, hardness readings verified that similar strength steels were used on the same column. From the group with uniform hardness readings, stub column specimens were fabricated by simply cutting one end of a long column using a band saw. This cut piece ranged in length from 1.06-1.91 m. End plates were welded on both ends of the specimen and placed in the 34.5 GPa capacity hydraulically controlled universal testing machine (Baldwin). Figure 7 depicts one stub column under compression in a Baldwin apparatus.

In addition, a set of fabricated stub columns were prepared for this study. Structural steel plate was cold rolled to form a cylinder and longitudinally welded. The cylinders also had end plates welded to both of the ends.

Four sensors were used for the stub column tests. The area of contact was cleaned with a electric grinder so that all of the oxides or corrosion products were removed. R6I sensors were used for all of the stub column tests.

Ultrage11 II was placed on the sensor head which was then attached to the specimen with magnetic hold-downs. The location of the sensors is shown in figure 8. Calibration for sensitivity as described previously was performed.

Linear variable displacement transformers (LVDTs) were utilized to measure the load and the overall displacement and were connected to the parametric inputs of the 3104. Note that the load measuring LVDT was connected to a mechanical arm in the Baldwin apparatus that moved a specific displacement depending on the load. The specimens were loaded in compression in a step wise sequence, i.e. the load was increased to a specific value and then held for a predetermined time. Data throughout the tests was saved on floppy disk for later analysis.

F. Long Column

A group of long column specimens were selected to be tested in the 34.5 GPa capacity Baldwin. Figure 9 shows one long column being tested in the Baldwin. Long column testing consisted of both salvaged and fabricated specimens. All of the fabricated specimens as well as most of the salvaged specimens were intentionally dented at the center of the column. One salvaged specimen had been accidentally dented in service.

The attachment procedure of the sensors to the long-columns was identical to that of the stub columns.

Attenuation and speed of sound was determined for these specimens because location plots were desired. The placement of the sensor array was changed for the testing of different columns to determine optimum location of the sensors. A total of three different sensor location geometries (Figure 10) were used in this study. Both linear and planar location plots were obtained.

G. Four point bending

A four point loading jig was used as shown in figure 11. Three R6 sensors were utilized in this experimental set-up. The outer two sensors were placed near the loading pins and acted as guard sensors while the inner sensor recorded the relevant acoustic emissions. The loading pins on the four point bend fixture were rapped with teflon tape and coated with a thin layer of oil in an attempt to limit the amount of noise generated from friction. A 413.8 MPa capacity Baldwin was utilized. Since this equipment was hydraulically controlled, a constant strain rate was not possible. The load and displacement were directly recorded in the acoustic equipment by utilizing LVTDs.

The same steel plate, (ASTM A572, nominal yield strength of 344.8 MPa) that was used to fabricate a long column and a stub column specimen (P2-LC,P2-SC) were used as four point bend specimens. The material had a coherent mill scale on the surface. An objective of this thesis was to determine if the

structural steel with different surface conditions would result in different AE. The material was cut into 5cm wide by 44.5cm long specimens by a band saw. Each fabricated four point bend specimen was cut out of the same plate so they initially had the same thickness of 0.95 cm. The following Table III gives the environmental history of each set (3 specimens in a set) of specimens. Cleaned and polished refers to the removal of the oxides by grinding and then roughly polished by 120 grit SiC abrasive paper. The ocean environment specimens were placed on a corrosion rack and totally immersed in a salt water bay at Long Beach Island which is located along the New Jersey shore line. The rack was placed approximately 30 cm below the water line at low tide. Each specimen at a 55 degree angle was placed on the wooden corrosion rack length wise and approximately 4 cm. apart from each other.

The specimens that were heat-treated were placed on alumina blocks in a Hayes furnace. The chamber was at ambient pressure and the specimens cooled to room temperature in the furnace by turning the furnace off at the end of their heat treatments. Prior to testing, any loose or noncoherent oxides and dirt were removed by using a hand held steel wire brush.

TABLE III

Surface Preparation and Environmental History of the
Fabricated Four Point Bend Specimens

Cleaned and Polished

As received Mill Scale

Cleaned and Polished / Heat-treatment 100 hrs at 560°C

Cleaned and Polished / Heat-treatment 200 hrs at 560°C

Cleaned and Polished / Heat-treatment 10 hrs at 900°C

Cleaned and Polished / Salt water environment 600 hrs

Cleaned and Polished / Salt water environment 1800 hrs

As received Mill Scale / Salt water environment 600 hrs

As received Mill Scale / Salt water environment 1200 hrs

As received Mill Scale / Salt water environment 2400 hrs

The second group (two specimens in a set) of specimens were cut out of a structural column that was salvaged from the Gulf of Mexico and their environmental histories are given in Table IV. Since, these salvaged four point bend specimens were fabricated from a column, the specimens were not flat and had a curvature to them.

TABLE IV

Surface Preparation and Environmental History of Four Point
Bend Specimens Fabricated From a Salvaged Column

As received with Oxides and Marine Life

Cleaned and Polished

Cleaned and Polished / Salt water environment 600 hrs.

Cleaned and Polished / Salt water environment 1200 hrs.

Cleaned and Polished / Salt water environment 2400 hrs.

Each specimen in table IV was 5 cm in width, 39.4 cm. in
length and 0.95cm. thick.

III RESULTS/DISCUSSION

A. Tensile tests

Two sets of tensile coupons were fabricated from ASTM A36 steel plate with the same dimensions except for different thicknesses (0.127 cm. and 0.0635 cm. their specimen identification was TP1 and TP2 respectively). The surface of the specimens were free of scale and corrosion products. Burst type of emissions occurred before the yield point of the steel. These events were very few and can be attributed to inclusion cracking in the material. The material became unusually quiet at the yield point. At the yield point of the material, dislocations become unpinned and start to move and this can be detected with AE equipment as continuous emissions only if the gain (amplification) is set high enough. It is postulated that the equipment was not set to high enough sensitivity to record this phenomena. Bursts of detectable emissions occurred during strain hardening of the material as shown in Figure 12.

All the tensile specimens fabricated from ASTM A 36 steel behaved similarly except that the thicker specimens exhibited more hits. This can be attributed to the volume effect. That is, as the volume of the material is increased, the number of events should also increase. This volume effect was first detected by Ying et al. with the study of steel plates.²⁹ Numerous types of steels were studied in this thesis and this

can be viewed by noting the Rockwell hardness readings of the specimens (Table V).

Tensile coupons were also fabricated out of two structural columns that were in service from the Gulf of Mexico (from columns E1 and E3). The surface of the specimens

TABLE V
Rockwell Hardness Measurements of The Specimens

<u>ROCKWELL HARDNESS (HRB)</u>		
	Tensile	Column
TP1	75	
TP2	83	
E1		83
E3	83	80
B3		80
P4P		86
P2P		82

were ground to remove all oxides and corrosion products. The steels yield points were determined to be 279.3 (E3) and 367.6 (E1) MPa. The hardness of the specimens can be viewed in Table V. The gain and threshold were set for maximum practical sensitivity which was a gain of 35dB and a threshold of 0.9 volts (only signals above 40dB would be recorded at these settings). The sensitivity values obtained from a specific gain and threshold setting are calculated and discussed in the

Appendix. The equipment has the capability of being more sensitive, but it is believed that frictional noise generated from the extensometer was being recorded at greater sensitivities. The frictional noise was indicated by continuous AE during the elastic region of the testing. Continuous emissions are not expected until yielding. After changing the gain to the values previously presented, there were some sporadic hits during the elastic region and silence at the yield point (Figure 13). The loading procedure for these specimens (coupons fabricated from salvaged columns) were different than the previous tensile tests in that the load was increased at a constant crosshead extension rate on a Tinius Olsen screw driven tensile machine. During the loading cycle, the specimens were loaded and then periodically stopped. In other words, the loading proceeded in a step wise sequence with intermittent pauses. During the pause period, the load would decrease. When the tensile machine was reactivated after the pause period, the load would slowly increase and surpass its previous maximum load. The material did not exhibit emissions until its previous maximum load was surpassed. This phenomena is called the Kaiser effect and it was noted for both of the steels being tested. This is an important phenomena to be aware of due to the fact that it can help determine if a member is being loaded at ever increasing stress levels.

It is possible to determine if mechanical vibrations such

as hydraulic flow through the testing apparatus (Baldwin) or if electromagnetic noise was recorded by the AE equipment. This is achieved by viewing correlation plots that may be prepared after testing. One such diagram is achieved by preparing counts (ordinate) versus amplitude (abscissa) plot. Mechanical noise has the attribute of many counts compared to their amplitude while electromagnetic interference has the characteristic of few counts compared to their amplitude. A correlation plot may be viewed in figure 14. Note that frictional and electromagnetic interference appears not to be a problem. This type of correlation plot was examined for all of the specimens tested in this thesis. All of the data presented in this thesis did not have a problem with recording these erroneous signals.

In summary, the tensile tests determined two factors: first if a Kaiser effect was present for the structural steel examined and second if continuous emissions at the onset of plastic deformation could be detected. The onset of yielding was not determined by the AE technique probably because the equipment could not be set at its most sensitive settings. The Kaiser effect, however, was present with all the tensile coupons tested.

B. Stub Column Testing

The purpose of these tests were to determine if yielding of the structural columns can be detected with the AE

equipment. The surface condition of these columns differed in that the severity of corrosion varied and some columns had a brittle marine growth (barnacles) on them. The specimens were inserted into a 34.5 GPa capacity Baldwin and compressed until gross buckling occurred.

The first specimen tested was E1-SC which was fabricated from a 359 MPa steel. The surface of the specimen was corroded and had marine life on it as shown in Figure 15. A large number of hits were recorded at a sensitivity setting of 1 volt threshold and a gain of 35dB (total sensitivity of 45dB). The sensitivity parameters for the remaining stub and long column test may be viewed in Table II. By viewing Figure 16 it can be seen that an increase in hits occurs at the yield point of the steel. As mentioned in the procedure, the load was increased in a step wise sequence. During the loading periods before yielding occurred, fewer hits are recorded when compared to the loading periods after the yielding. It is speculated that these hits are the result of the oxides and other surface material spalling off of the specimen. This is reinforced by the fact that at the yield point of the specimen the spalling was visibly apparent and could be heard with the unaided ear. During the hold period, the load would decrease (Figure 17). It was noted that the spalling of the oxide occurred only when the previous maximum load was surpassed. In other words, the surface material exhibited the Kaiser effect. Detail about the surface material will be discussed

later in this section.

Specimen E3-SC was tested and further supported the speculation above. By viewing figure 18, it can be seen that there is an increase of hits at the yield point. The Kaiser effect was also present for this material. The surface condition of E3-SC was very similar to specimen E1-SC in that they both had a layer of corrosion products and residual dried marine life (barnacles).

The final salvaged stub column to be tested was S2-SC. This column had a monel sheet on it during service to protect it from corrosion. Prior to testing this sheet was removed, and it was noted that marine life was not present on the surface of the column. (Figure 19). This material was more acoustically active than the previous two specimens in that more hits were recorded. At the yield point, there was an increase in hits but they were so frequent that it overloaded the equipment and data was not recorded. The AE equipment used in this project requires time to process the incoming acoustic signals. During this 'dead' time the processor does not allow any new signals to be recorded. When signals are generated at a rapid rate, the AE equipment can not process the signals fast enough and will essentially remain in dead time. When this occurs, all data acquisition is halted and no data is recorded.

Due to the halting of data acquisition during the yielding of specimen S2-SC, post analysis was difficult and

conclusions could not be drawn from the data that was recorded. The onset of yielding of the column was identified by viewing the load vs. displacement diagram, and it was noted that spalling of the surface layer (corrosion products and possibly mill scale) occurred at the yield point. In an effort to avoid the "overloading" of the AE instrumentation, the sensitivity was decreased during the testing. This was successful because the equipment again began to collect data. It should be noted that changing the sensitivity during the test complicates post analysis, and should be avoided if at all possible.

Since only one end plate was welded on this specimen (S2-SC), the inside surface of the column was examined after the test. By viewing figure 20. it can be seen that spalling also occurred on the inside of the tubes. The corrosion products appear light in this photograph, and the areas where spalling occurred appear brown. The inside of the stub columns experiences compression forces while the outer surface is in tension. It is evident by this photograph that spalling, of the surface layer, occurs in both compression and tension.

The above three stub column specimens support the theory that yielding or plastic deformation of structural columns can be detected by monitoring the emissions of the spalling. It should also be noted that the surface condition of S2-SC appeared different than E1-SC and E3-SC. Therefore, different

corrosion products or mill scale may exhibit similar AE information during the onset of yielding.

Three fabricated stub columns were also tested (P1-SC, P2-SC, and P3-SC). Their dimensions are shown in table II. The fabricated columns exhibited a similar surface scale in that the surface material was composed of a layer of mill scale and rust (Figure 21). The scale spalled off all of the specimen prior to yielding, and the yield point could not be determined by the AE. The emissions given off however were very large in amplitude and the sensitivity had to be lowered to Threshold 1V and Gain of 10 dB (at these settings, the signal had to have an amplitude of 70dB or greater to be recorded). This is a lower sensitivity than was required for the salvaged stub column specimens.

The fabricated stub columns were cold rolled and welded longitudinally to form a specimen. Steel end plates were then welded to the ends of the column. The AE technique was not successful in detecting the onset of yielding in these specimens. Numerous hits occurred prior to the yielding of the stub column. It is speculated that the premature AE activity was caused by localized deformation. The cold rolling and welding of the specimens created a complex residual stresses and localized yielding occurred near the longitudinal weld prior to gross yielding. This may explain the increase in hits prior to gross yielding. It should be noted that localized yielding is not apparent by examining the

load versus displacement diagram.

The following trend seems to be present, the uncorroded mill scale produces the most hits at the greatest amplitude. This was apparent by the sensitivity settings that were required for the AE equipment not to overload. The more severe the mill scale is corroded or replaced with other oxides, the lower the amplitude. For example, the fabricated columns generated the most hits, then the monel protected column followed by the generalized corroded columns. This trend can be viewed in table II. A lower sensitivity indicates that the material was not as acoustically active as a material which required a high sensitivity.

C. Long Column Tests

Two sets of long column specimens were tested which were cut from salvaged columns that were taken from the Gulf of Mexico and from columns that were fabricated for this study. The lengths, circumferences and thickness of each column can be viewed in Table II. Hardness readings are located in table V.

The first long column to be tested was E1-LC which is from the same column as stub column E1-SC. The center of this column was intentionally dented at Lehigh University by compressing a 5cm diameter 61cm long indenter into the center of the column by a screw driven universal tensile machine. A more detailed discussion of this procedure is written in B.

Wood's masters thesis⁵. Four sensors were staggered along the length of the column, see Figure 10a, so that a location plot of the damaged area would be attainable. The location of the damaged area was possible by utilizing a linear location plot as previously discussed (Procedure). The column plastically deforms around the damaged area (dent) and due to this localized plastic deformation, a true yield point of the column could not be determined. It should be noted that determination of the yield point was not the purpose of using AE on these specimens, rather the purpose was to determine if a column is being overloaded (loading which caused plastic deformation) and locating the plastically deforming area. As in the stub column tests, all of the long column specimens were loaded in a step wise sequence in the Baldwin. As the load increased, the number of hits increased. This was expected because as the load is increased, the plastic zone grows and this is the area where spalling occurs. In essence the area of spalling increases as the load increases. The greatest number of hits occurred at the maximum load of the column, Figure 22.

A linear location plot was utilized for the four salvage columns. To review, if a hit occurs between two sensors, then by utilizing time of arrival analysis the location of the source of the hit can be ascertained. Generally the data is viewed by plotting a histogram of hits versus location. Such a plot is shown in figure 23 which is the data for E1-LC. It

can be readily observed that the location of damaged area which produced the greatest number of hits is positioned between sensors two and three. This was where the dented region was located. Closer examination of this figure reveals that there appears to be two Gaussian types of distribution of hits in the region between sensors 2 and 3. It is speculated that the equipment was able to resolve the two ends of the dent where the plastic zones were located. This speculation was further studied and supported by testing another long column specimen with a different set-up of sensors. The results of this test will be discussed later in this report.

The next specimen tested was E3-LC and it produced similar results as E1-LC. Again, this specimen was intentionally dented and subsequently compressed in the Baldwin. A problem encountered with this specimen was that the sensitivity of this test was initially set the same as the previous test E1-LC, and this was determined to be too high. This was apparently because too many hits were being recorded near the specimens maximum load that the equipment could not process them fast enough. The end result was that the computer did not record the signals and they were lost. The stoppage of data acquisition was noted during the loading sequence, so the sensitivity was decreased in the middle of the test so that data could again be recorded. It should be noted, as it was previously, that one of the critical parameters that has to be set with this AE technique is the

sensitivity level and this appears to be very difficult to predict before the testing.

Even though some data was lost with this specimen (E3-LC) the trend of increase in hits with increase in load is again observed (Figure 24) as was the fact that the maximum load produced the greatest number of hits.

The next salvaged long column (B3-LC) had a dent from service. This dent was much more gradual and not as severe as the previous two. Again the similar results of the previous two test were obtained. The maximum load produced the maximum number of hits (Figure 25).

The fabricated specimens were tested in a similar manner except the sensor arrays were changed. The specimens had a coherent mill scale on the surface. Removal of this mill scale for sensor mounting required a grinding wheel. The first specimen to be tested was P4-LC and it was decided to change the software so that a planar location plot could be obtained. Four sensors (R6I) were positioned on the middle section geometrically around the dent (Figure 26). The purpose of this arrangement was to determine if the two plastic zones, previously detected with the linear location, can be resolved. Figure 27 is a planar location plot for this specimen. The points on the plot indicate the location of a hit. From this figure it can be readily observed that this technique can resolve the growth of the plastic zone with increasing load. The purpose of this exercise was to

determine the resolution of the equipment.

The sensitivity of this test was set so only signals above 70dB would be recorded. This was chosen because earlier stub column testing at a sensitivity of 65dB was too sensitive and resulted in lost data by overwhelming the computer (as previously discussed). While this long column (P4-LC) was being tested, it was determined that 70dB was not sensitive enough and it had to be changed to 65dB. This again shows the difficulty encountered with initial settings before testing.

A linear location plot was used for the remainder of the tests because this format has a more practical use for inspection of offshore structures. The planar array described for specimen P4-LC would require too many sensors and the resolution it renders is not required for the proposed application of general location. Rather than a staggered array as previously used in the salvaged columns, it was decided to place the sensors on one line of specimen P2-LC, a fabricated column. Figure 28 shows the placement of the sensors. The two end sensors were placed as far away from each other as possible on this column with a length of 10.67 m. The purpose of this test was to determine the minimum distance required to effectively locate the damaged area. Figure 29 shows a linear location plot that utilizes all four of the sensors. Note that the damaged area is readily identified between sensors 2 and 3. The other peaks that are present between sensors 1-2 and 3-4 are from the transverse

welds that connect the cylinders. A bursts of hits occurred at these welds early in the test and they subsequently became quiet when the maximum load was surpassed (compare figures 29 & 30). At first glance this may appear as posing a problem with later analysis because the welds may be misidentified as damaged areas, but it should be noted that the Kaiser effect was observed. Therefore, these areas will only give readings when a new maximum stress is applied otherwise they will be quiet.

A limitation with the software used (supplied by Physical Acoustics) is that linear location can only be used with two adjacent channels. In other words, locations between 1-2, 2-3, and 3-4 are possible, but plots for 1-3, 1-4, or 2-4 can not be obtained. The distance between 2-3 was 3.68 meters and it can be readily seen in figures 29 and 30 that these sensors where placed close enough for an accurate location of the damaged area. Dunegan ²³ claims that sensor spacing of 61 meters is realistic for offshore oil structures. This of course depends on many factors such as the amplitude levels of the signals at the damaged area and the attenuation factor. It should be noted that all of the columns studied in this thesis were tested in a dry environment and it is speculated that attenuation may be more severe if the columns were immersed in water.

The next fabricated column to be tested was D3-LC. It was decided to use two sensors on this column and to place

them as far away from each other as possible. The spacing between them was 8.23 meters. By viewing the location plot (Figure 31) it can be readily ascertained that spacing of 8.23 meters between sensors was not too far apart to enable determination of the location of the damaged area.

The final long column (D1-LC) studied was a salvaged column that was protected from corrosion with an organic coating (Paint). In preliminary equipment calibration, it was noted that the attenuation in this column was severe. For example a pencil break could be detected on all the other columns tested at least 9.14 meters away from the sensor. This signal (pencil break) however could not be resolved 8.53 meters away from the sensor (resolution was possible at 5.7 meters). Hence, it was predicted that a higher sensitivity setting would be required for this test. The high attenuation may have been due to the surface condition of the column. Apparently corrosion occurred underneath the painted surface and the interface between the paint and corrosion may not have transmitted sound efficiently. Once the test began however, this specimen was observed to produce the most hits with the highest amplitudes. Due to the amount of signals, a reduction in the sensitivity settings was required so that only signals above 73dB would be recorded. If the sensitivity was not lowered to 73dB, then it is speculated that data acquisition would have been too fast for the computer to process.

In summary, the long column tests have shown the success

of resolving the location of the damaged area. The actual plastic zone can be mapped if the sensors are placed close enough to each other (view figure 26 for distances) and the dent. However, the most efficient arrangement of sensors would be in a linear array because it would require the lowest number of sensors. A possible limitation of this technique is the difficulty in selecting the sensitivity settings. It is recommended that the equipment should be set at its most sensitive settings just above the unwanted background noise. If a column begins to plastically deform and emit a cascade of signals, then the inspector would be informed that something is occurring with that column. The sensitivity can subsequently be lowered if an accurate location plot is desired.

D. Four Point Bending Tests

As previously discussed in the introduction, it was concluded that a more in-depth study of the mill scale and other oxides on the surface of the specimens needed to be undertaken. A four point loading jig (Figure 11) was used for bending tests. There would be both a compression and tensile side similar to what is observed in the structural columns. One sensor was utilized to record the relevant hits generated between loading pins 3 and 4. All other emissions outside this window were discarded by the two guard sensors situated between the loading pins. A more detailed discussion of guard

sensors was presented in the introduction.

Two sets of specimens were studied. The first set was cut from a salvaged column that was also used for long column specimen E1-LC. The second set was from the 0.96 cm. thick ASTM A572 fabricated plate. Both materials were initially tested with there surface films (corrosion products and mill scale) ground off. The purpose of studying polished specimens was to determine whether or not the equipment possessed the required sensitivity to record continuous emissions (generated from dislocation movements) at the yield point of the steel.

Specimens from the 0.96 cm. thick fabricated plate were polished to a 120 grit finish with SiC abrasive paper and all oxide and pits were removed. By viewing figure 32 it can be seen that the continuous emissions of plastic deformation was not recorded. This was the case because the amplifiers were not preset to their most sensitive scale. The limit of the sensitivity was dictated by the frictional noise at the loading pins. If the equipment was set at its highest sensitivity, then the frictional noise at the pins would have been overwhelming in that it would continuously trigger the guard sensor. Hits generated between loading pins 3 and 4 would not be recorded if the guard sensors are continuously being excited. Hence, the sensitivity had to be decreased to a threshold of 0.3V and a gain of 30dB giving a net sensitivity of 38dB. It was noted that very few hits were recorded at these sensitivity settings. The results indicate

that the yield point could not be determined by acoustic emissions on these specimens. The recorded hits during the elastic region can be attributed to inclusion cracking and debonding as was seen by Kwon et al³⁰.

Specimens with the as received coherent mill scale on them were tested (Figure 33). They all exhibited a burst of hits at the yield point (Figure 34). The amplitude of these hits are also comparatively high when compared to the polished specimens. The average amplitude of a polished specimen was 45 dB while a specimen with the mill scale averaged 65 dB. This leads to the conclusion that the generated hits from the structural columns were indeed from the mill scale spalling.

The next group of specimens were cut from the same plate (ASTM A572), and the mill scale was left on the surface. The specimens were exposed to a salt water environment for varying lengths of time (600, 1200, 2400 hrs.) and their surface appearance is shown in figures 35,37,39. This study was undertaken to determine if the mill scale would deteriorate and reduce the amount of emissions after various exposure times in an ocean environment. By viewing Figures 36,38, and 40, it can be deduced that the burst of hits still occurs at the yield point of the material and significant deterioration with time does not occur up to the maximum exposure time of 2400 hrs.

To determine the acoustic emissions of only the corrosion products, it was decided to remove the mill scale and expose

the polished specimens to a salt water environment. This would help determine if the bursts of hits at the yield point can also be obtained by just the corrosion products. The corrosion product grown in the two time spans (600, and 1800hr.) appeared different (Figure 41 and 43). The 600 hr exposure resulted in a soft noncoherent corrosion product, while the 1800hr exhibited a coherent layer. The 600hr exposed specimen did not exhibit a burst of hits at the yield point. Rather it was somewhat continuous throughout the test (Figure 42). The 1800 hr exposed specimen resulted in an increase in hits at the yield point (Figure 44).

The final set of specimens were placed in a furnace, in air, at various temperatures and times to determine the acoustic emission characteristics of different oxide layers. The first group (100hrs at 560°C) exhibited a thin oxide layer that easily flaked off the specimen (Figure 45). This resulted in a continuous increase of emissions with stress. The yield point could not be determined with the AE signal (Figure 46). The second set was heat treated at the same temperature but for a longer time (300 hrs.). This resulted in two layers of oxide, a loose outer layer and a coherent inner one. The surface layer of this specimen can be viewed in Figure 47. The yielding of this material could be determined by the AE (Figure 48). The last group was placed in a furnace for 10 hrs at 900°C. This specimen had a very hard and brittle outer layer that was somewhat coherent in that it

could not be completely removed by hand (Figure 49). To be more explicit, the loose surface layers of the specimens were removed prior to testing by rubbing a hand held steel wire brush across the specimens surface. The acoustic information from the higher temperature heat treatment specimens did not supply any information about the yield point (Figure 50).

In summary, it has been shown that the mill scale exhibits a burst of hits at the yield point. This characteristic is still present up to 2400 hrs of exposure to salt water. If a mill scale is not present then it will take approximately 1800 hrs for a brittle corrosion product to form which will give similar results as the mill scale. Loose and thin mill scale will not be beneficial in determining the yield point, but it should be noted that mill scale is generally not thin, and any semicoherent product would be removed (spall off) during the rolling process of the plate into a cylinder.

The specimens that were fabricated from a column that was removed from service presented similar results as the fabricated bend specimens. Direct comparison between the fabricated specimens and the specimens from a salvaged column can not be made because the geometries of the two sets were different. The four point bend specimens fabricated from a salvaged column had a curvature and their dimensions were different than the specimens fabricated from the steel plate. The polished specimens exhibited sporadic hits and the onset

of yielding could not be determined by viewing the acoustic emissions data (Figure 51). Specimen IE 1 (Figure 52) , which was exposed to ocean environment for 600hrs, had a very noncoherent corrosion product on the surface similar to the fabricated specimen that was exposed for the same amount of time (Figure 41). Specimen IE 1 did not generate a detectable burst of emissions at the yield point of the material (Figure 53).

Specimen IE 3 (Figure 54) was exposed to an ocean environment for 1200 hrs. The surface was more severely attacked by corrosion and the products were more coherent to the surface than after the 600 hr exposure specimen. This layer (1200hr exposure), however, was still easily removed by hand. The AE generated from this specimen were not beneficial in determining the yield point of the material (Figure 55).

The 2400 hr. marine environment exposure specimen (Figure 56) did not produce meaningful data. It appears that a burst of emissions occurred prior to yielding and then subsided. It is believed that the acoustic sensor began to slip during testing and resulted in this burst of hits (Figure 57).

The final four point bend specimen was tested in its as received condition. It can be seen (Figure 58) that the surface of the specimen consisted of marine life (white areas) and corrosion products (brown areas). An increase in emissions has been observed near the yield point of this specimen (Figure 59).

In summary, the specimens fabricated from the column that was in service behaved similarly to the fabricated specimens. The determination of yielding was most readily apparent from the as received specimen (specimen with remnants of marine life and corrosion products).

E. Equipment Evaluation

Two randomly selected sets of data were analyzed to determine the reliability of the recorded data on the 3104/3000. The data for P1 long column and a fabricated polished 4pt bend were printed (Tables VI and VII). An event that is recorded with a value of zero for any of the following variables; duration, energy, or counts is meaningless and should be discarded.

TABLE VI

A Representative Group Of Data That Was Recorded

For A Fabricated Long Column (P1-LC).

<u>Dat#</u>	<u>Channel</u>	<u>Timing</u>	<u>Duration</u>	<u>Count</u>	<u>Energy</u>	<u>Amp.</u>	<u>Rise</u>
542	3	74.8	6	2	1	49	4
542	4	0	11	1	0	40	12
543	2	1070.6	5	3	1	53	1
543	3	0	232	20	22	52	0
543	4	291	0	1	0	40	1
544	1	153	1075	54	122	63	25
544	2	97.4	2740	164	422	65	110
544	3	0	3326	225	605	73	34
544	4	47.6	1877	98	251	66	32

The "dat#" column in Table VI indicates the number of hits that were recorded e.g. this table starts at hit number 542 and ends on 544. The same data number can appear for more than one row because different sensors (1-4) can record the same event. This can be seen by viewing the last four rows in the above chart. Column two indicates which sensor recorded a particular event. The remaining columns have the pertinent parameters that were measured for the recorded event. A recording time of zero indicates that the sensor was the first to record the event. A value of zero in any of the above mentioned parameters (Duration, Count, or Energy), indicates erroneous data. Therefore row two and five should be discarded from data analysis.

A different loading system (4pt bending instead of uniaxial compression) with different acoustic sensors (R6 instead of R6I) also generated the erroneous data (Table VII). Therefore it is speculated that the bad data may be generated with the 3000 processor or the 3104 amplifier.

TABLE VII

A Representative Group Of Data From A Polished
Fabricated 4pt. Bend Specimen.

<u>Dat#</u>	<u>Channel</u>	<u>Timing</u>	<u>Duration</u>	<u>Count</u>	<u>Energy</u>	<u>Amp.</u>	<u>Rise</u>
81	1	0	2148	62	75	46	1500
81	2	574.4	61	10	4	42	16
81	3	496.2	141	16	4	41	0
82	1	0	4	3	0	40	3
83	1	0	3355	113	139	50	187
83	2	197.8	585	35	17	46	56
83	3	20.2	1401	84	48	45	30
84	1	0	1	2	0	40	2
85	1	0	3081	119	118	46	273
85	2	322.2	456	29	15	45	137
85	3	57.4	1844	98	73	47	44
86	1	0	50	3	0	42	25
86	3	1287.4	0	1	1	38	0

A random population of 100 recorded hits for each specimen were selected, and it was determined that over 17% of the data for long column and 25% for the four point bend specimen should be discarded. A possible source for these erroneous readings may be from the conversion process from an analog to digital format. It was also noted that this type of data can also be recorded if the transducer lost sensitivity or slipped during a test. Another possible source may have been caused by the great number of events that occurred, in essence, signals were being superimposed on top of each other.

This erroneous data can be filtered with the current

equipment by utilizing graphical filters. This technique can only be incorporated after the data is collected and recorded. Misleading interpretation can result if this filtering is not incorporated in the post data analysis. The most affected plots are average duration and average energy diagrams. In essence without the filtering, averages would be computed with zero energies and durations and this leads to artificially low values. Figure 60 gives plots of energy, duration and hits verses displacement. The greatest effect of artificially low averages can be viewed at low displacements. Note that the least affected data appears to be plots of hits versus displacement. Hence, for the purposes of this study it is recommended that histograms of hits versus displacement or cumulative time be the criteria for plastic deformation. If AE technology is to be utilized on these structures, then on-the-fly filtering is a must, or use equipment that does not produce these artificial hits. On-the-fly filtering is currently available on the latest version of Physical Acoustic's AE equipment which is called the "Spartan".

If location plots are to be utilized, then the operator has to calibrate the equipment at one sensitivity level and should not change it during a test. It was noted that as the sensitivity of the sensors was increased, the velocity of the recorded signal also increased. This is the result of the pressure wave having a precursor wave of smaller intensity that travel faster in the material. At proper setting of the

sensitivity, this precursor wave would not be detected. At high sensitivities, the precursor wave will travel faster and be detected by the other sensors in a shorter time period. This deleterious effect can be shown by the following example. A 0.5 mm. diameter pencil lead break was performed next to sensor 1 and it required 719 micro seconds for the pressure wave to arrive at sensor 2. A 0.9 mm. thick lead pencil break at the same location produced a greater amplitude signal and arrived at sensor 2 in 571 micro sec. This shows that a greater amplitude signal may be recorded on the AE equipment as having a greater velocity and this can result in a shifted location plot if the operator is not aware of the change.

IV CONCLUSIONS

It has been shown that AE technology has the potential to be utilized as a nondestructive evaluation technique for offshore oil platforms. The onset of yielding has been identified with a bursts of acoustic emissions on stub columns and four point bend specimens. It has been determined that the bursts of emissions is the result of a brittle surface layer spalling off the specimen during plastic deformation. It has been shown that the intrinsic acoustic emissions generated from inclusion cracking and dislocation movements are not a significant factor in this analysis in that the spalling of the oxides is greater in intensity (amplitude) and more frequent.

Corrosion products that form on a ASTM A572 structural steel, after a minimum exposure of 1800 hours in a salt water environment, emit similar AE signals compared to mill scale, and can be used to determine yielding in a material. It should be noted that not all corrosion products emit at the onset of yielding. This depends on the thickness and coherency of the product to the surface of the steel. Corrosion products that formed in less than 1800 hours were not beneficial in determining yielding of the material. The corrosion of the mill scale in a salt water environment (immersed up to 2400 hrs.) does not significantly reduce the emissions during the onset of yielding.

The AE technique can be used to determine the location of an overloaded area (dents). The actual growing plastic zone can be mapped by utilizing a planar location plot. For practical applications, of this AE technique to offshore structures, it is recommended that a staggered linear array of sensors to be used. The sensor spacing can be as great as 8.23 meters to obtain meaningful data. This is by no means a limiting distance between sensors, rather it was the farthest distance tested in this thesis. For data analysis, it is recommended that only diagrams containing a histogram of hits versus time to be used. The other parameters such as duration, rise time, and energy should not be used because the equipment generates false hits and this erroneous data can lead one to false conclusions.

Further equipment improvements have to be entailed if this technique is to be placed into service, such as on-the-fly filtering of bad data, a more efficient analog to digital converter and a faster processor.

V SUGGESTIONS FOR FUTURE WORK

Since in service structural columns are completely or partially immersed in water during service, it is imperative to determine how an immersed column generates AE. It is possible that attenuation may be greater in water which would require closer spacing of the transducers. Also it is not certain that the high amplitude hits encountered in this study would be present in a wet environment. A possible experimental set-up would be to use an immersed four point bend specimen.

It would be beneficial to attempt monitoring on a real structure in service. This would present valuable data in determining the magnitude of the actual noise level present and to attempt filtering of background noise with the present equipment.

REFERENCES

- 1 Street, R. , "The Requirements for the Testing and Inspection of Offshore Installations Under The Mineral Workings (Offshore Installations) Act, 1971", British Journal of NDT, May 1975.
- 2 Silk, M.G.; Williams, N.R.; Bainton, B.A. "The Potential Role of NDT Techniques in the Monitoring of Fixed Offshore Structures", British Journal of NDT, May 1975 pp. 83-87.
- 3 Marshall, P. , "Strategy for Monitoring, Inspection and Repair for Fixed Offshore Structures", Second International Conference on Behavior of Off-Shore Structures, Held at Imperial College London, England August 1979, pp. 369-379.
- 4 Sawant, S.S; Wagh A.B.; Venugopalan, V.P., "Corrosion Behavior of Mild Steel in Offshore Waters of the Arabian Sea". National Institute of Oceanography (India), Corros. Prev. Control, Apr. 1989, 36, (2), 44-47.
- 5 Wood, B., Masters Thesis to be published. Civil Engineering, Lehigh University Bethlehem, PA 18015.

- 6 Pollock, A , "Acoustic Emission Inspection" Metals Handbook Ninth Edition, Vol 17, ASM International, Metals Park, OH, 1989. pp. 278-294.
- 7 Gilbert, B, Private telephone conversation, Physical Acoustics Corp. representative. Aug. 1991.
- 8 Zhang, B.Q. , "Acoustic Emission On-Line Monitoring for Petrochemical Plants", Materials Evaluation, 47, March 1979 pp. 351-355.
- 9 Hutton, P.H. , "Acoustic Emission for Continuous Monitoring of Light-Water Reactor Systems: A Status Review". Materials Evaluation, 46, Feb. 1988. pp. 241-246.
- 10 Parry, D.L. , "Nondestructive Examination of Subsea Structures Using Acoustic Emission Technology". 9th Annual Offshore Technology Conference, Houston, Tex., 1977. pp.467-474.
- 11 Rogers, J.P.; Hansen J.P.; Webborn,T.J.C., "Application of Acoustic Emission Analysis to the Integrity Monitoring of Offshore Steel Production Platforms" Materials Evaluation Aug, 1980., pp. 39-49.

- 12 Bassim, M.N.; Hay, D.R.; Lantaigne, J., "Wave Analysis of Acoustic Signals from Mild Steel", Materials Evaluation, Feb. 1975, pp. 109-113.
- 13 Hartman W.F.; Klin, R.A., "Variations in Frequency Content of Acoustic Emission During Extension of HF-1 Steel", Materials Evaluation, July 1977, pp. 47-51.
- 14 Wadley, H.N.G.; Scruby, C.B.; Speake, J.H., "Acoustic Emission for Physical Examination of Metals", International Metals Reviews, Vol 2, 1980, pp. 41-63.
- 15 Hadjicostis A.N.; Carpenter, S.H., "An Investigation Of The Acoustic Emission Generated During The Deformation Of Mild Steel", Materials Evaluation, February 1980, pp. 19-23.
- 16 Glass, J.T.; Green, R.E., "Acoustic Emission during Deformation and Fracture of Three Naval Alloy Steels", Materials Evaluation, Vol 43, June, 1985, pp. 864-872.
- 17 Holt, J.; Goddard, D.J., "Acoustic Emission during the Elastic-Plastic Deformation of Low Alloy Reactor Pressure Vessel Steels I: Uniaxial Tension", Materials Science and Engineering, Vol 44, 1980, pp. 251-264.
- 18 Ono, K.; Yamamoto, M., "Anisotropic Mechanical and

- Acoustic Emission Behavior of A533B Steels", Materials Science and Engineering, Vol 47, 1981, pp. 247-261.
- 19 Halmshaw, R. , "Offshore NDT Forum" British Journal of NDT, March 1977, pp. 18-32.
 - 20 Chandler, K.A. and Bayliss, D.A. Corrosion Protection of Steel Structures., Elsevier Applied Science Publishers, New York, 1985, pp. 36.
 - 21 Gaylarde, C.C.; Beech, I.B., "Molecular Basis of Bacterial Adhesion to Metals". Microbial Corrosion. [Proc. Conf.], Sintra, Portugal, Mar. 1988, pp. 20-28.
 - 22 Drew. M.W.; Wood. B.R.A.; Harris, R.W., "Acoustic Emission During Deformation and Crack Initiation of Pipeline Steels", Journal of Acoustic Emissions, Vol 6, Number 4, 1987, pp. 239-248.
 - 23 Dunegan, H.L., "Acoustic Emission - New Inspection Technique", 9th Annual Offshore Technology Conference, Houston, Tex, 1977, pp. 349-356.
 - 24 Dunegan, H.L. "Using Acoustic Emission Technology to Predict Structural Failure", Metals Engineering Quarterly, Feb. 1975, pp. 8-16.

- 25 Ostapenko, A; Wood, J., "Proposal for Research on Residual Strength of Damaged and Deteriorated Offshore Structures" Lehigh University, Bethlehem, PA 18015, 1989.
- 26 Ultragell II Contact Ultrasonic Couplant, ECHO Ultrasound, P.O. Box 552, Lewistown, PA 17044.
- 27 Annual book of ASTM Standards, "Standard Guide for Mounting Piezoelectric Acoustic Sensors.", Vol. 03.03 Designation E650-85, ASTM Committee on Standards, 1916 Race St. Phila, PA 19103, Jan. 1985.
- 28 Annual book of ASTM Standards, "Standard Guide for Determining the Reproducibility of Acoustic Emission Sensor Response." Vol 03.03 Designation E976-84, ASTM Committee on Standards, 1916 Race St. Phila, PA 19103 July, 1984
- 29 Ying, S.P.; Grigory, S.C., "Acoustic Emission from Flawed Heavy Section Steel Plates", Materials Evaluation, Feb. 1975, pp. 30-36.
- 30 Kwon, O.Y.; Roman, I.; Ono, K, "Burst-type Emission Behavior of Structural Steels", The Second International Conference on Acoustic Emission, pp. S106-S110.

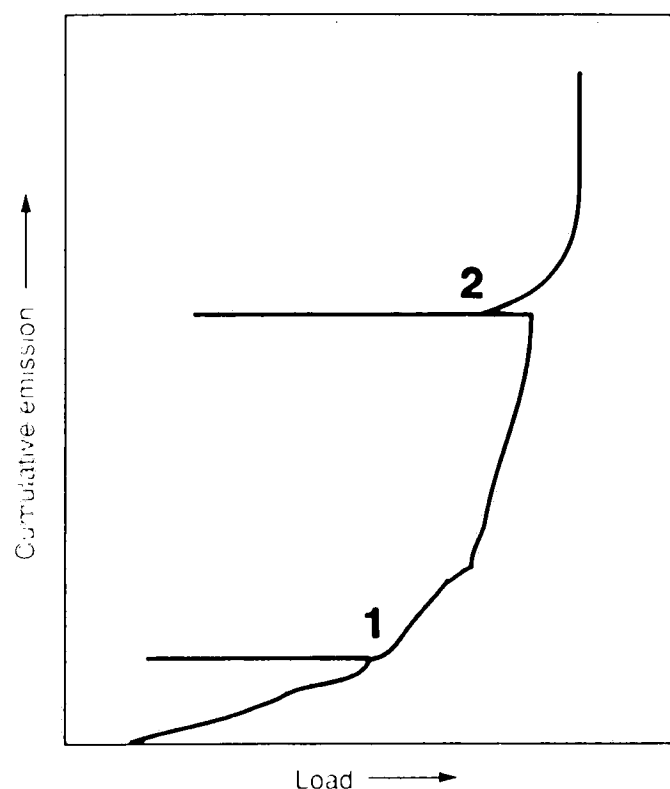


Figure 1. Cumulative Emissions Versus Load Diagram Showing The Kaiser Effect. At position 1 the load is decreased and no new emissions are generated. The load is then increased, and new emissions are generated only after the previous maximum load was surpassed. Position 2 is an example of the Felicity effect, which is simply the breakdown of the Kaiser effect.⁶

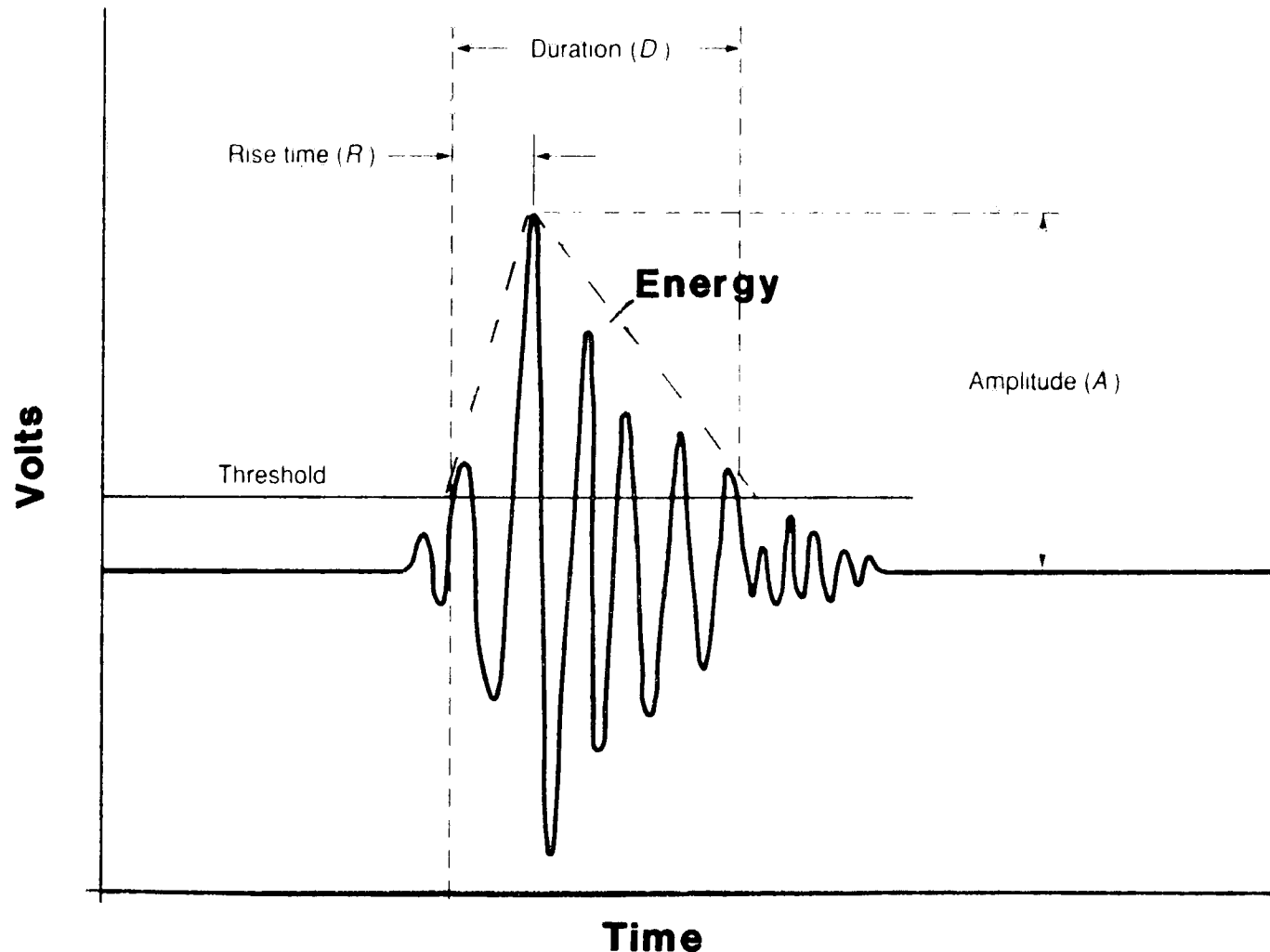


Figure 2. Schematic of A Typical Wave Form From A Burst Type Emission. Commonly measured parameters are indicated.⁶



Figure 3. Two R6I Acoustic Sensors With Built-in 40dB Preamplifiers. A magnetic hold-down can be viewed in the upper right.

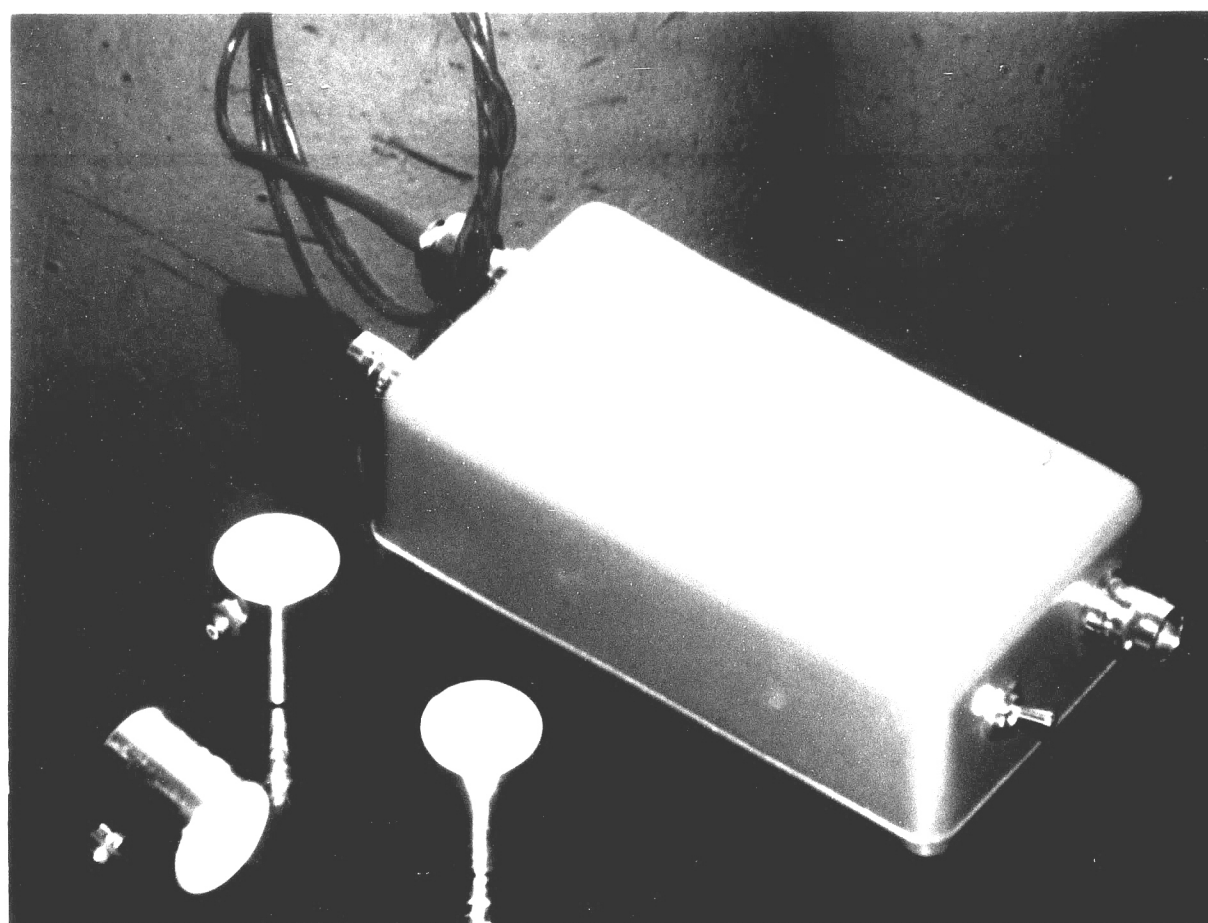


Figure 4. Three R6 Acoustic Sensors Shown With One P.A.C. 1220-A Preamplifier

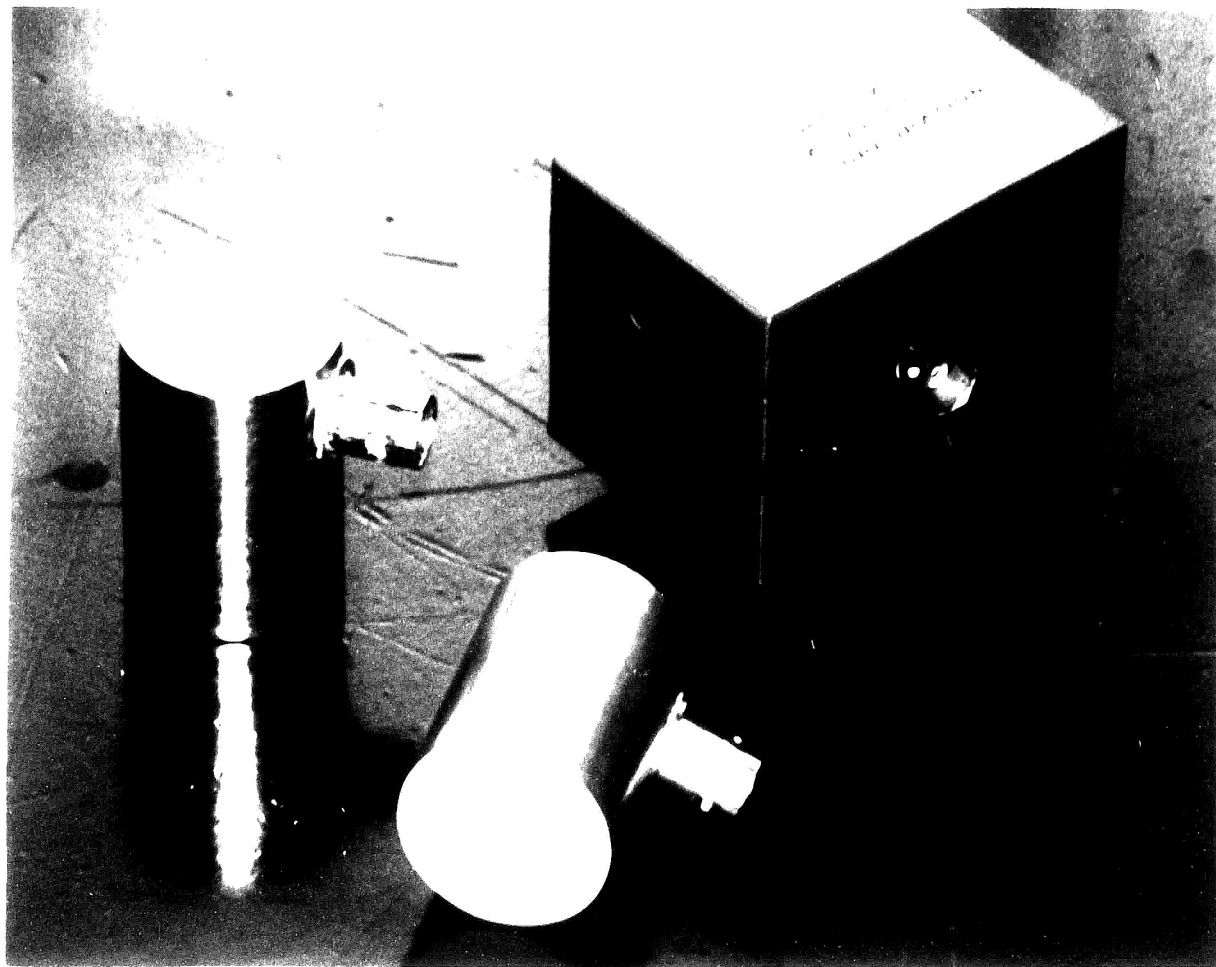


Figure 3. Two R6I Acoustic Sensors With Built-in 40dB Preamplifiers. A magnetic hold-down can be viewed in the upper right.

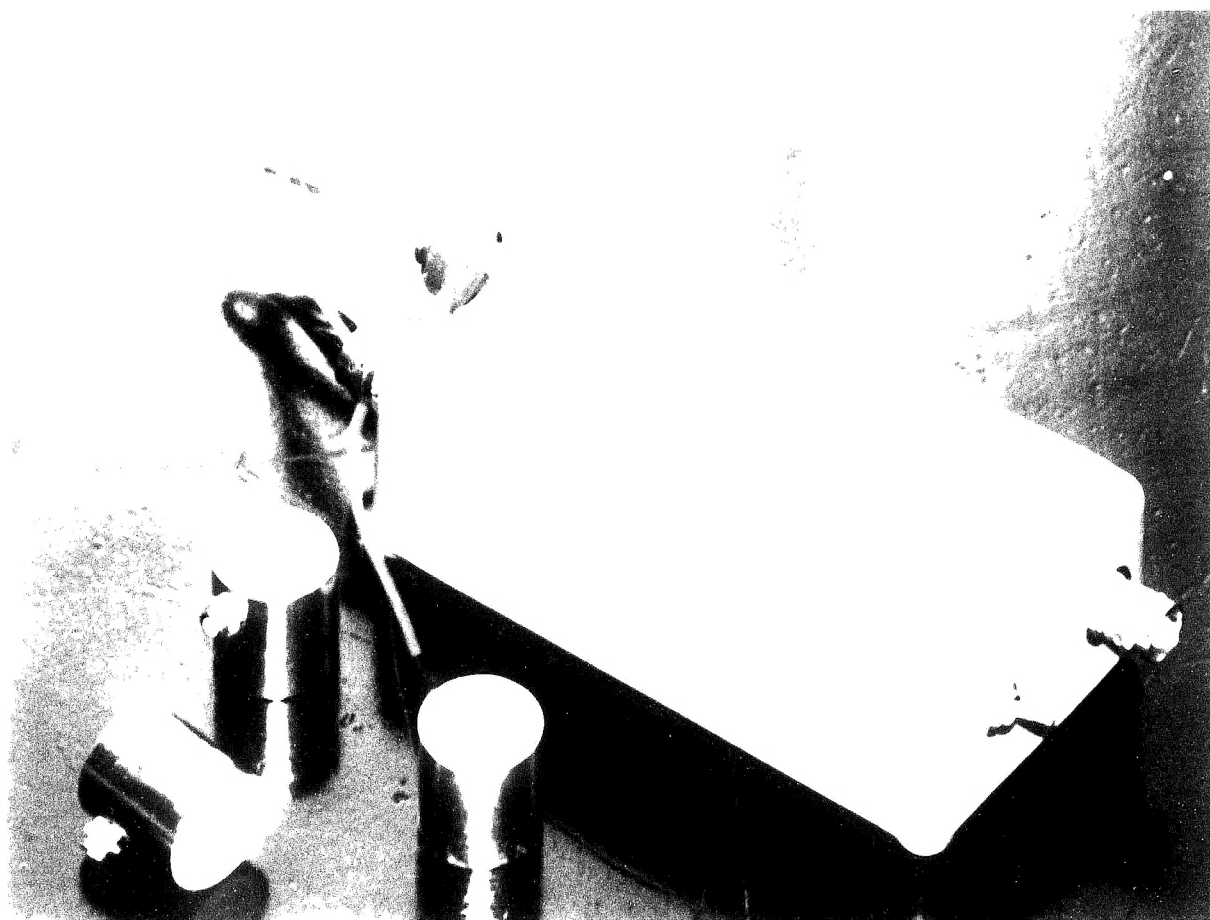


Figure 4. Three R6 Acoustic Sensors Shown With One P.A.C. 1220-A Preamplifier

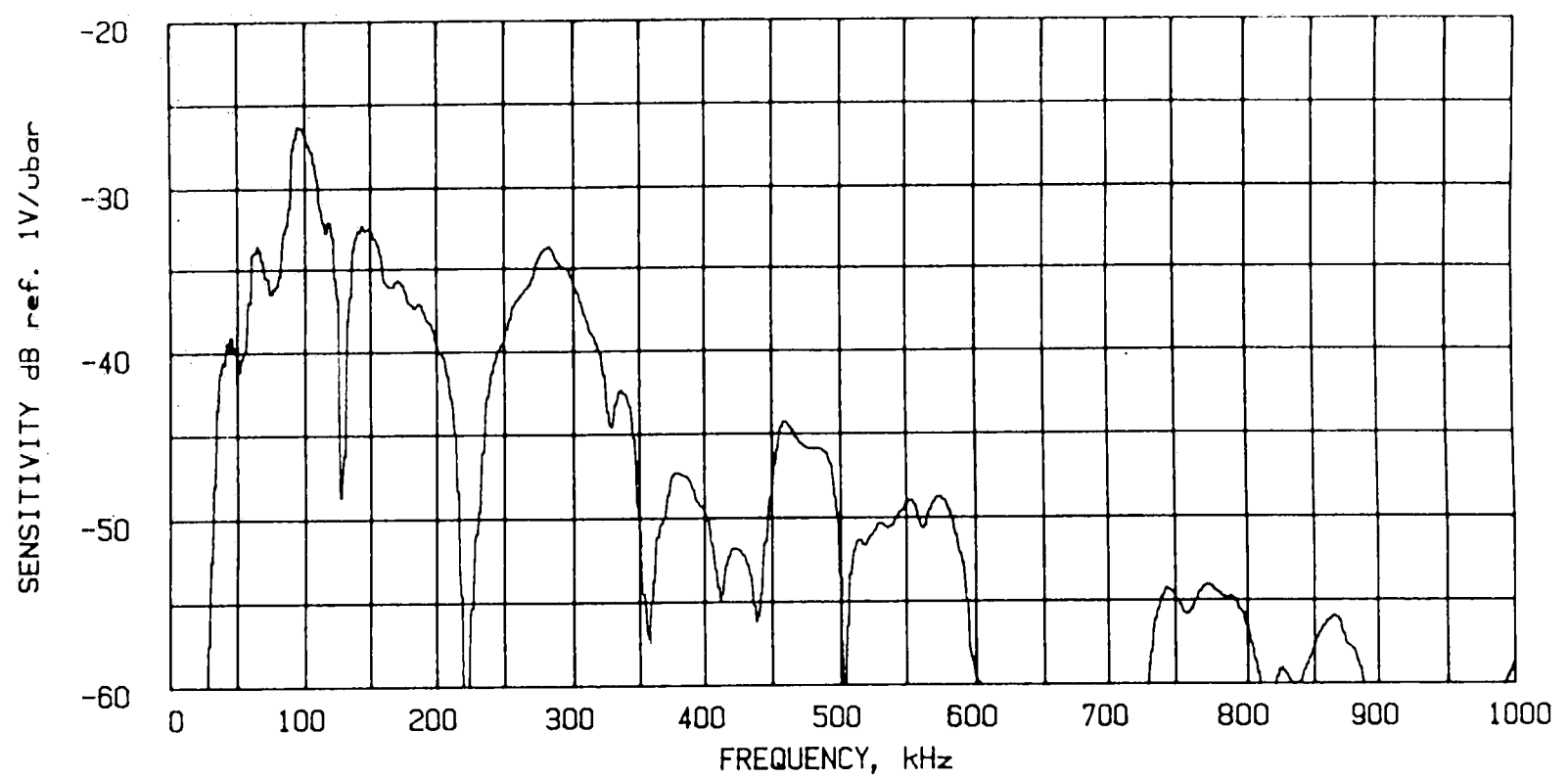


Figure 5. A Typical Frequency Response Plot for R6 and R6I Sensors.

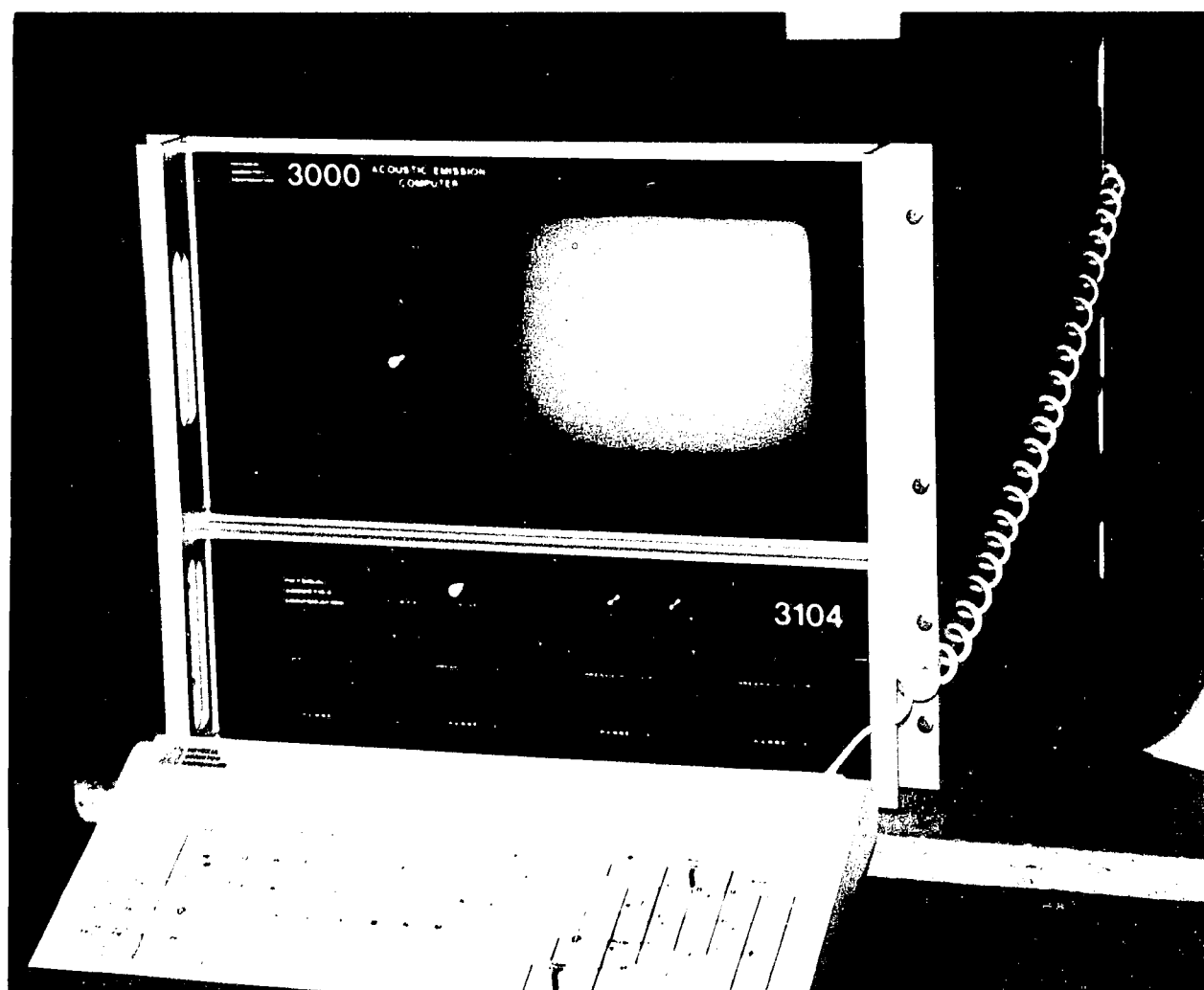


Figure 6. Physical Acoustic's 3000 Processor with a 3104 Amplifier.

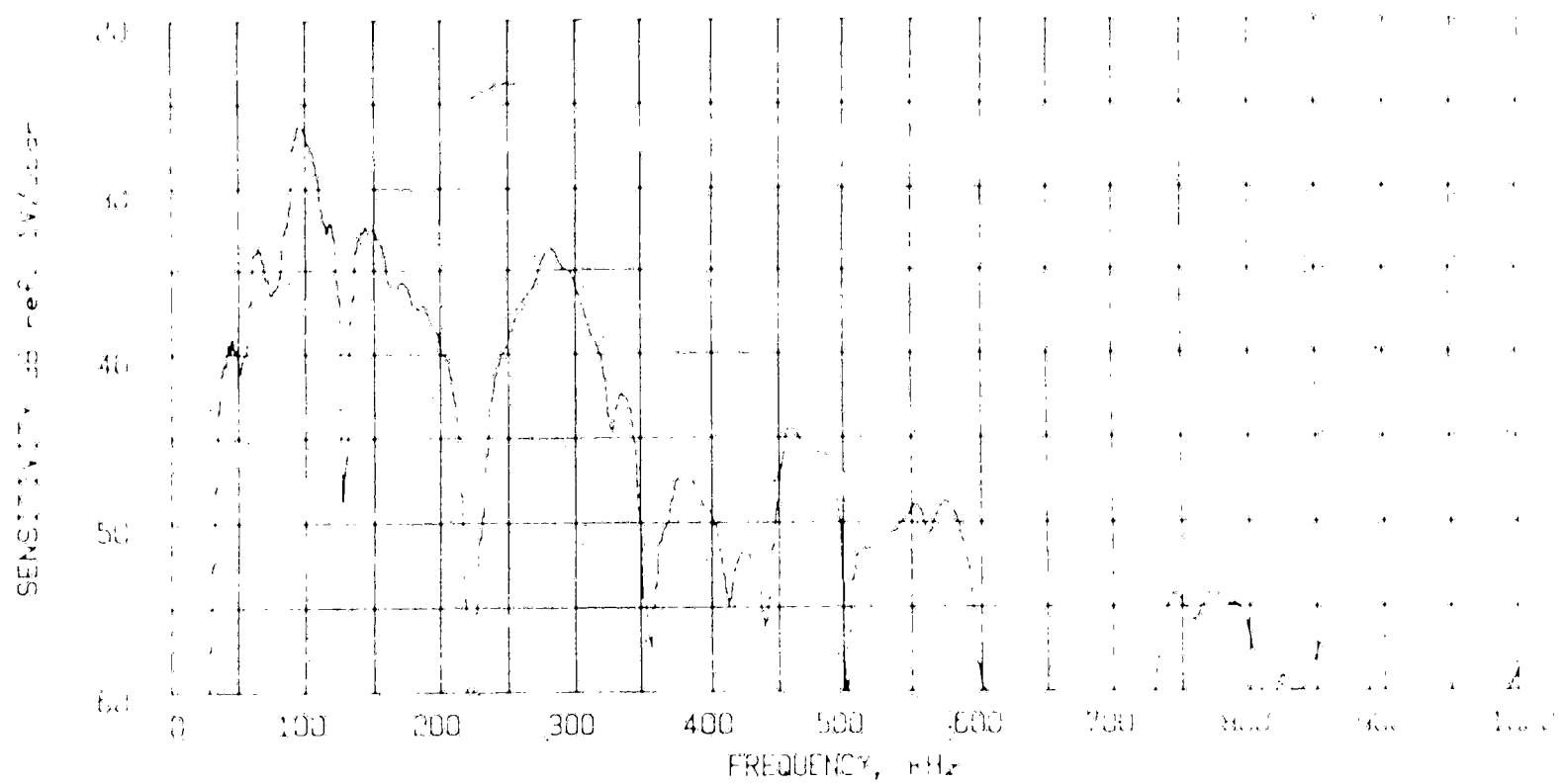


Figure 5. A Typical Frequency Response Plot for R6 and R6I Sensors.

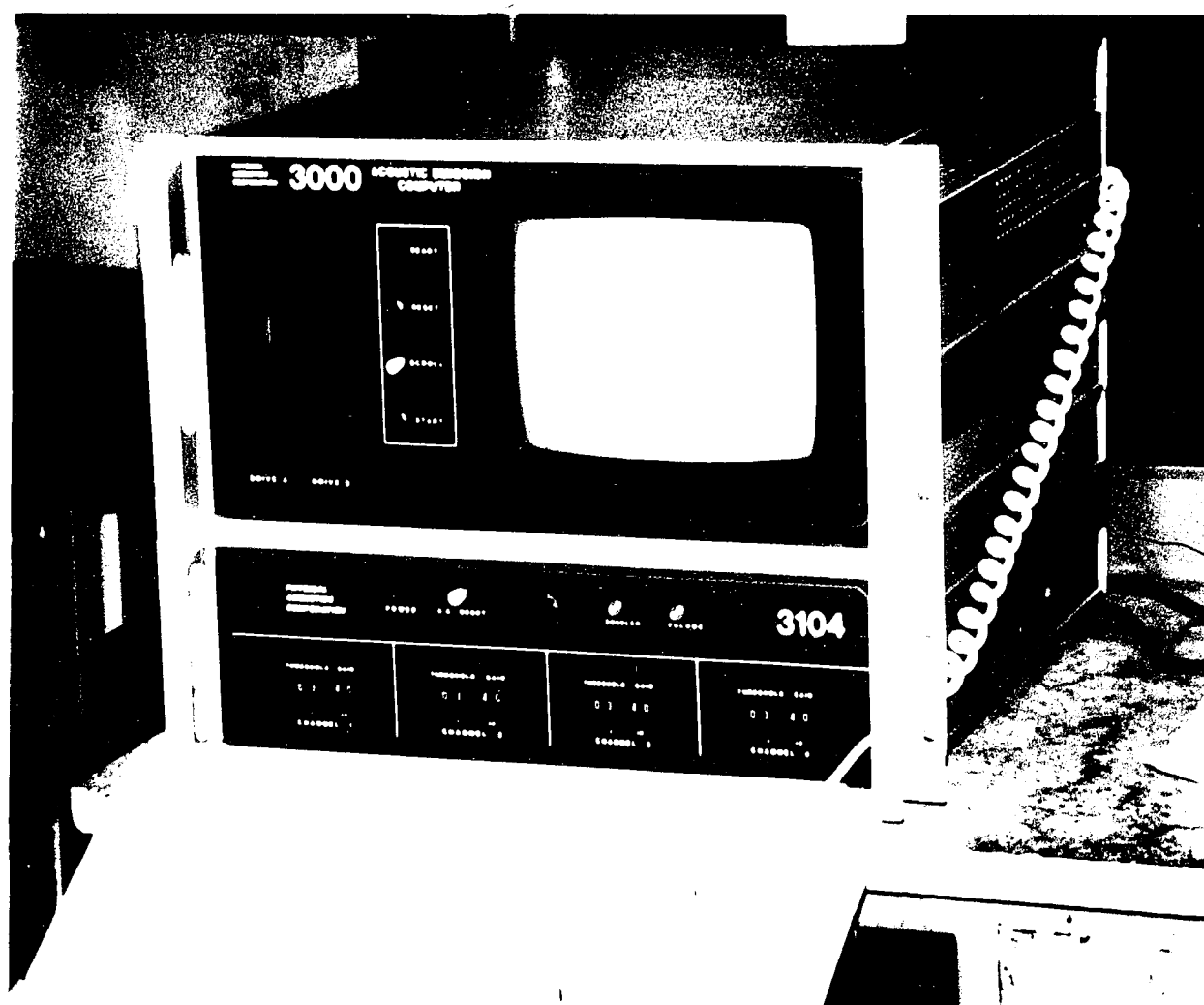


Figure 6. Physical Acoustic's 3000 Processor with a 3104 Amplifier.



Figure 7. Stub Column P1-SC Being Compressed in a 34.5 GPa Capacity Universal Testing Apparatus (Baldwin)

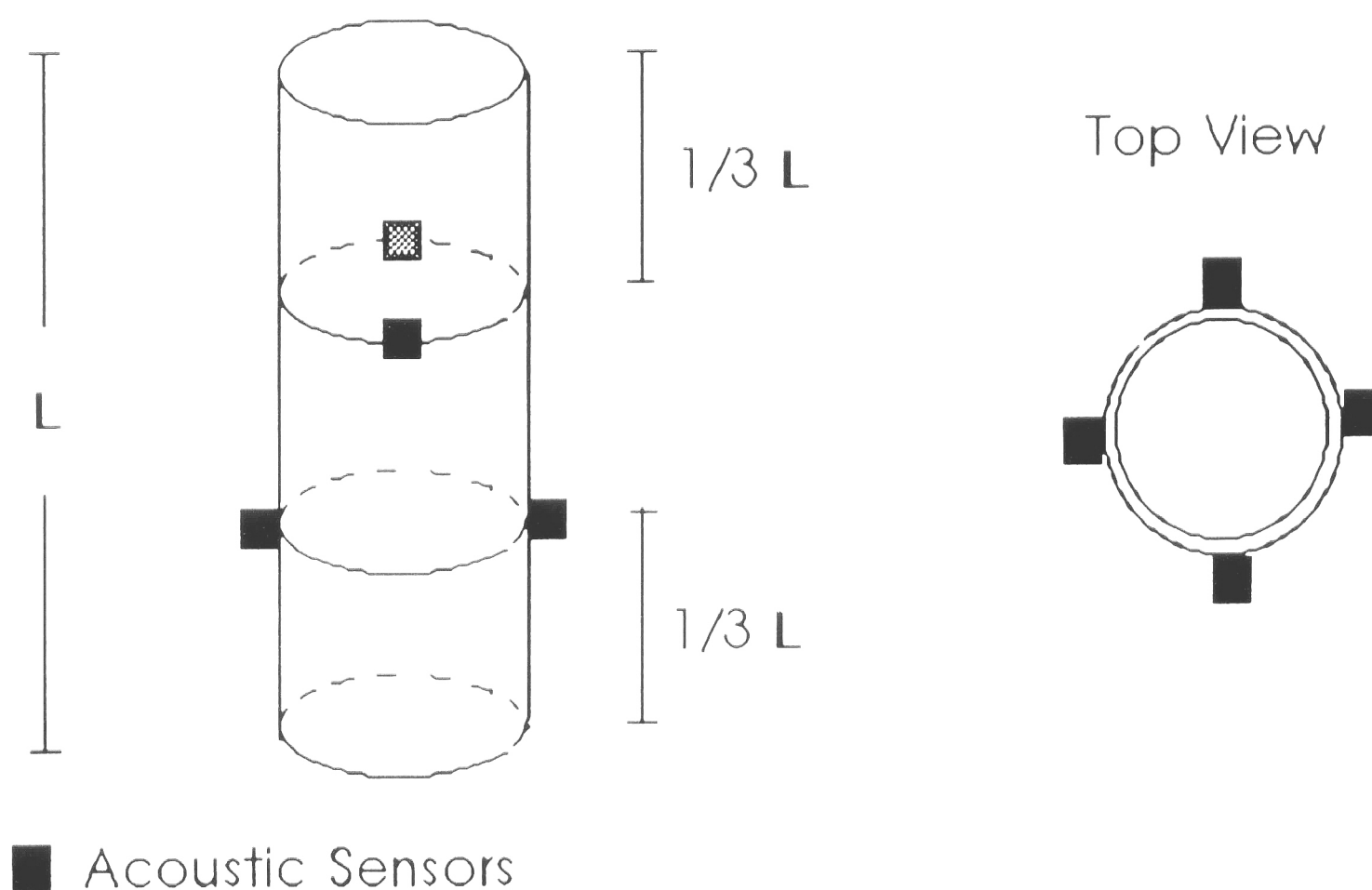


Figure 8. Schematic of A Stub Column Showing The Location of AE Sensors.

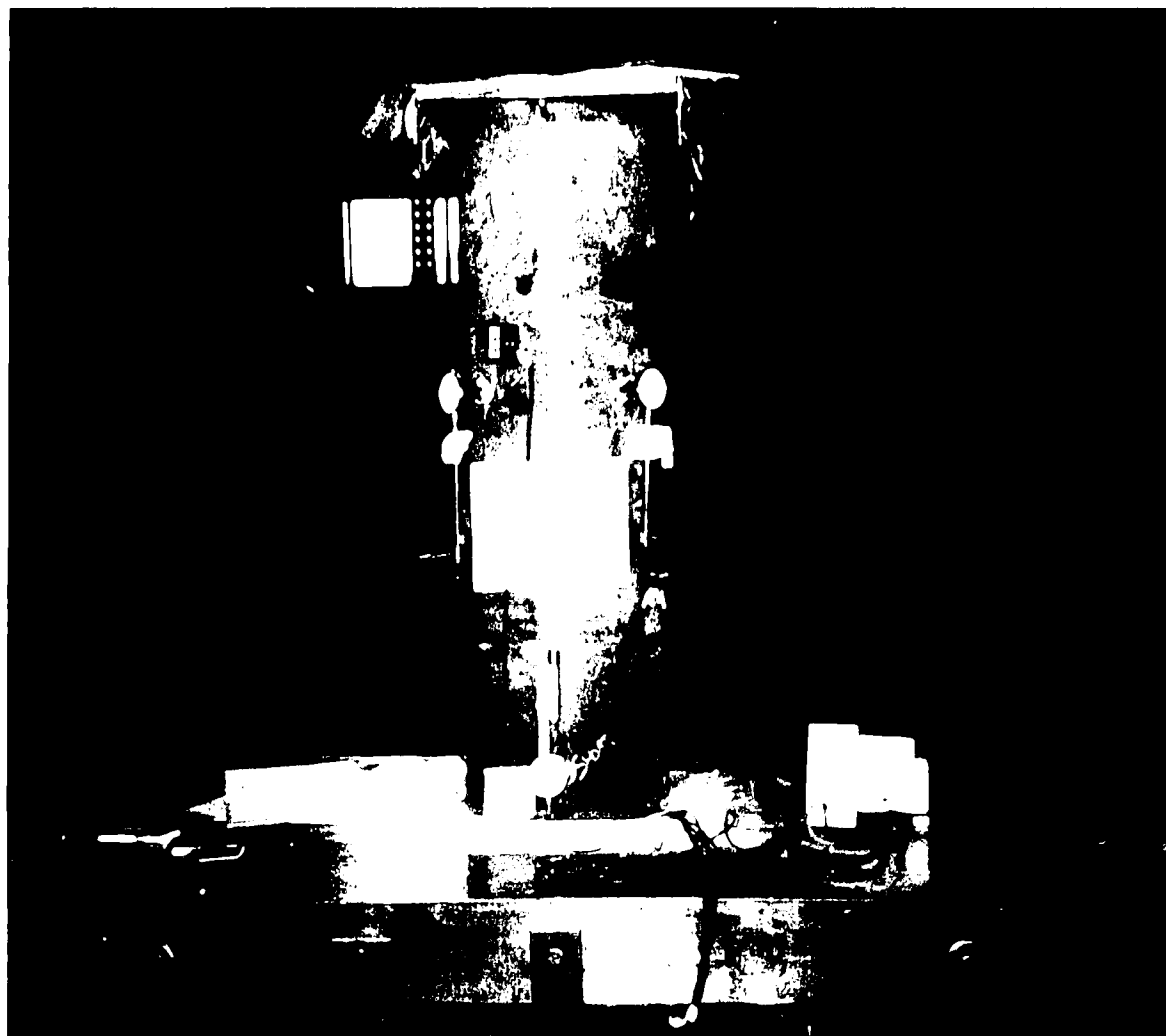


Figure 7. Stub Column P1-SC Being Compressed in a 34.5 GPa Capacity Universal Testing Apparatus (Baldwin)

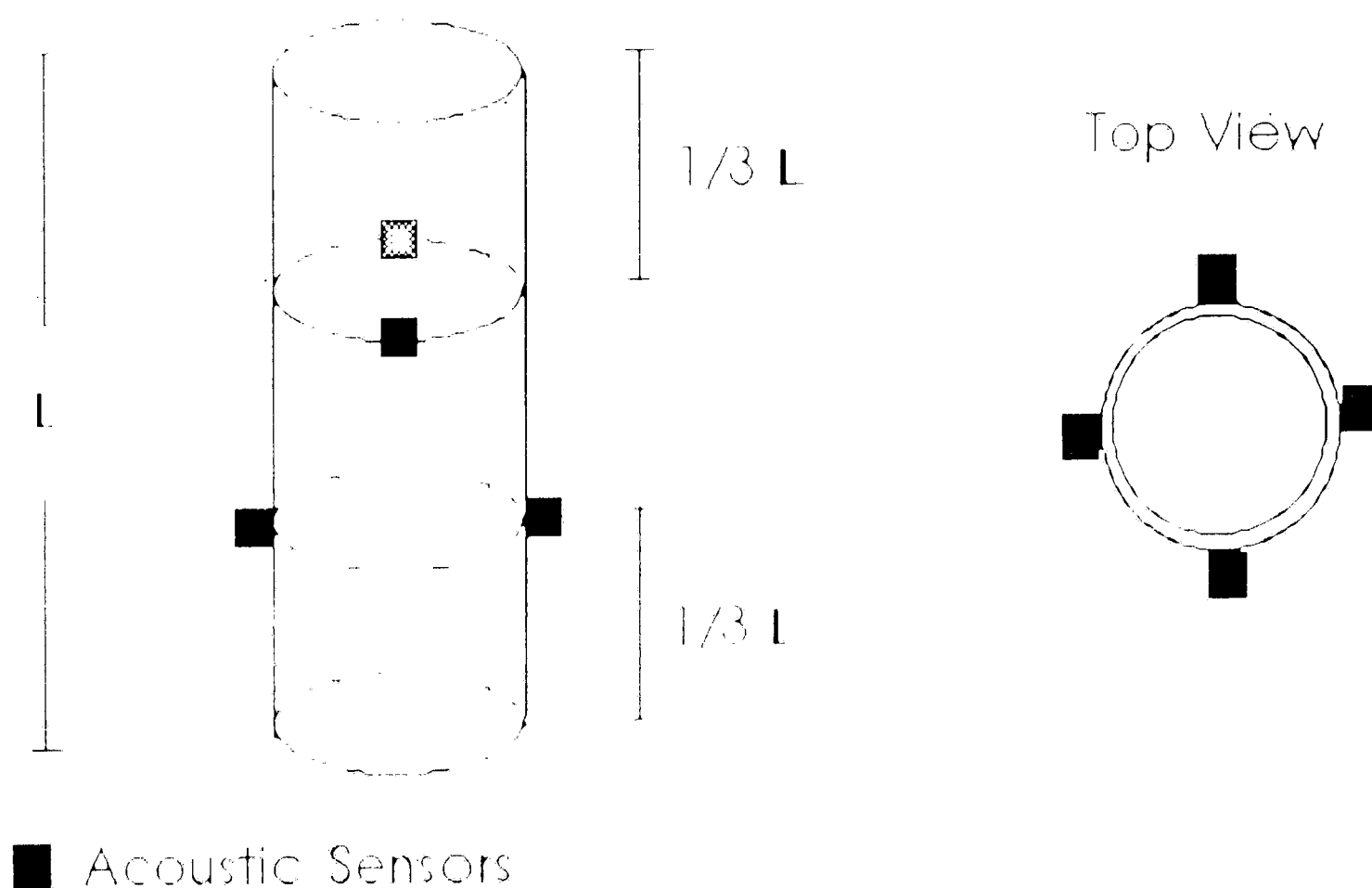


Figure 8. Schematic of A Stub Column Showing The Location of AE Sensors.

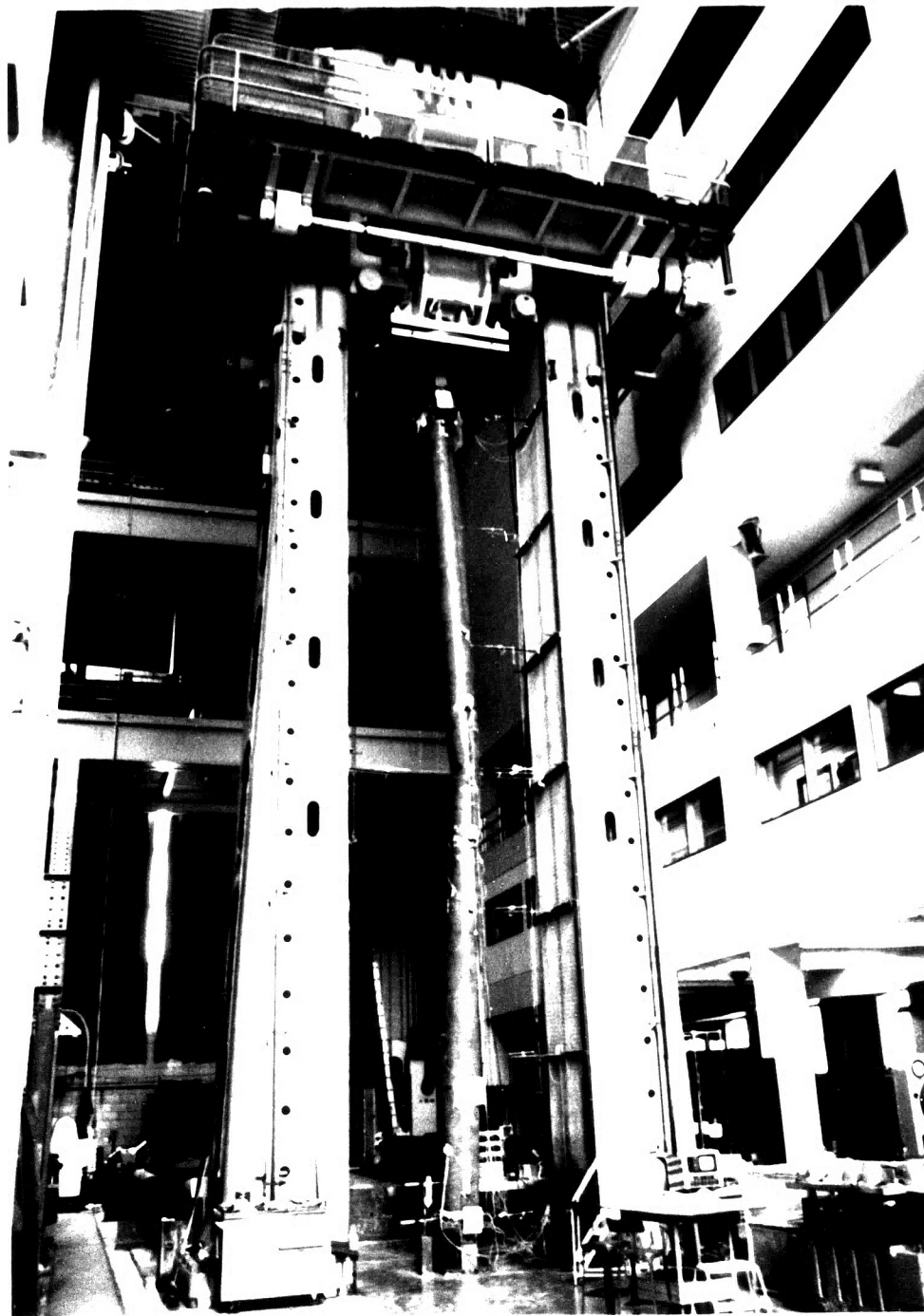


Figure 9. Long Column P2-LC Under Compression In A 34.5 GPa Capacity Baldwin.

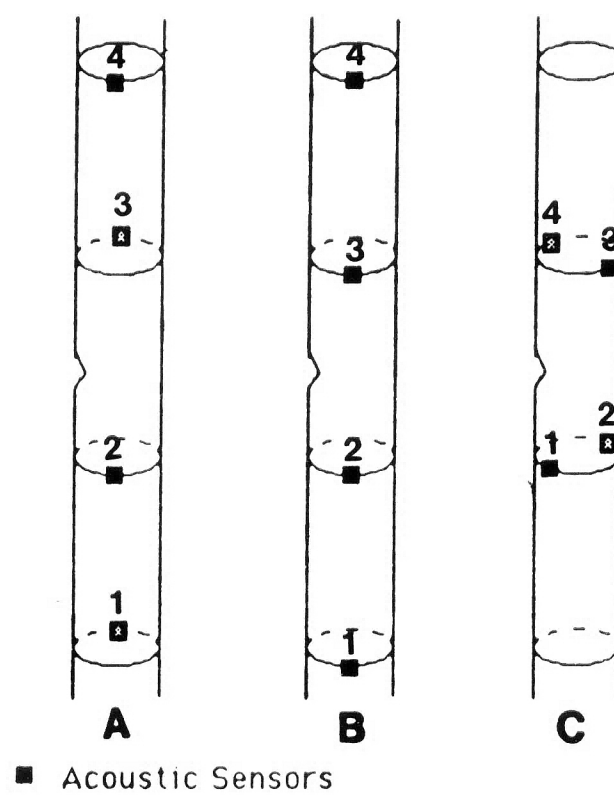


Figure 10. Three AE Sensor Arrays Used For Long Column Tests.

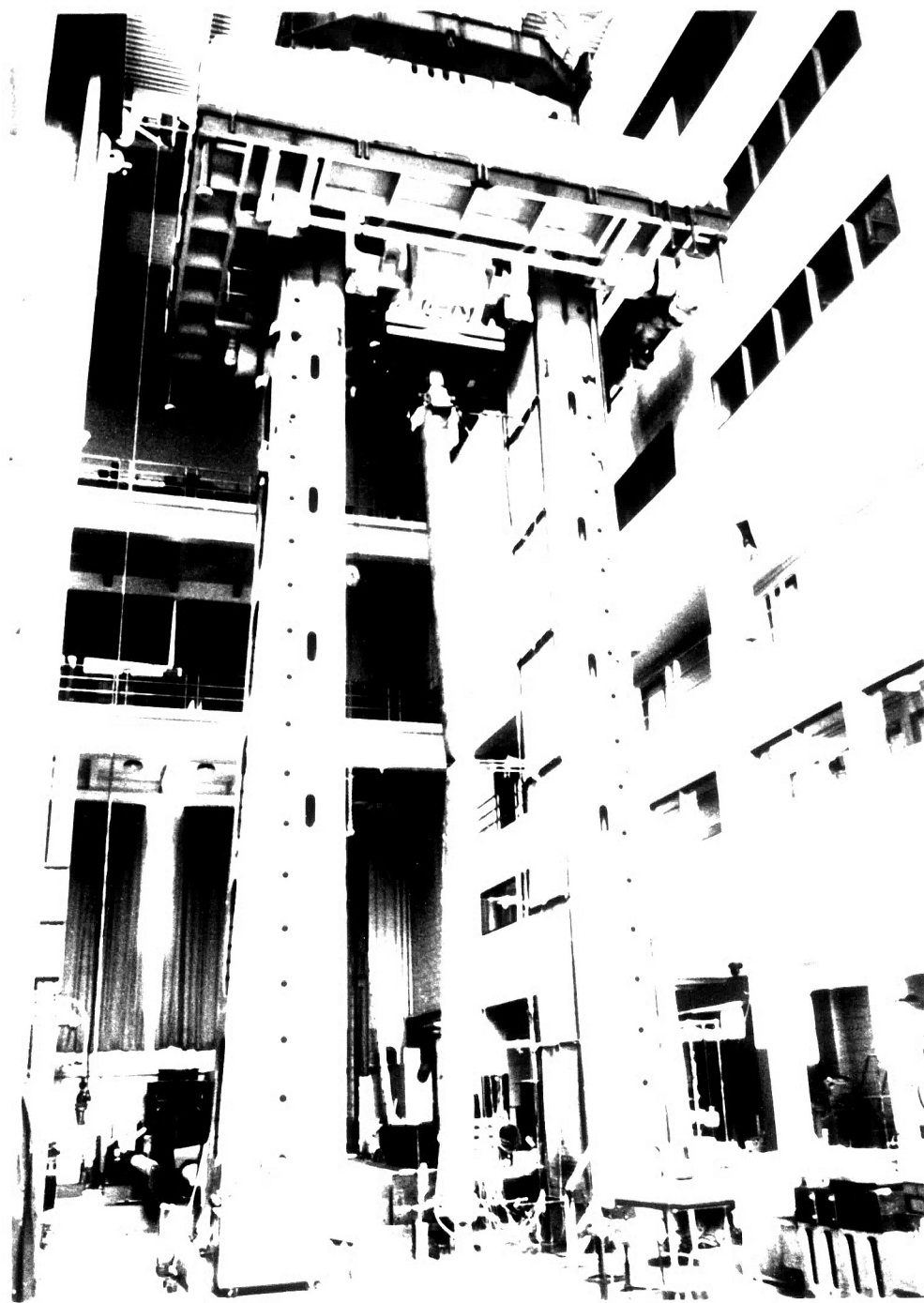


Figure 9. Long Column P2-LC Under Compression In A 34.5 GPa Capacity Baldwin.

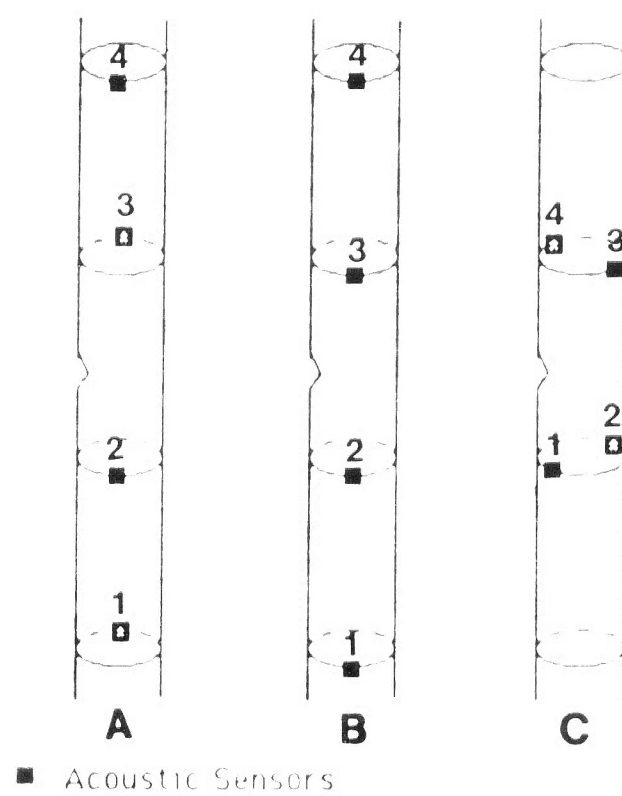


Figure 10. Three AE Sensor Arrays Used For Long Column Tests.

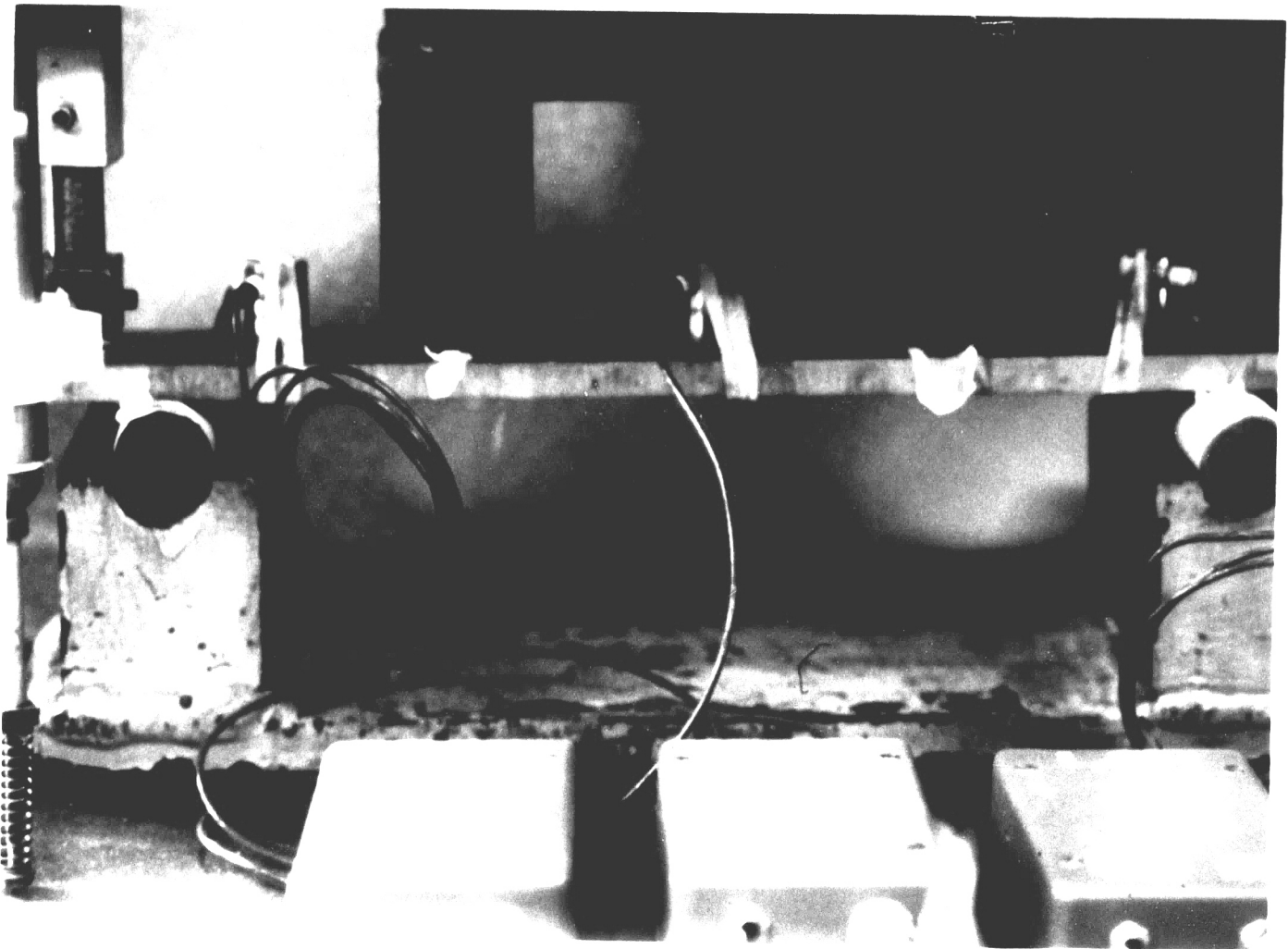


Figure 11a. Four Point Bending Set-up. The acoustic sensors were connected to the specimen with elastic bands.

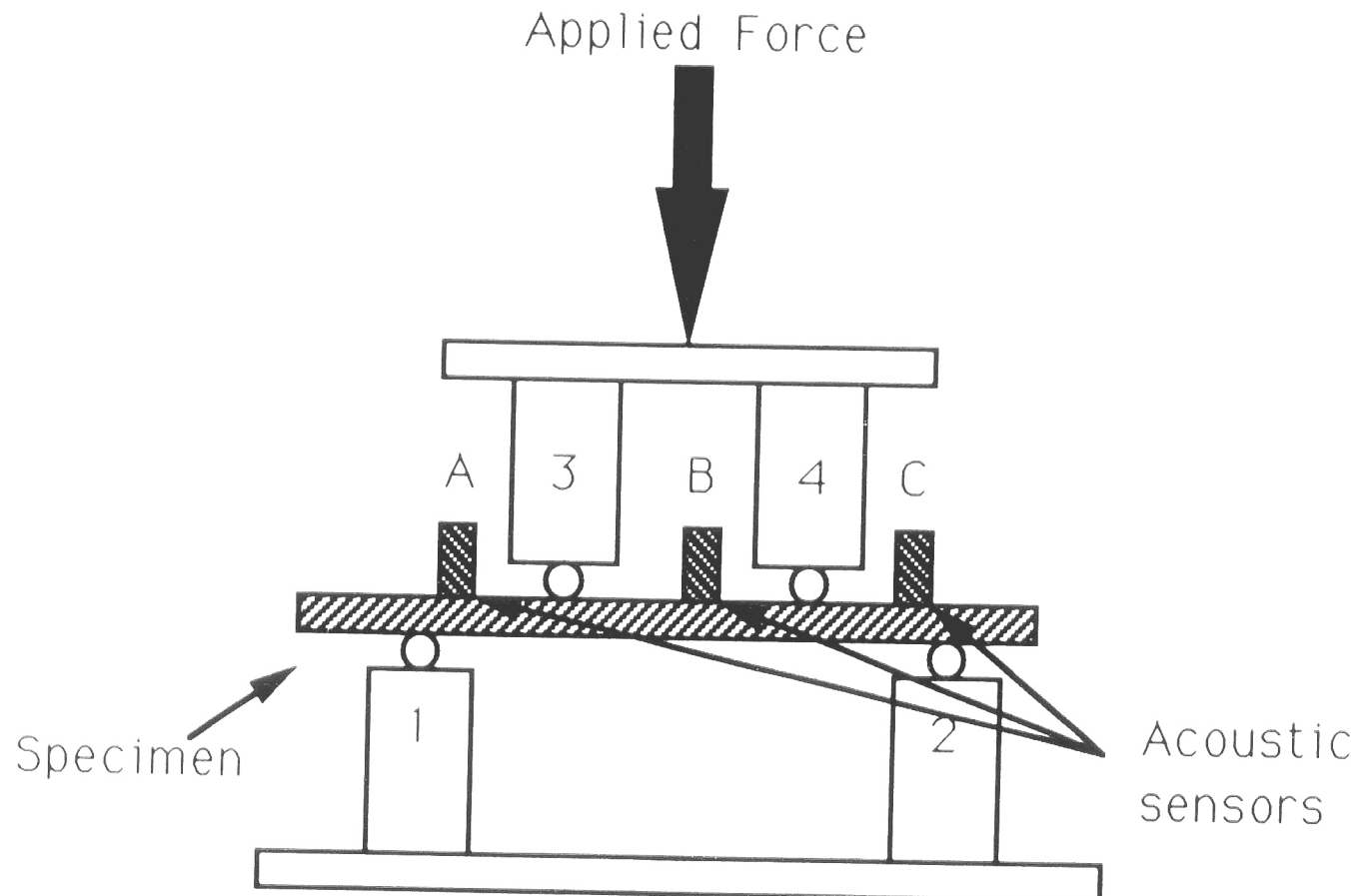


Figure 11b. Schematic of The Above Four Point Bend Set-up. Sensors A and C were guard sensors that ensured that noise from loading pins 1,2,3, and 4 was not recorded. Sensor B recorded the relevant AE.

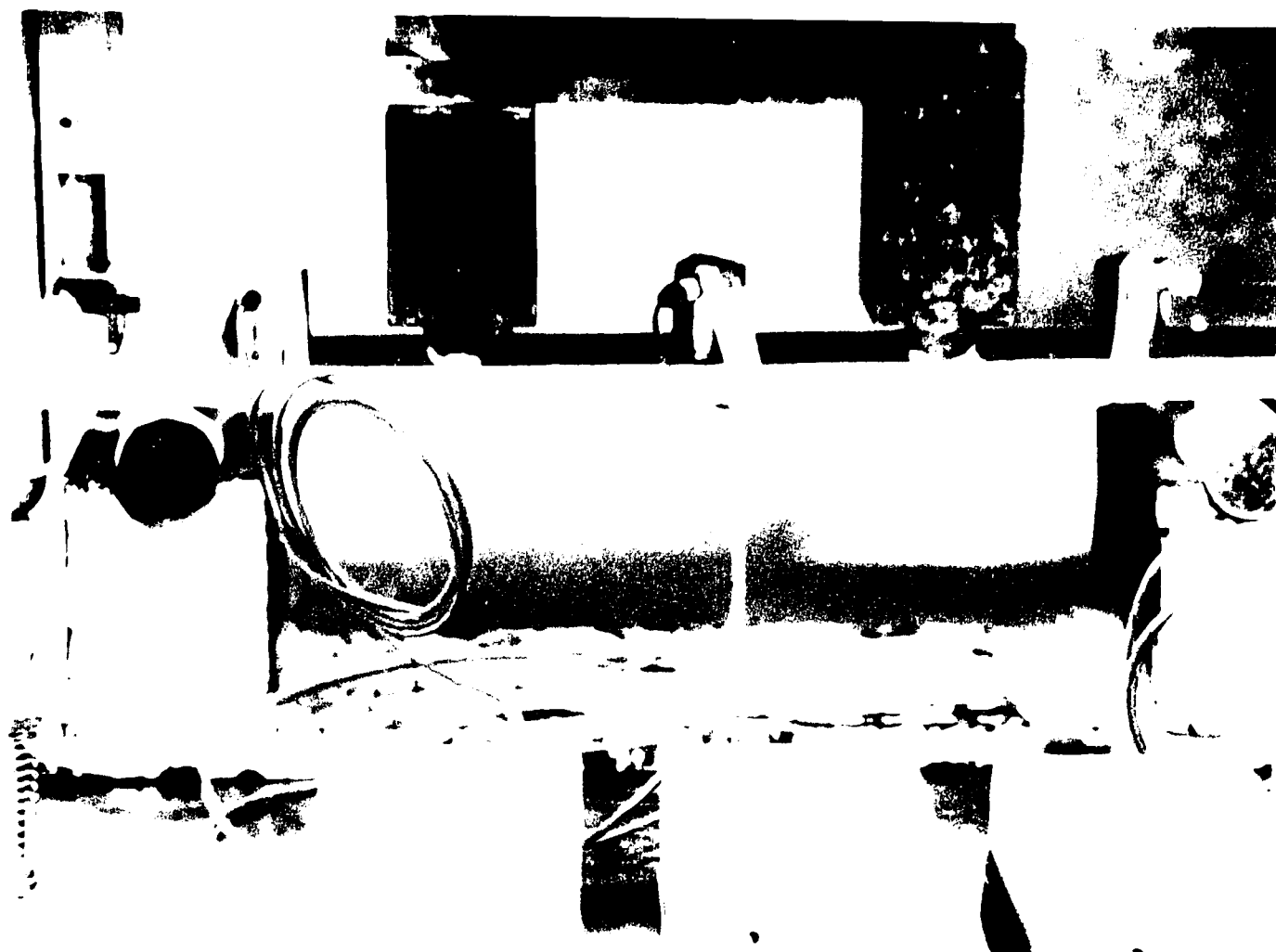


Figure 11a. Four Point Bending Set-up. The acoustic sensors were connected to the specimen with elastic bands.

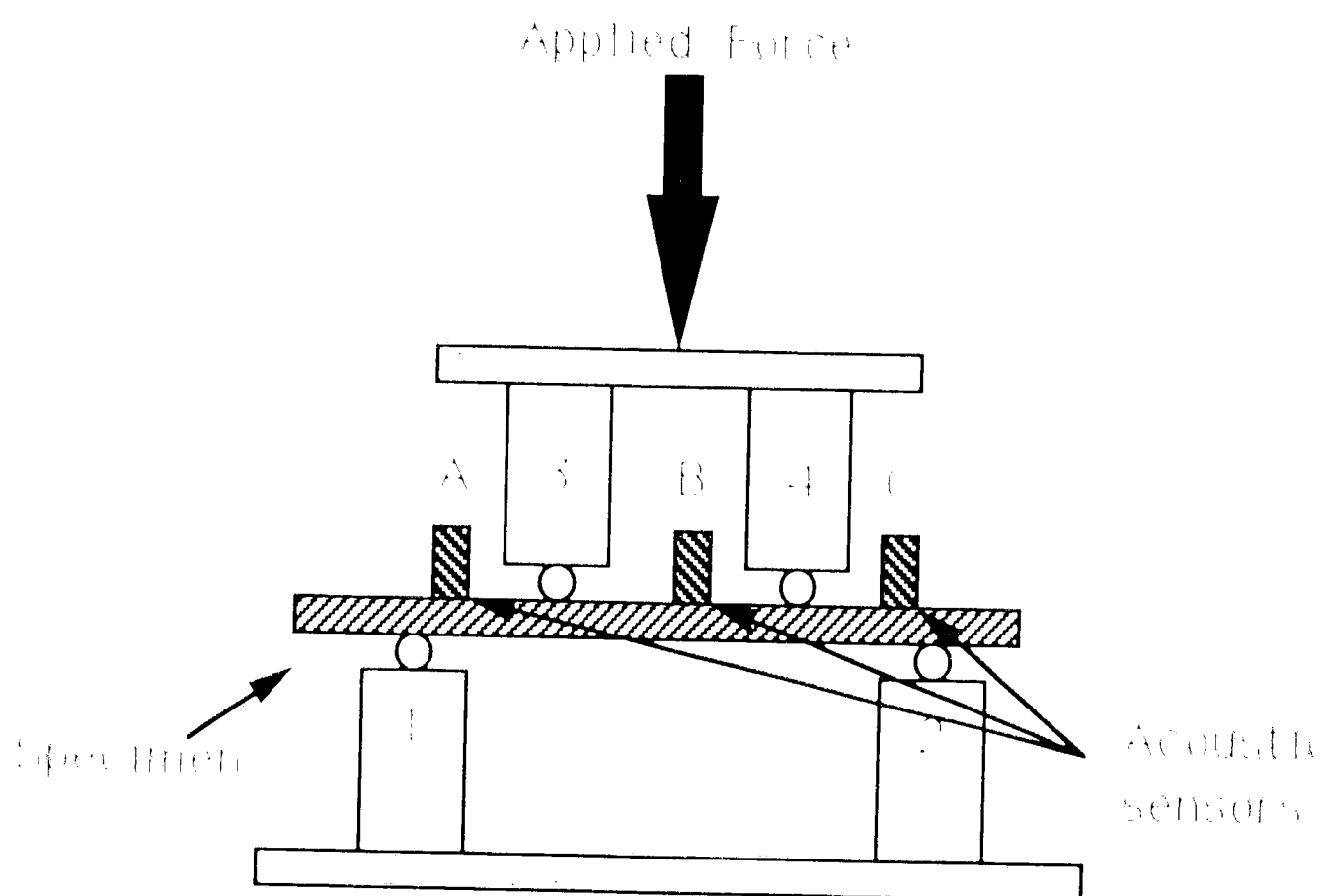


Figure 11b. Schematic of The Above Four Point Bend Set-up. Sensors A and C were guard sensors that ensured that noise from loading pins 1, 2, 3, and 4 was not recorded. Sensor B recorded the relevant AE.

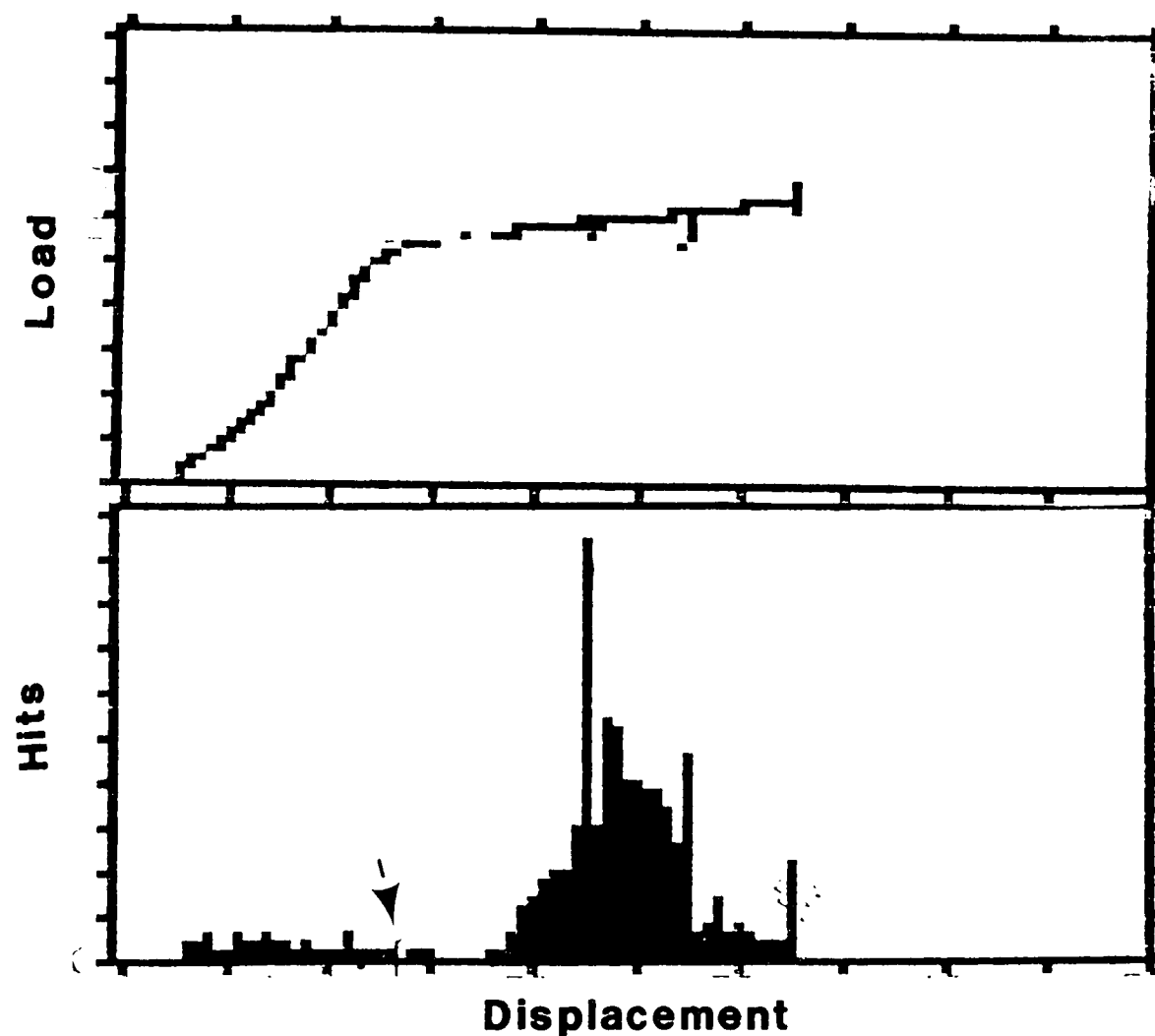


Figure 12. AE Data Generated From A Tensile Coupon Frabricated From AN ASTM A36 Steel Plate. The top diagram represents load vs. displacement while the bottom figure is total number of hits (histogram) vs. displacement. Note, at the yield point, denoted by arrows, there is not a significant increase in hits. (Sensitivity 80dB)

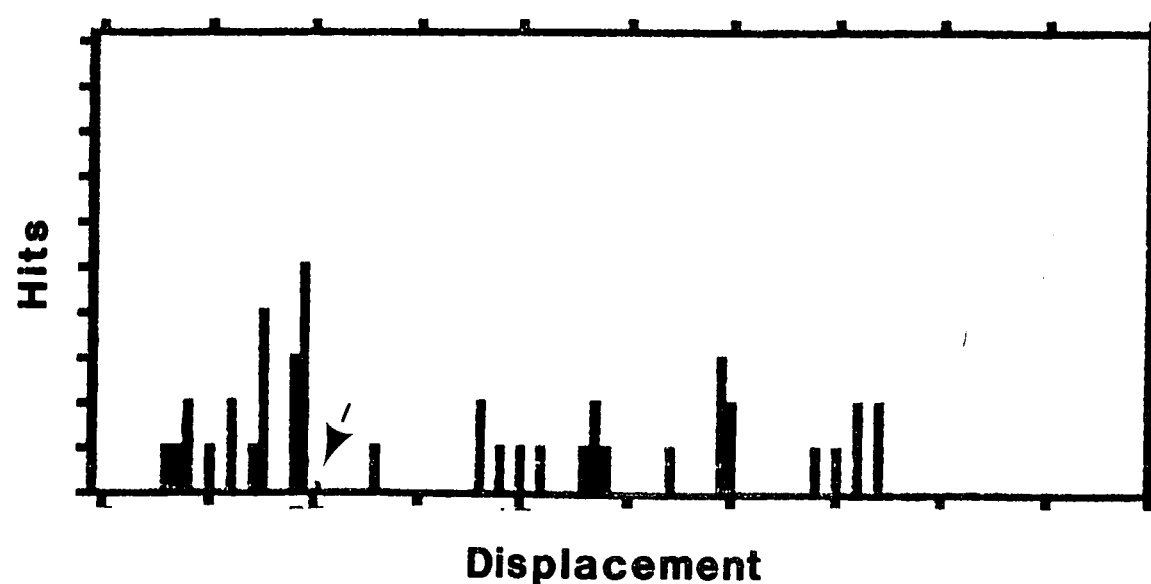


Figure 13. Tensile Specimen Fabricated From A Salvaged Column With All Oxide Layers Removed Prior To Testing. The yield point is denoted by an arrow. Note that there is a lack of emission at that point. (Sensitivity 50dB.)

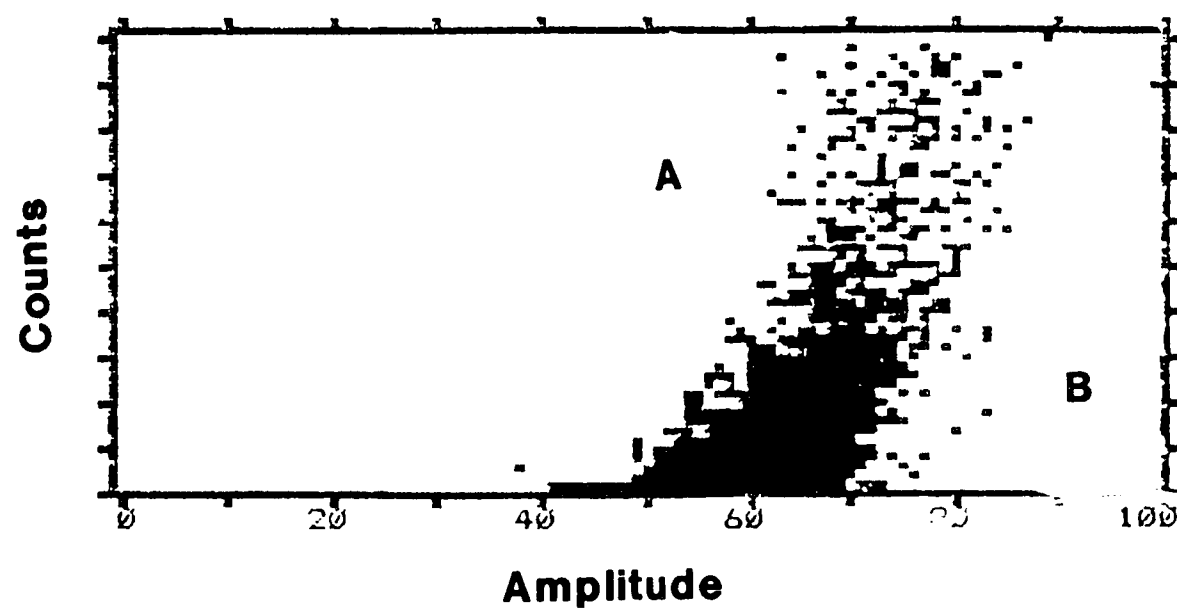


Figure 14. A Representative Correlation Plot Showing That Mechanical Noise (A) And EMI Noise (B) Were Not Recorded. A cluster of hits at these locations would indicate the presence of recorded noise.

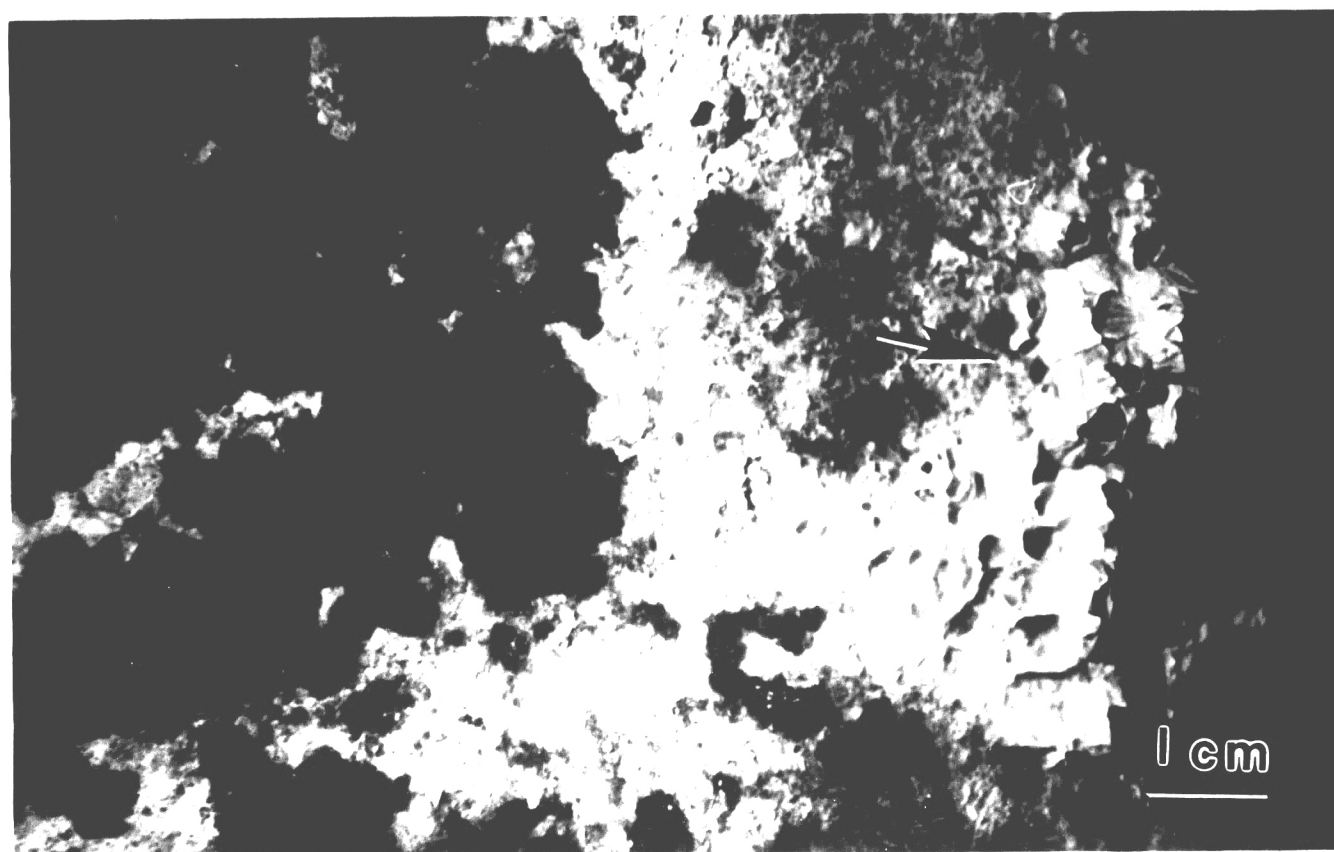


Figure 15. Surface Condition of A Salvaged Column (E1). Arrow points to the marine growth.

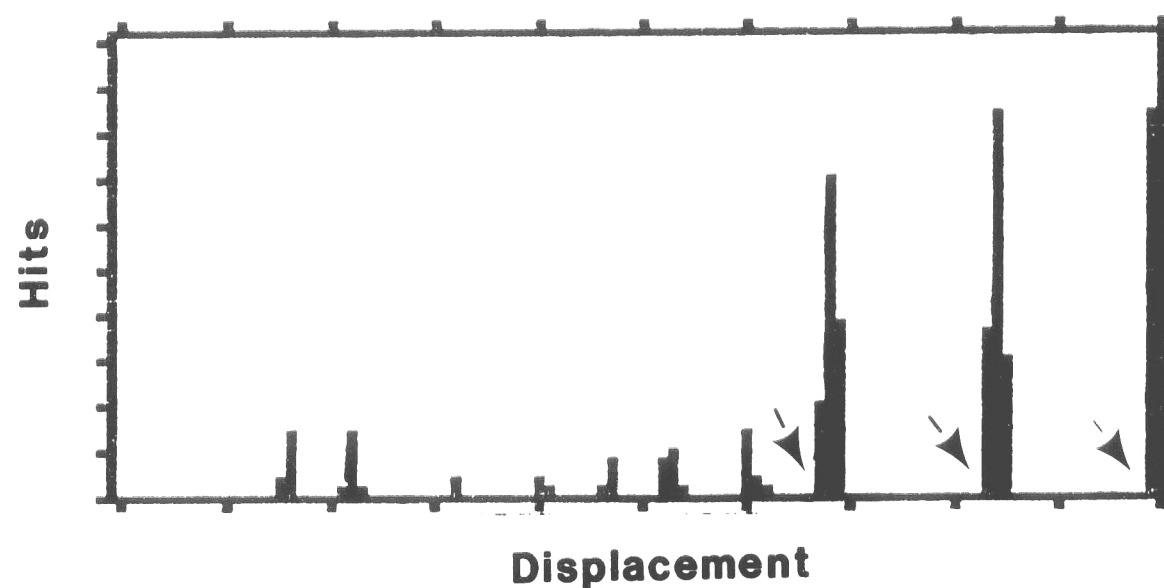


Figure 16. AE Data Generated From Stub Column E1-SC. Note the increase of emissions at each yield point. The onset of yielding is denoted by the arrows. (Sensitivity 45dB)

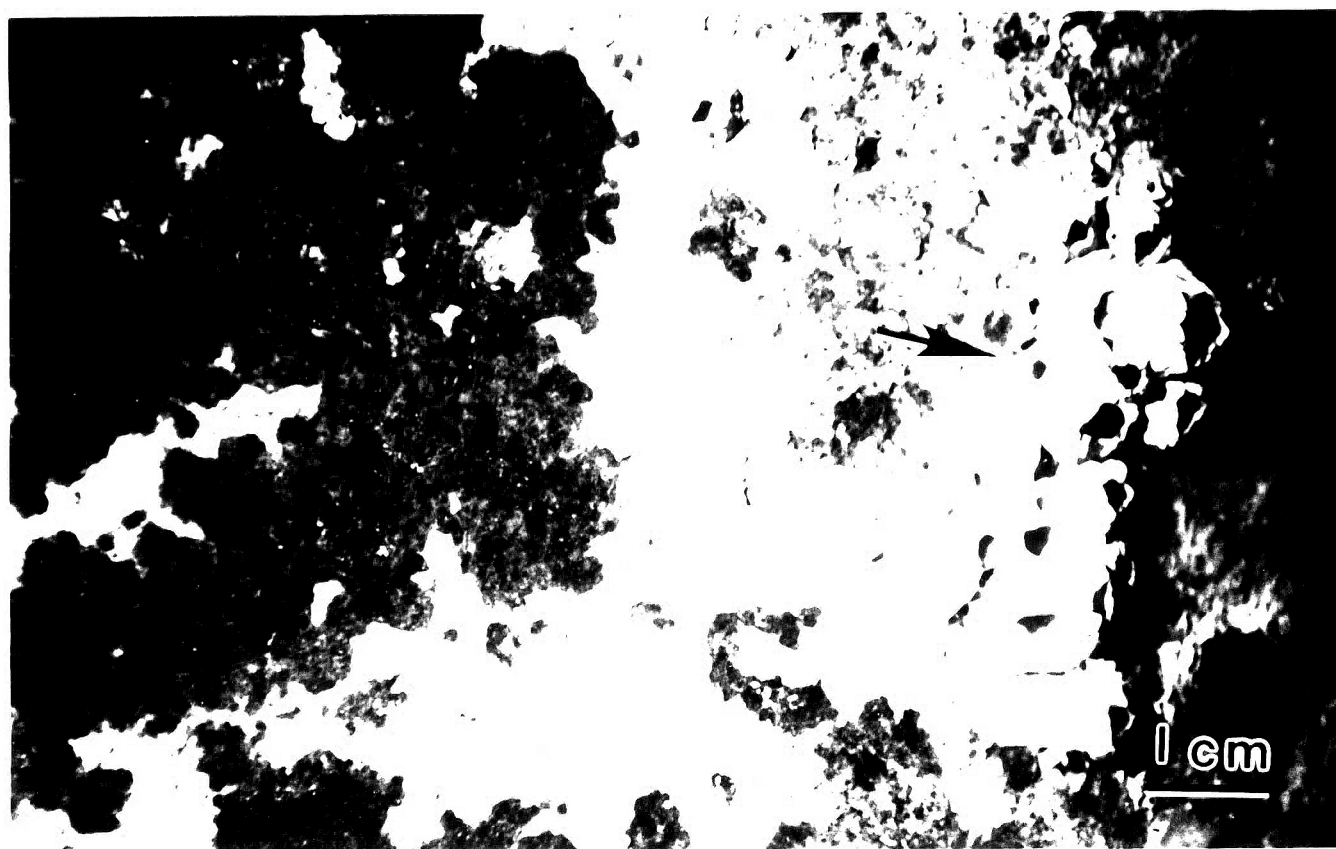


Figure 15. Surface Condition of A Salvaged Column (E1). Arrow points to the marine growth.

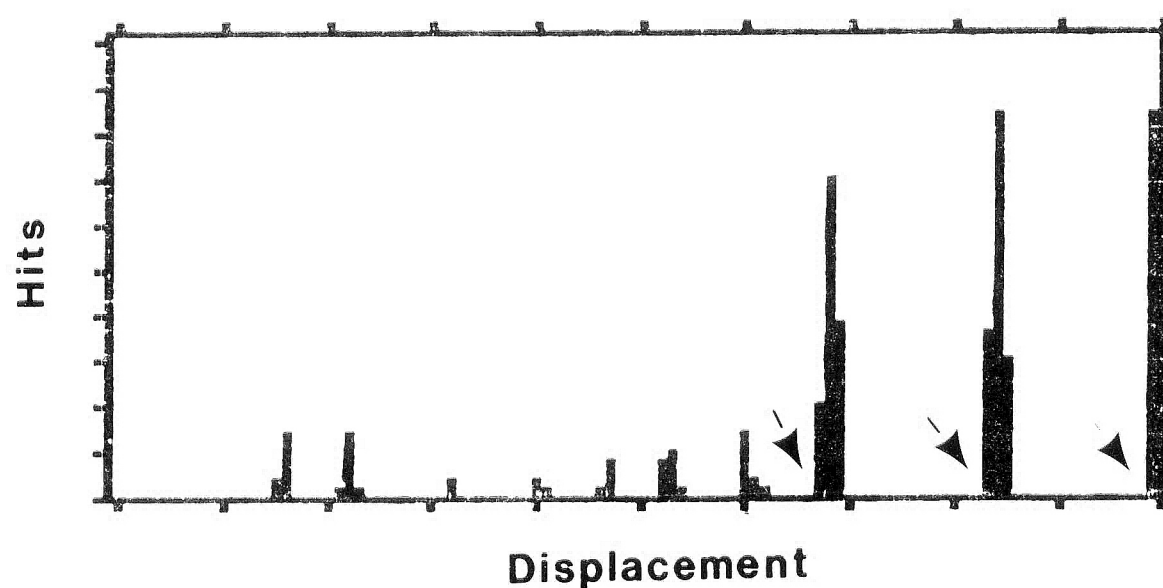


Figure 16. AE Data Generated From Stub Column E1-SC. Note the increase of emissions at each yield point. The onset of yielding is denoted by the arrows. (Sensitivity 45dB)

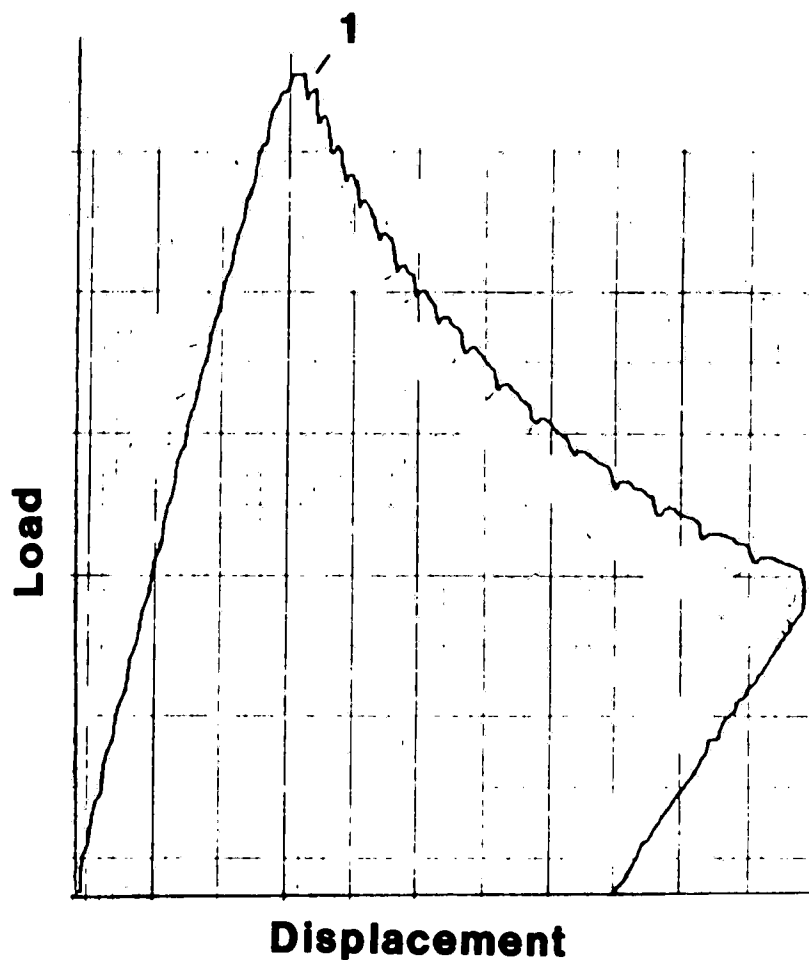


Figure 17. A Representative Load vs. Displacement Diagram For A Long Column. Note that at position 1, the load drops. This occurred when there was an intentional pause in the testing. There are 18 visible hold periods in this diagram.

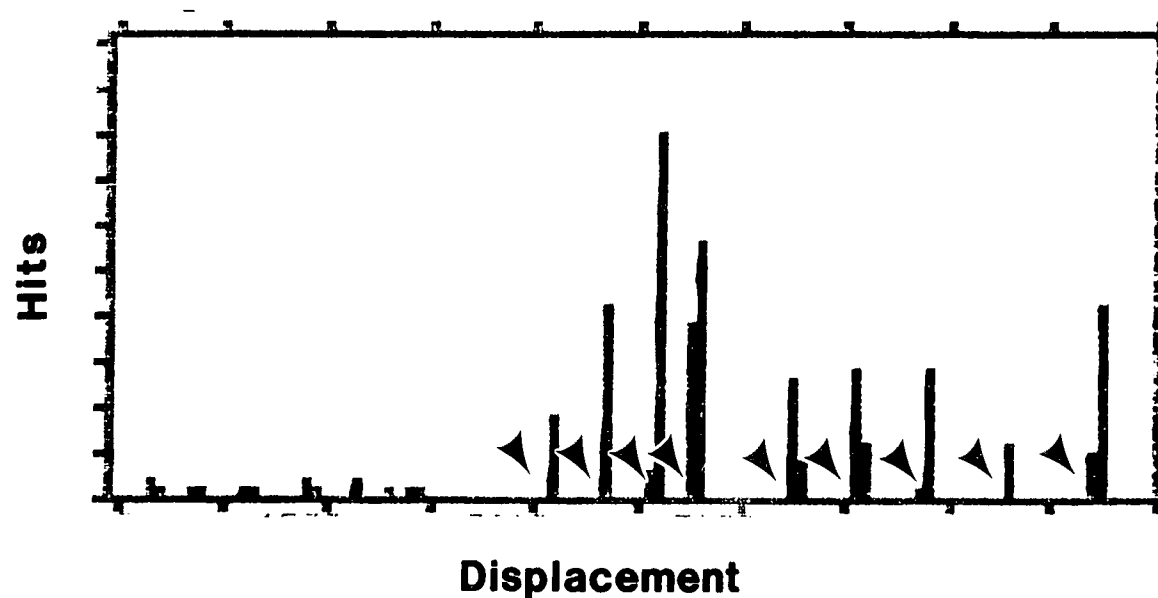


Figure 18. AE Data For Stub Column E3-SC. Note that there is an increase of hits at each yield point. The onset of yielding is denoted by the arrows. (Sensitivity 50dB)

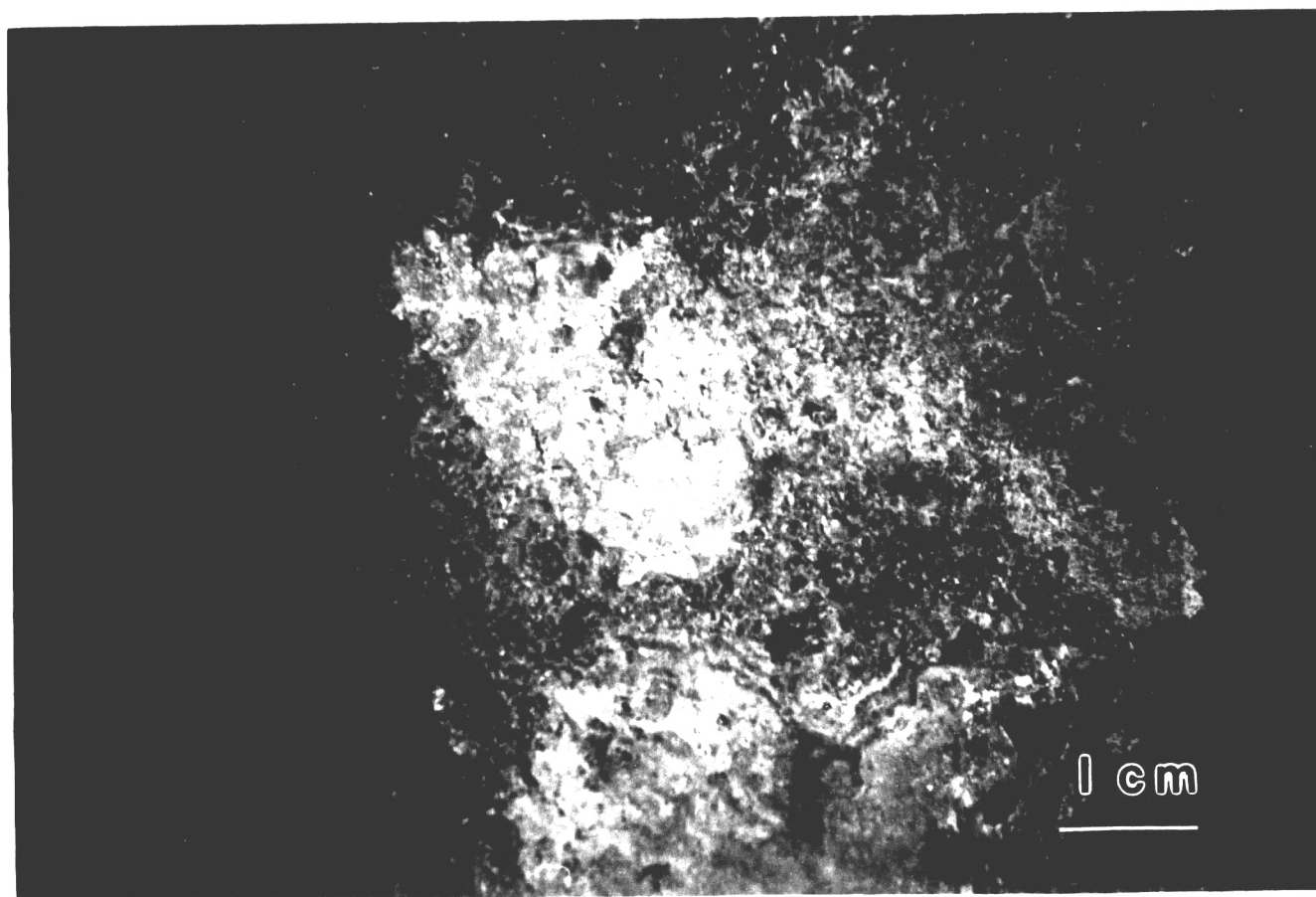


Figure 19. Surface Condition of Stub Column S2-SC. Note that general corrosion rather than localized corrosion occurred.

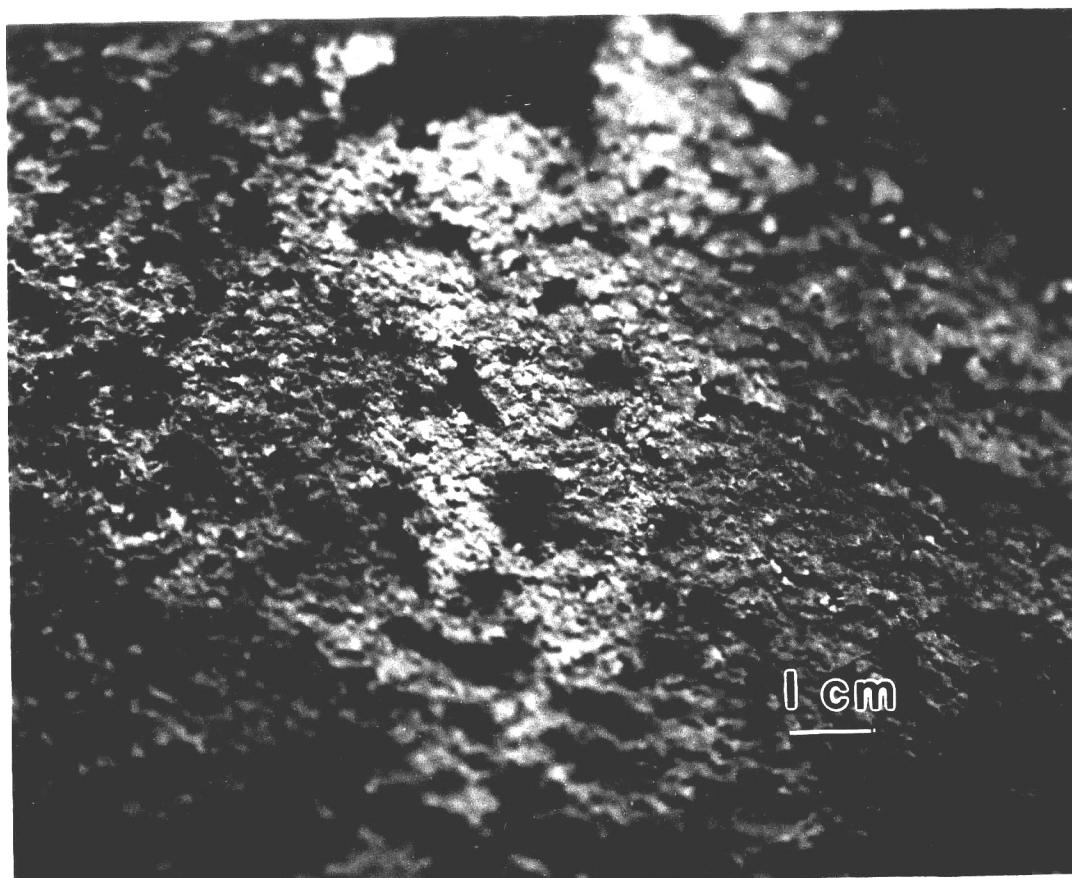


Figure 20. Surface Condition Inside Stub Column S2-SC. The light tan areas represent corrosion products while the darker areas indicate where spalling occurred.

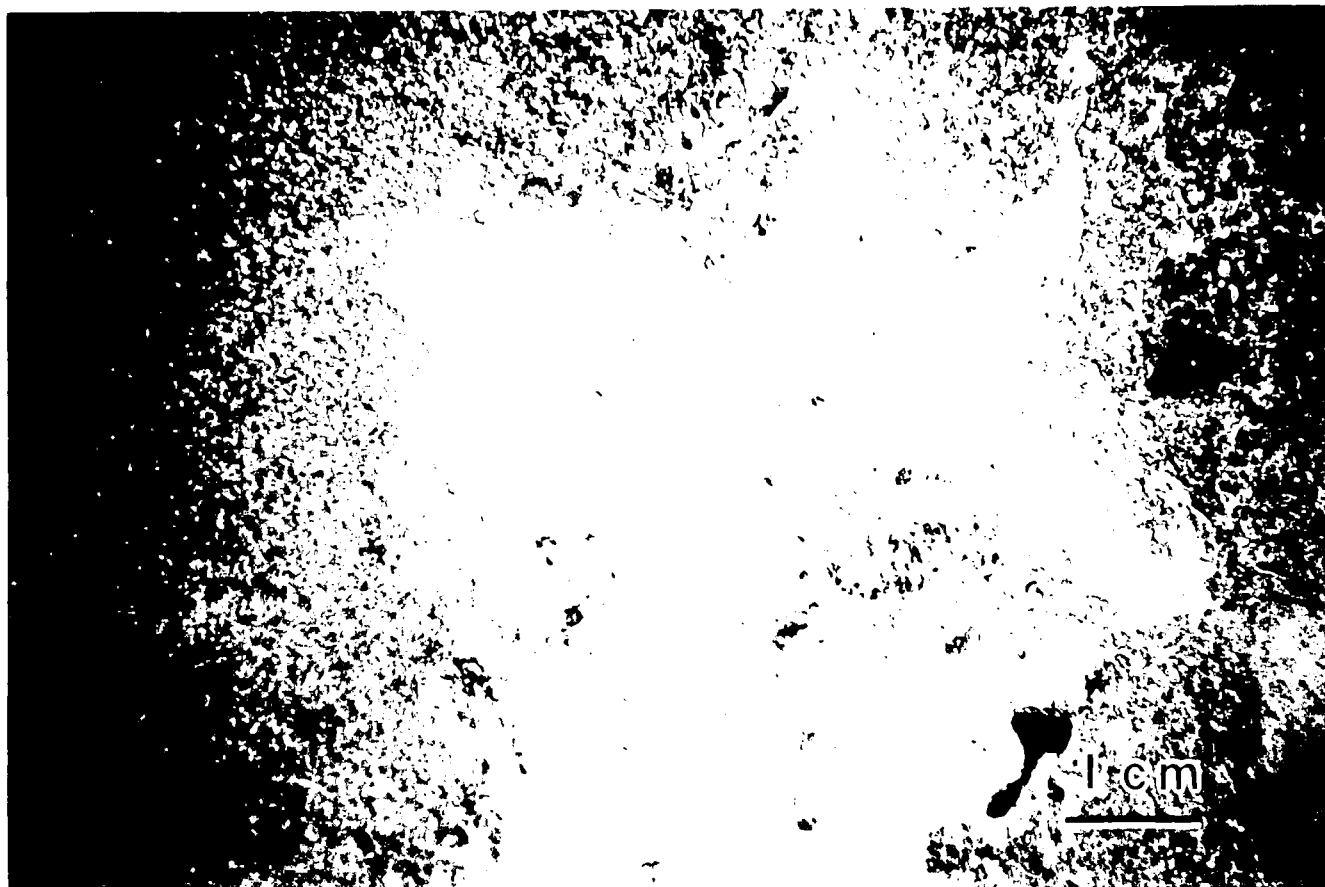


Figure 19. Surface Condition of Stub Column S2-SC. Note that general corrosion rather than localized corrosion occurred.

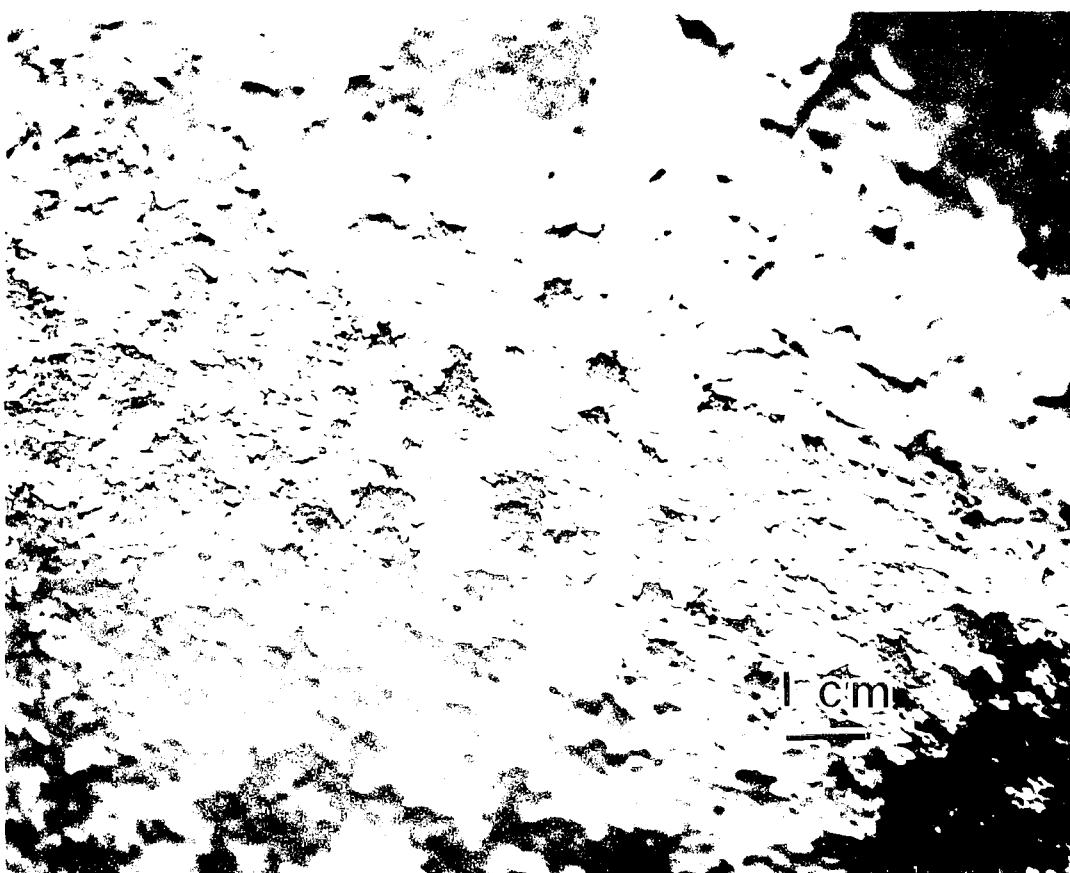


Figure 20. Surface Condition Inside Stub Column S2-SC. The light tan areas represent corrosion products while the darker areas indicate where spalling occurred.

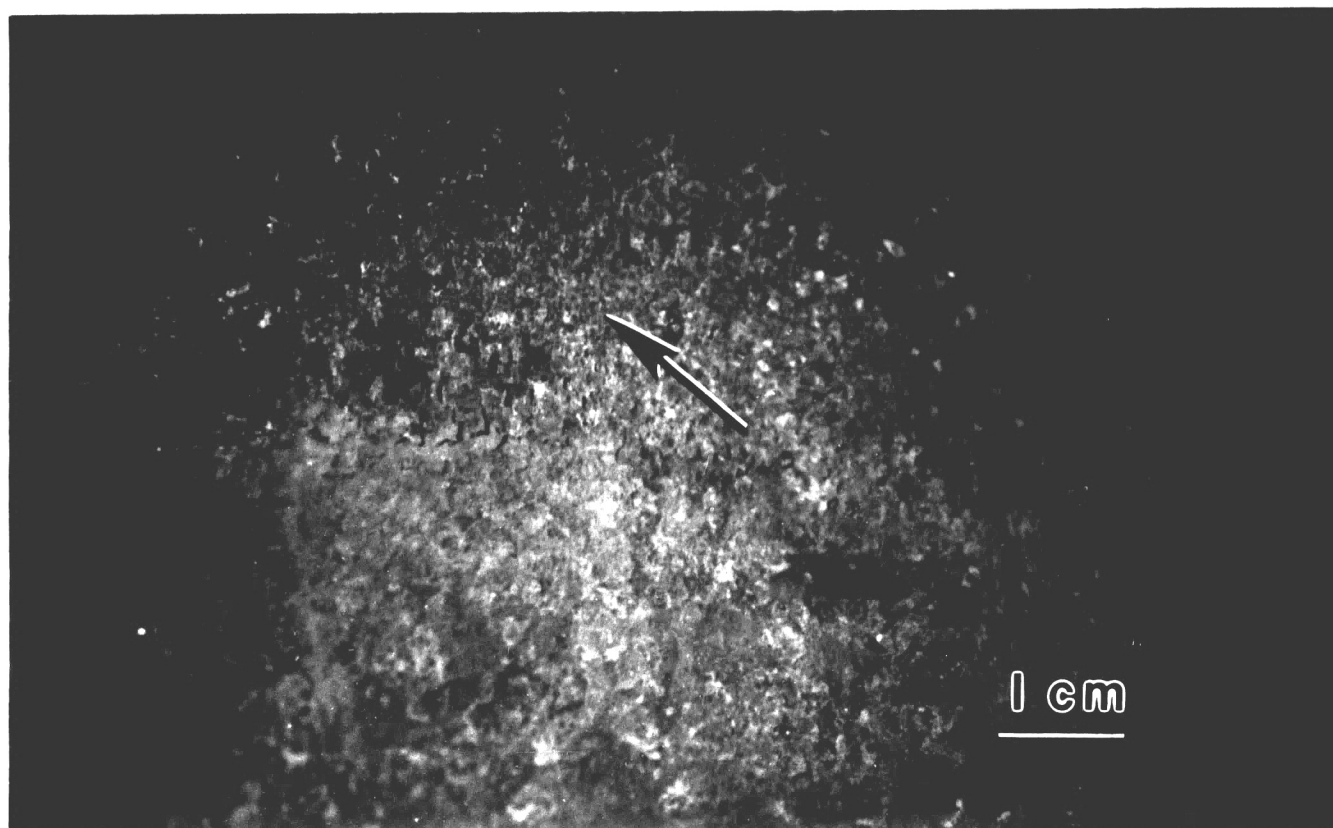


Figure 21. A Representative Photograph of The Surface Condition of The Fabricated Specimens. The arrow points to areas where spalling occurred.

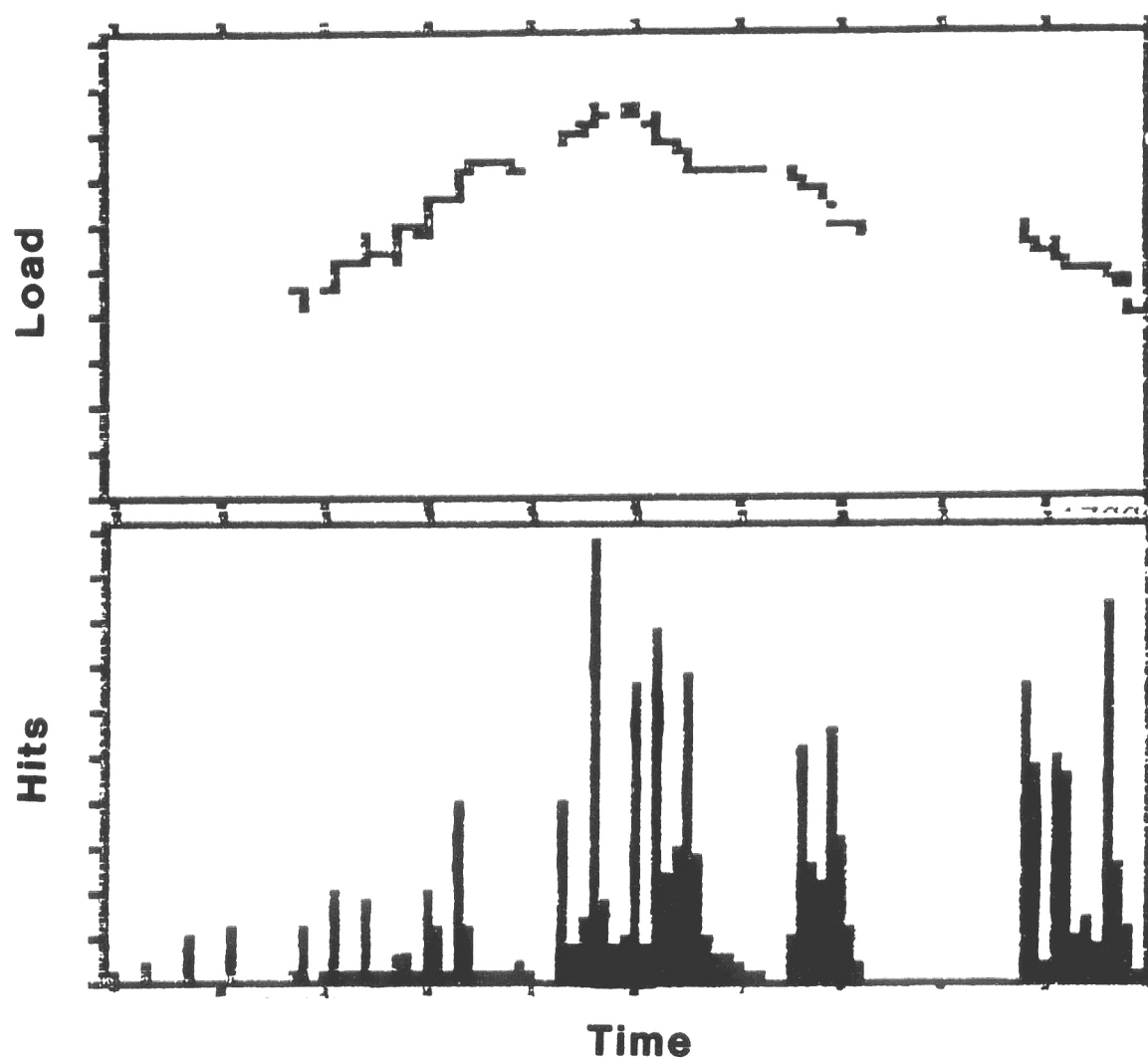


Figure 22. AE Data Generated From A Long Column (E1-LC). Top figure represents the loading history of the column. The maximum compression load is depicted by the highest point on this graph. Below is a histogram of the number of hits. Note that the greatest number of hits coincides with the maximum load.



Figure 21. A Representative Photograph of The Surface Condition of The Fabricated Specimens. The arrow points to areas where spalling occurred.

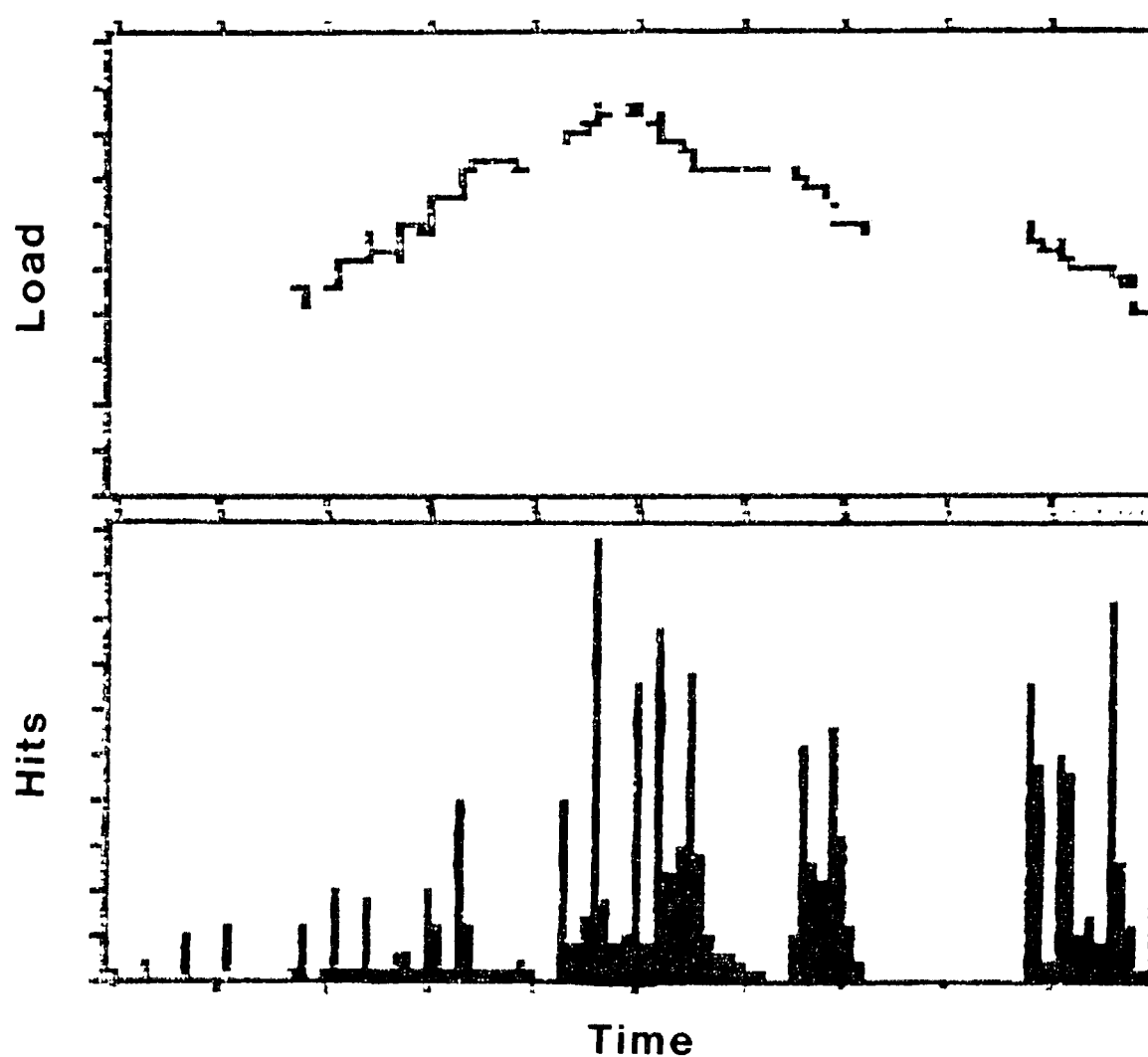


Figure 22. AE Data Generated From A Long Column (E1-LC). Top figure represents the loading history of the column. The maximum compression load is depicted by the highest point on this graph. Below is a histogram of the number of hits. Note that the greatest number of hits coincides with the maximum load.

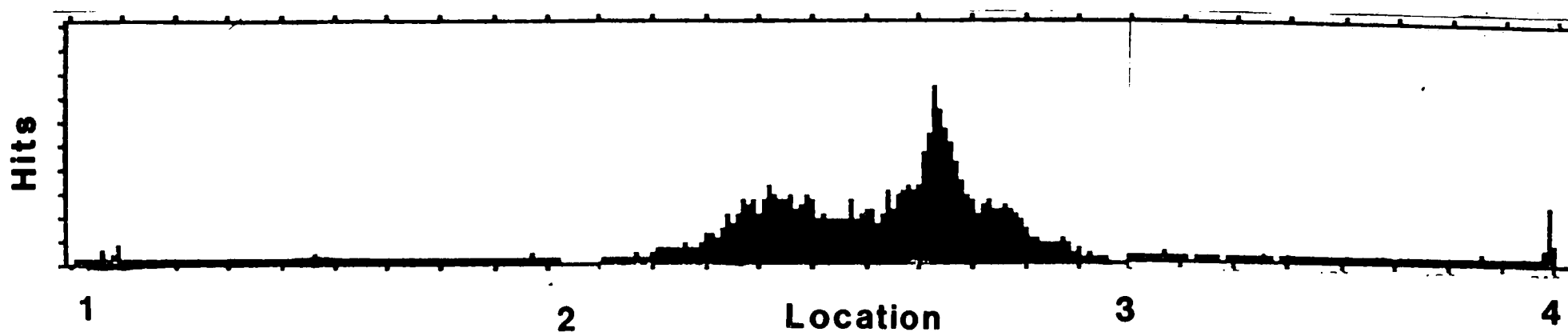


Figure 23. A Linear Location Diagram of Long Column E1-LC. Numbers represent location of AE sensors. Note that the maximum number of hits occurs between sensors 2 and 3. This coincides with the location of the dent.

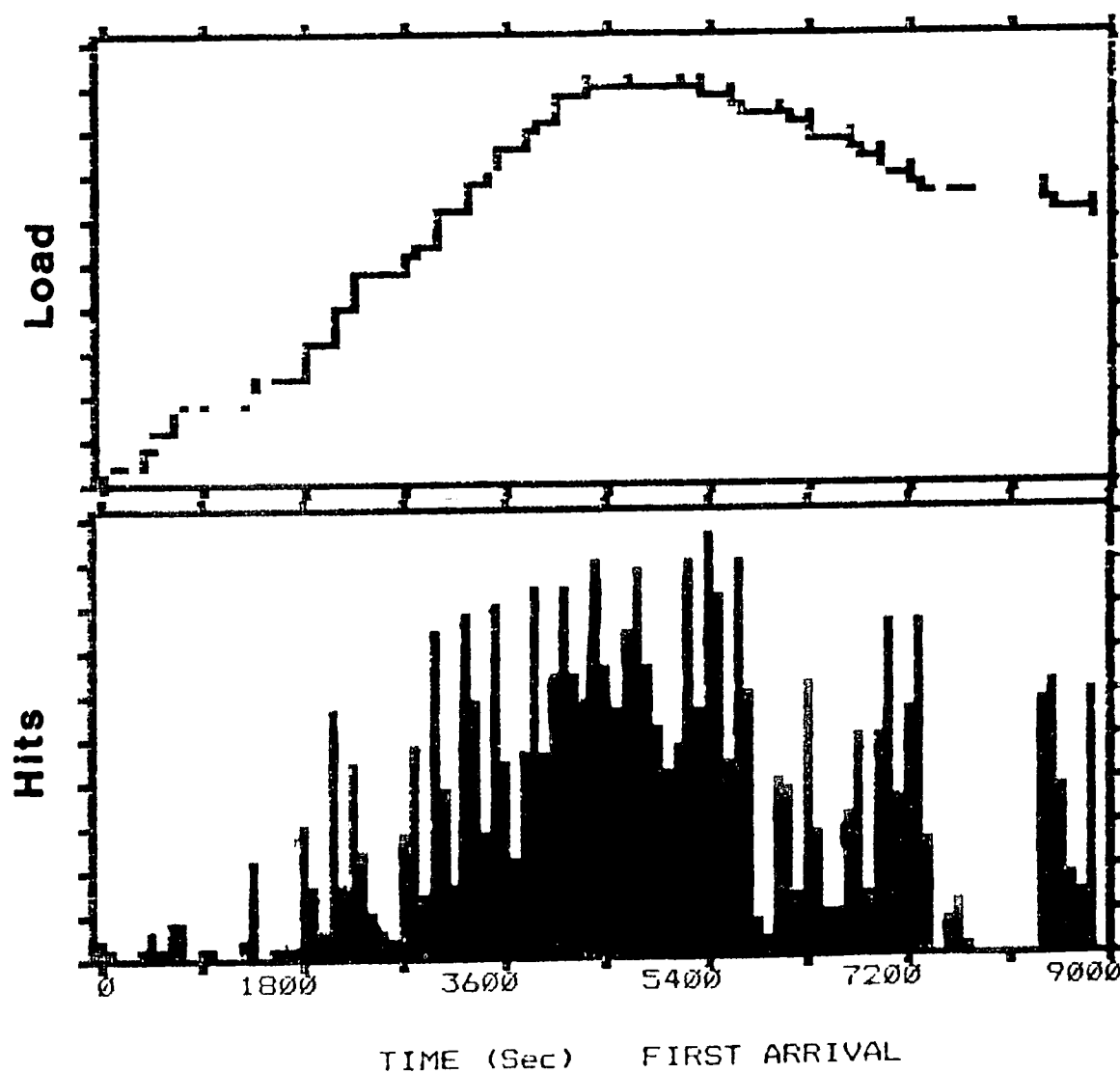


Figure 24. AE Data From Long Column E3-LC. Note that the greatest number of hits occurred near the maximum load.

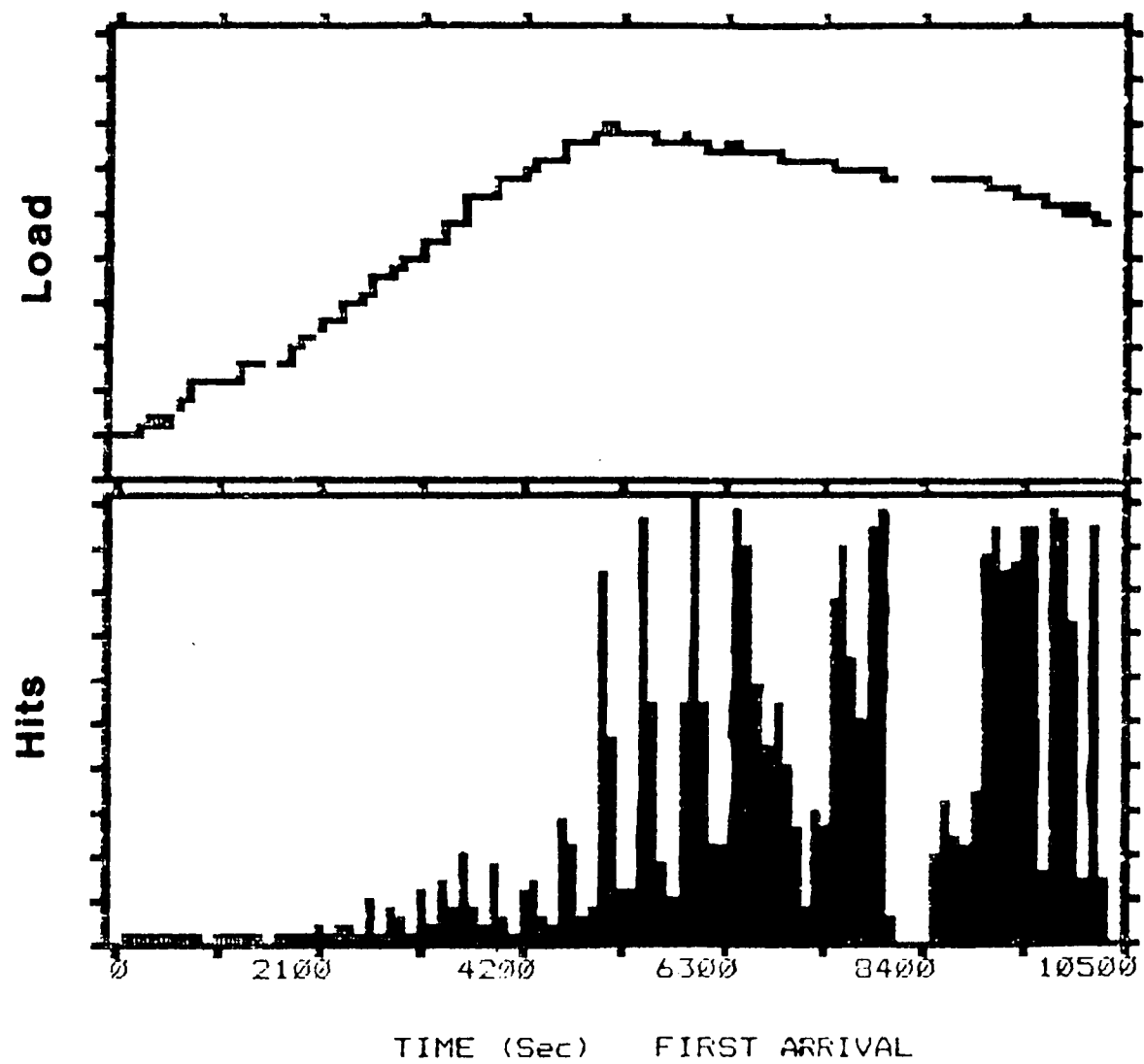


Figure 25. AE Data From Long Column B3-LC. Note that the greatest number of hits occurred near the maximum load.

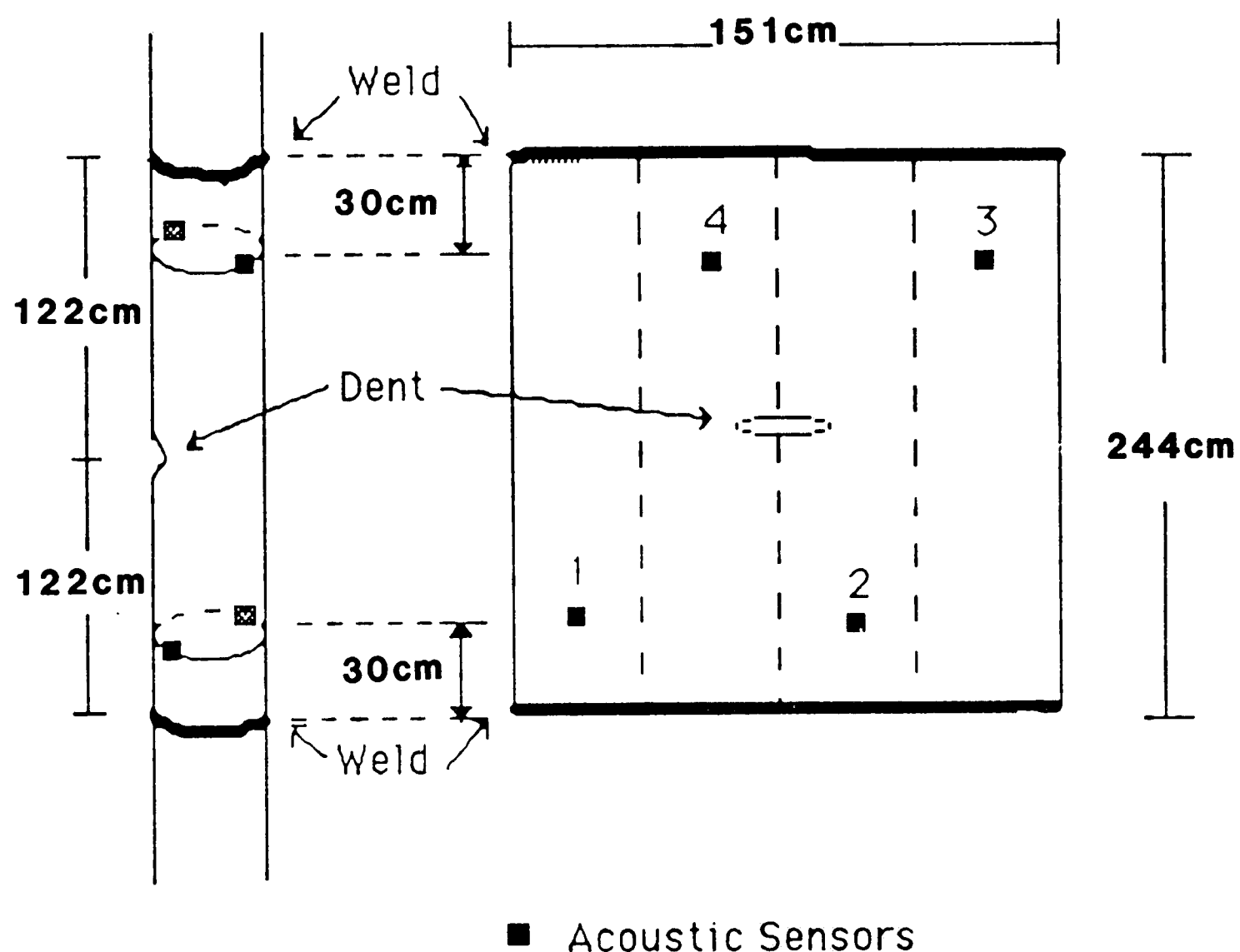


Figure 26. Location of AE Sensors On Long Column P4-LC. The left figure is a schematic of the long column showing the location of the AE sensors. The right figure depicts the column as it would appear as a plate. Imagine that the column was cut longitudinally and unfolded. The dent is represented by the ellipse in the center of this figure.

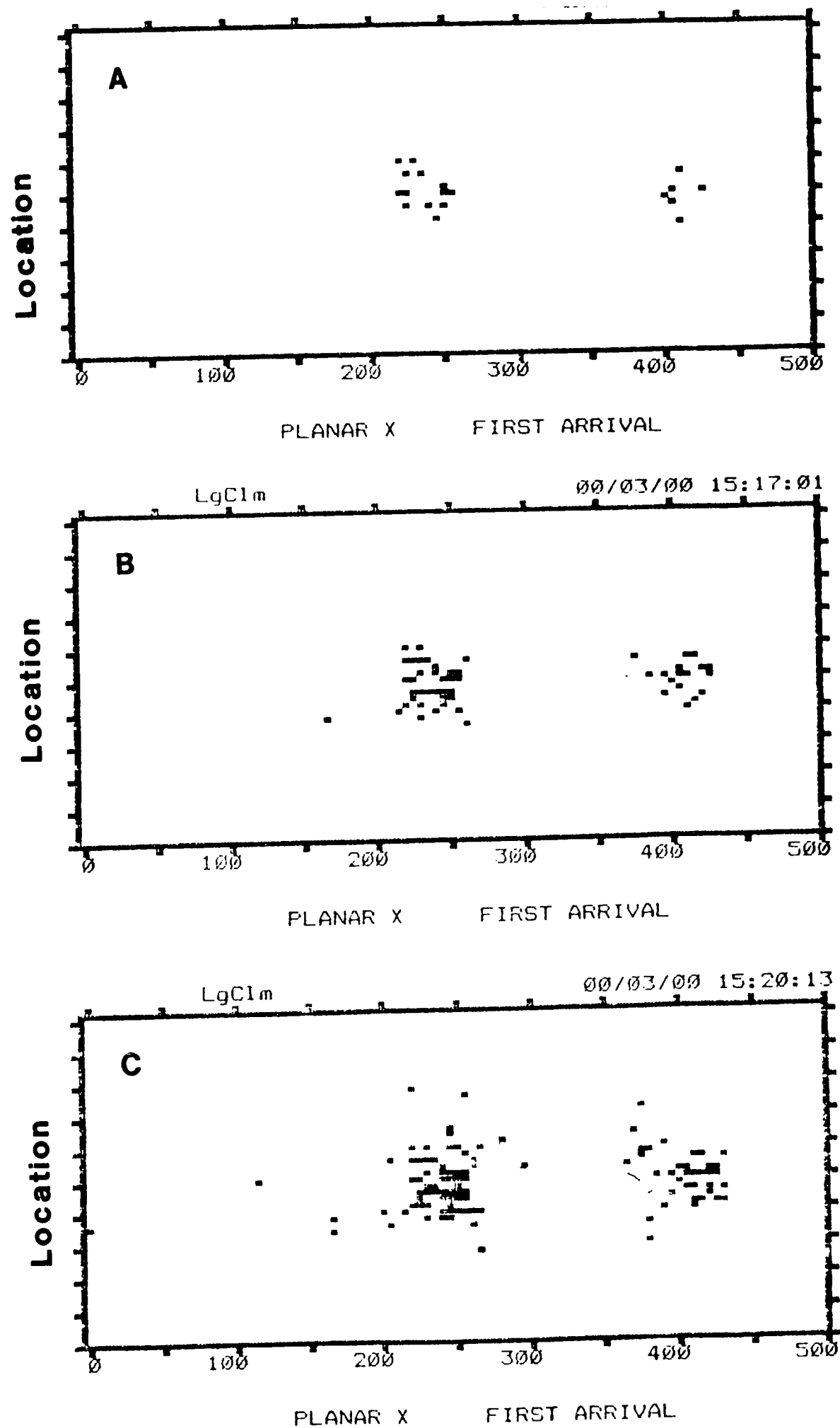


Figure 27a. Planar Location Plots of Long Column P4-LC. Imagine the specimen as a plate rather than a column (refer to fig. 26). Each dot in these figures represents a hit. There are two clusters of hits for each figure and they represent the two ends of the dent. Between these clusters is the location of the dent. The regions at the end of the dent grow with time. This can be seen by viewing figures A through F. Figure A was plotted at the beginning of the test while F was at the end.

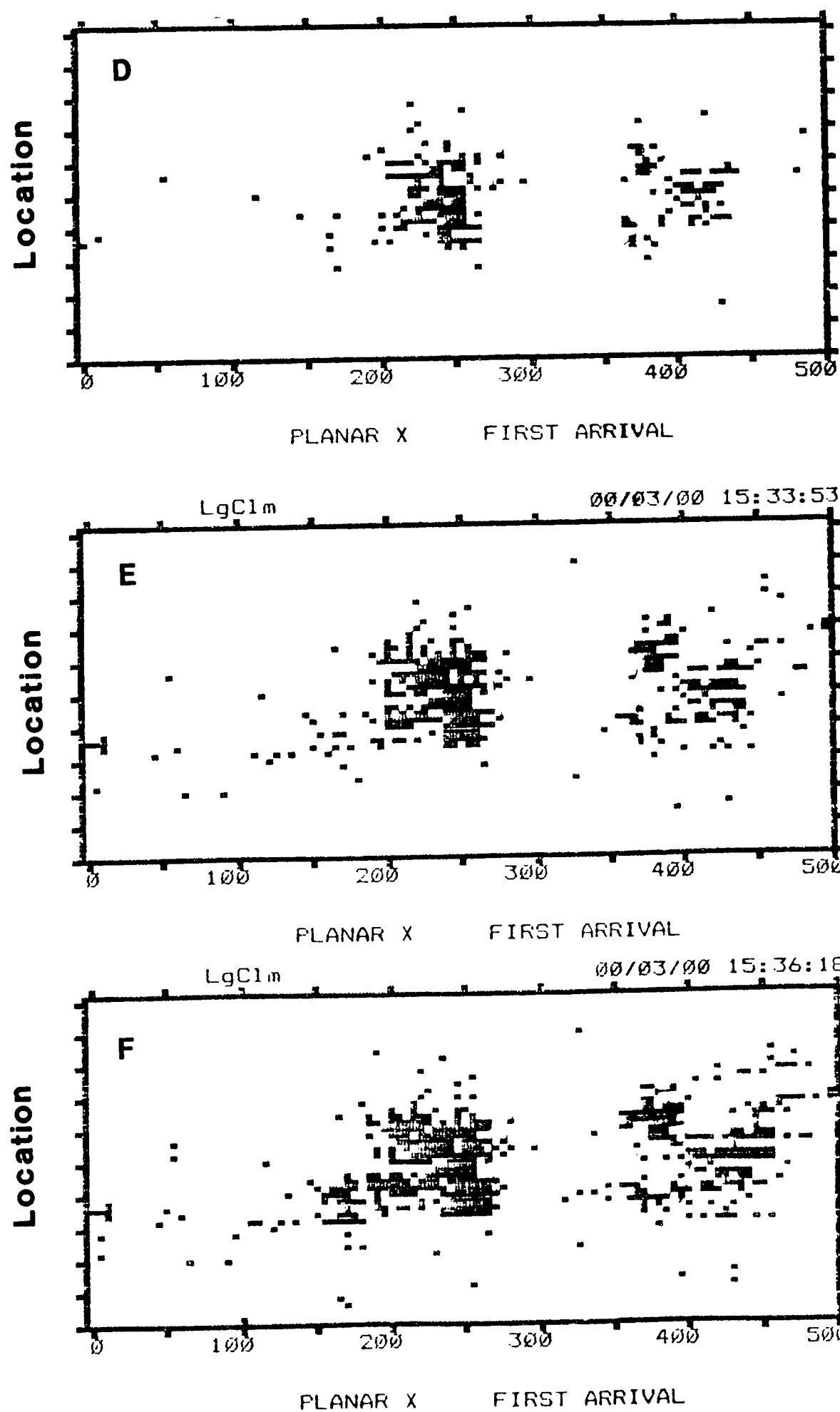
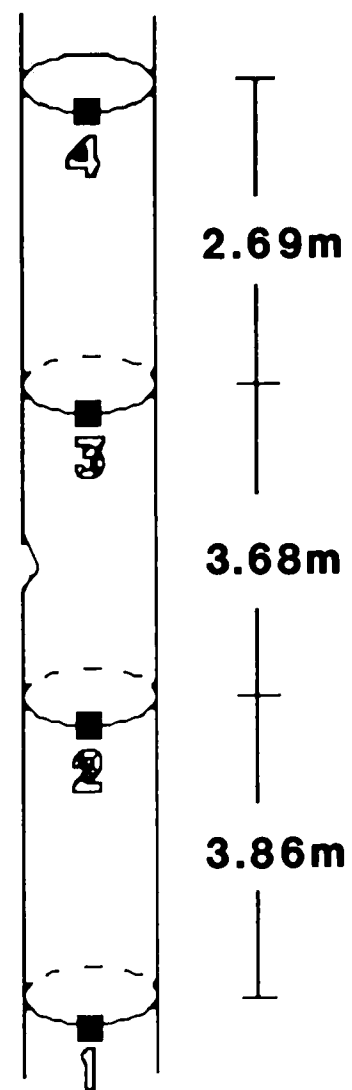


Figure 27b. Planar Location Plot Of Long Column P4-LC
(continued from figure 27a)



■ Acoustic Sensors

Figure 28. Placement of AE Sensors On Long Column P2-LC. All the sensors were position on the same plane of the column.

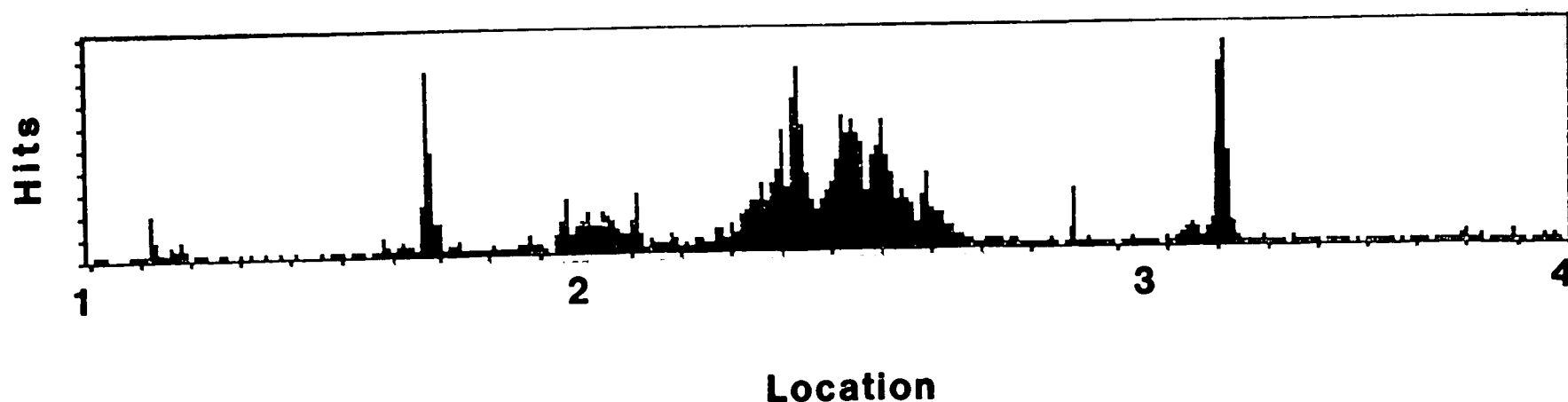


Figure 29. Linear Location Plot of Long Column P2-LC. The numbers along the abscissa represent the location of the AE sensors. Note that the greatest number of hits occurred between sensors 2 and 3. This coincides with the location of the dent. A peak occurred between sensors 1 and 2 and also between 3 and 4. These two peaks coincide with the location of transverse welds.

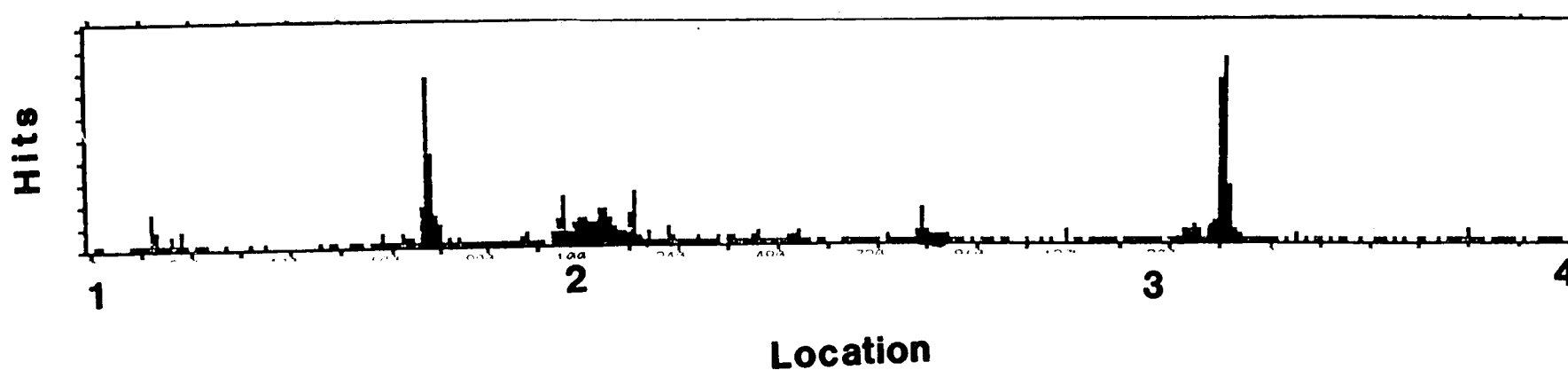


Figure 30. Linear Location Plot of Long Column P2-LC. This diagram was taken at the early stages of the test. Note that the transverse welds generated large number of hits early, but subsided as the test continued. This can be seen by comparing figure 29 and 30. Note that no appreciable number of hits occurred between sensors 2 and 3.

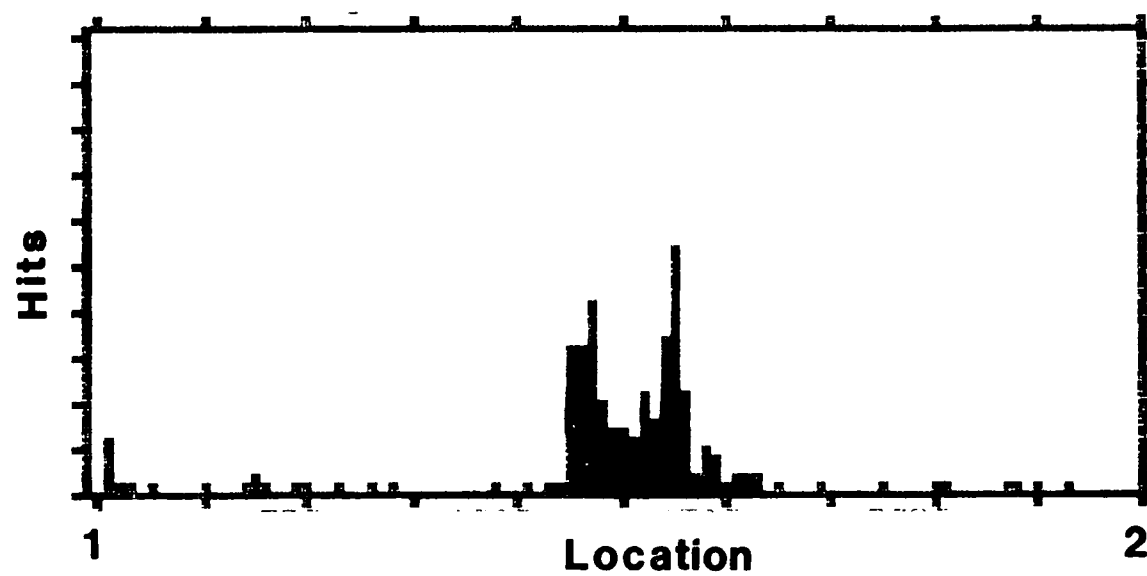


Figure 31. Linear Location Plot of Long Column D3-LC. Only two AE sensors were used for this test and they are designated by the 1 and 2. Note that a burst of hits occurred at the center of the column, and this coincides with the damaged area.

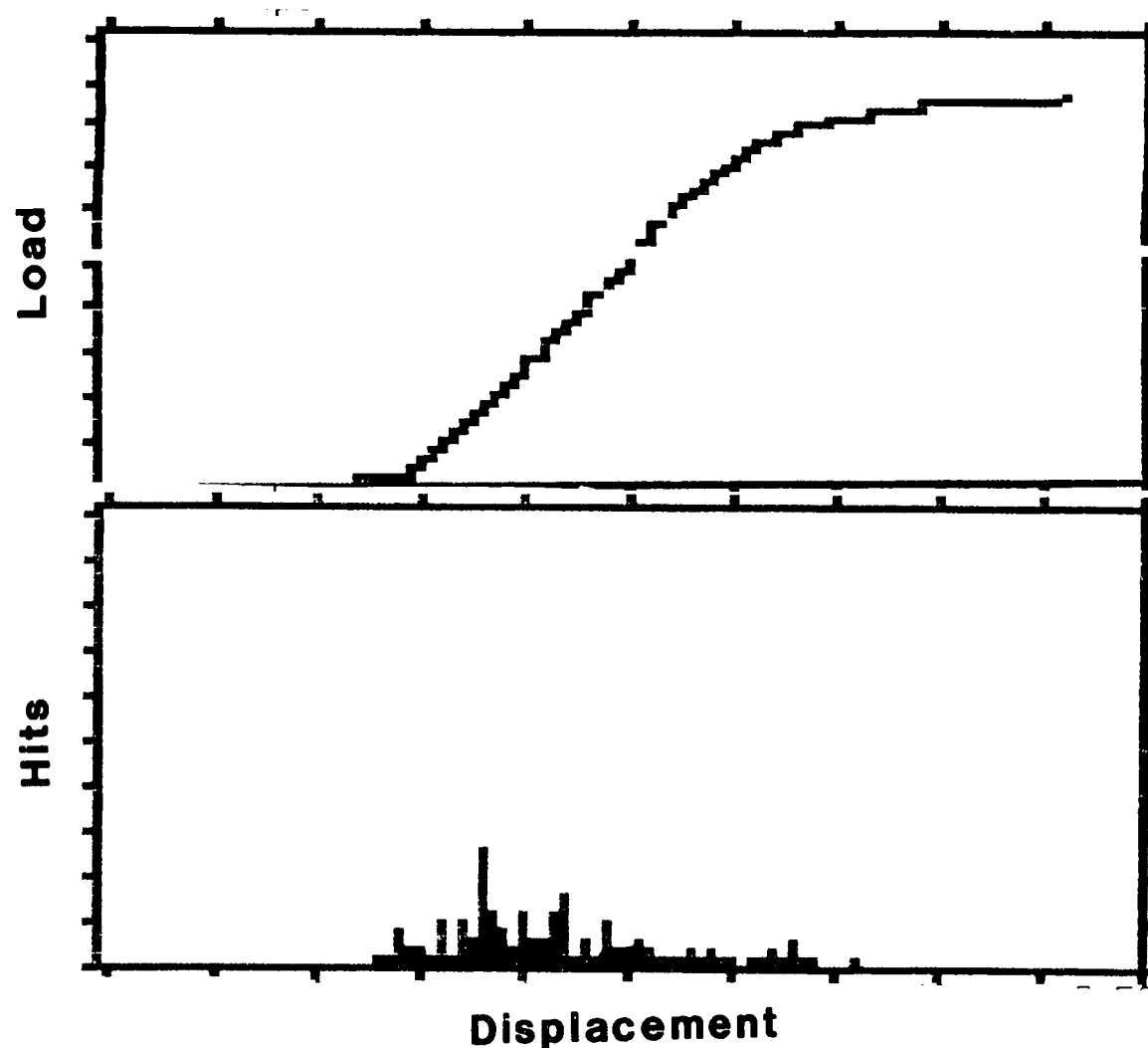


Figure 32. Four Point Bend Specimen Fabricated From A Polished ASTM A572 Steel Plate. The top figure depicts load vs. displacement while the bottom figure represents a histogram of hits verses displacement. Note that the yield point can not be determined from the AE data. The equipment sensitivity was 38dB which means that only signals with amplitudes greater than 38 dB were recorded.

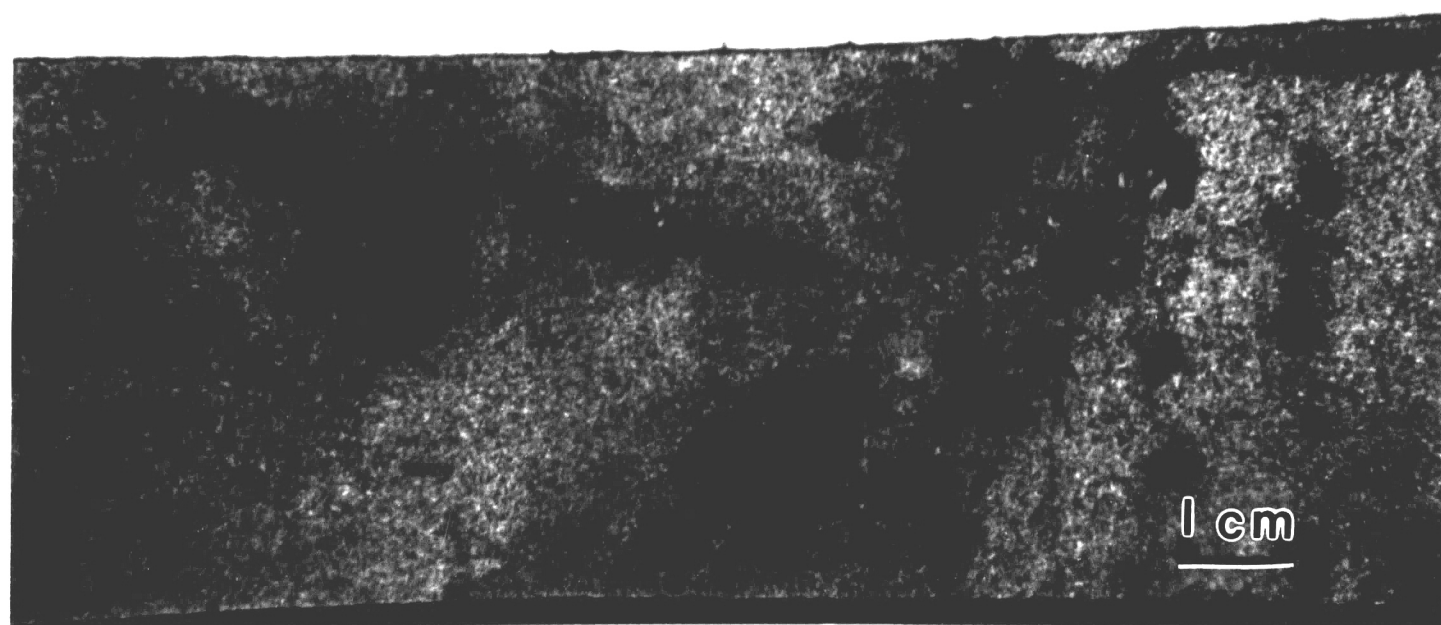


Figure 33. Surface of As Received ASTM A572 Steel Plate With Mill Scale. (Specimen F1).

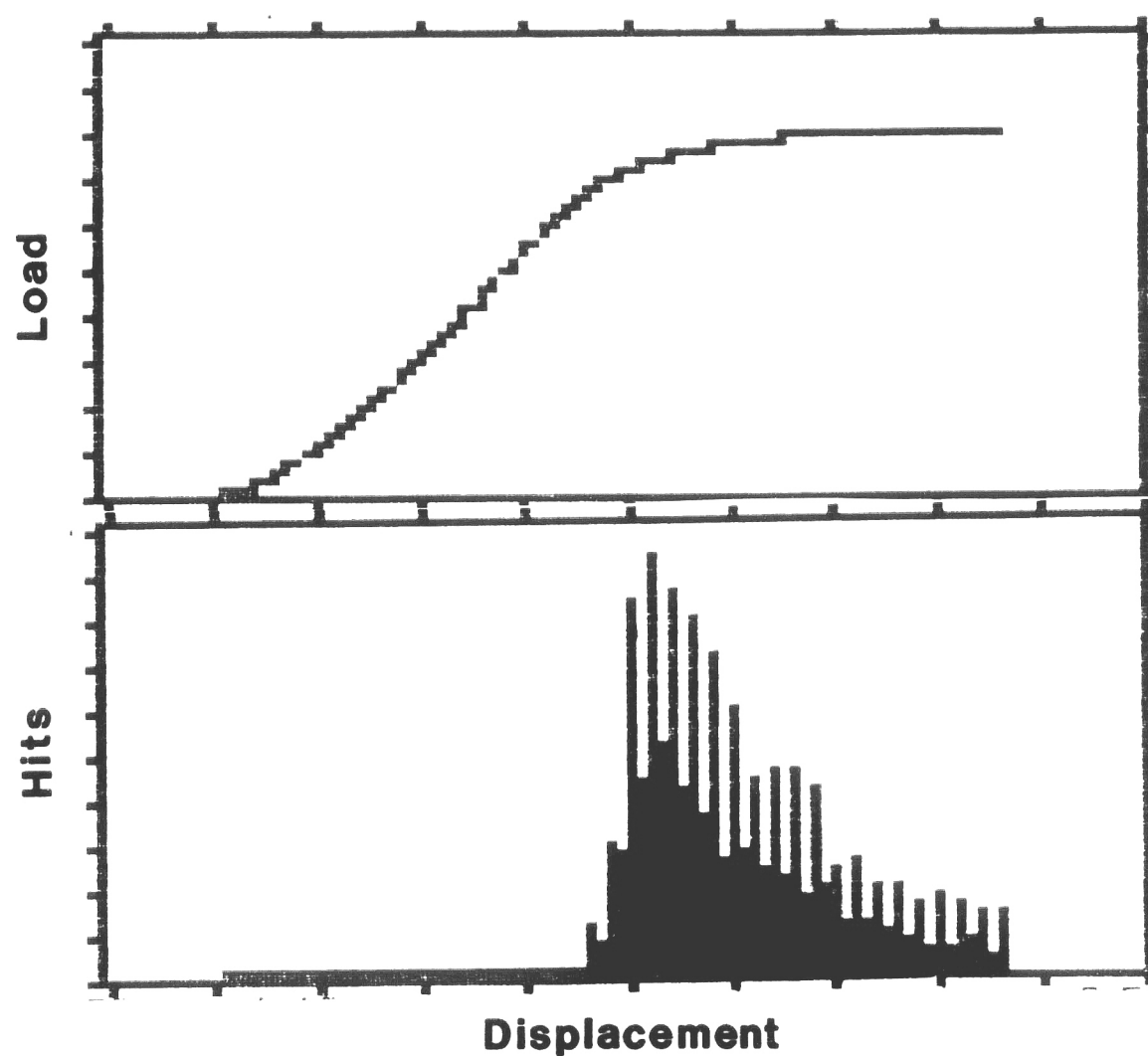


Figure 34. Four point Bend Data for A572 Steel with Mill Scale (Specimen F1). Note that the onset of yielding produced a significant increase in hits. (Sensitivity 38dB)



Figure 33. Surface of As Received ASTM A572 Steel Plate With Mill Scale. (Specimen F1).

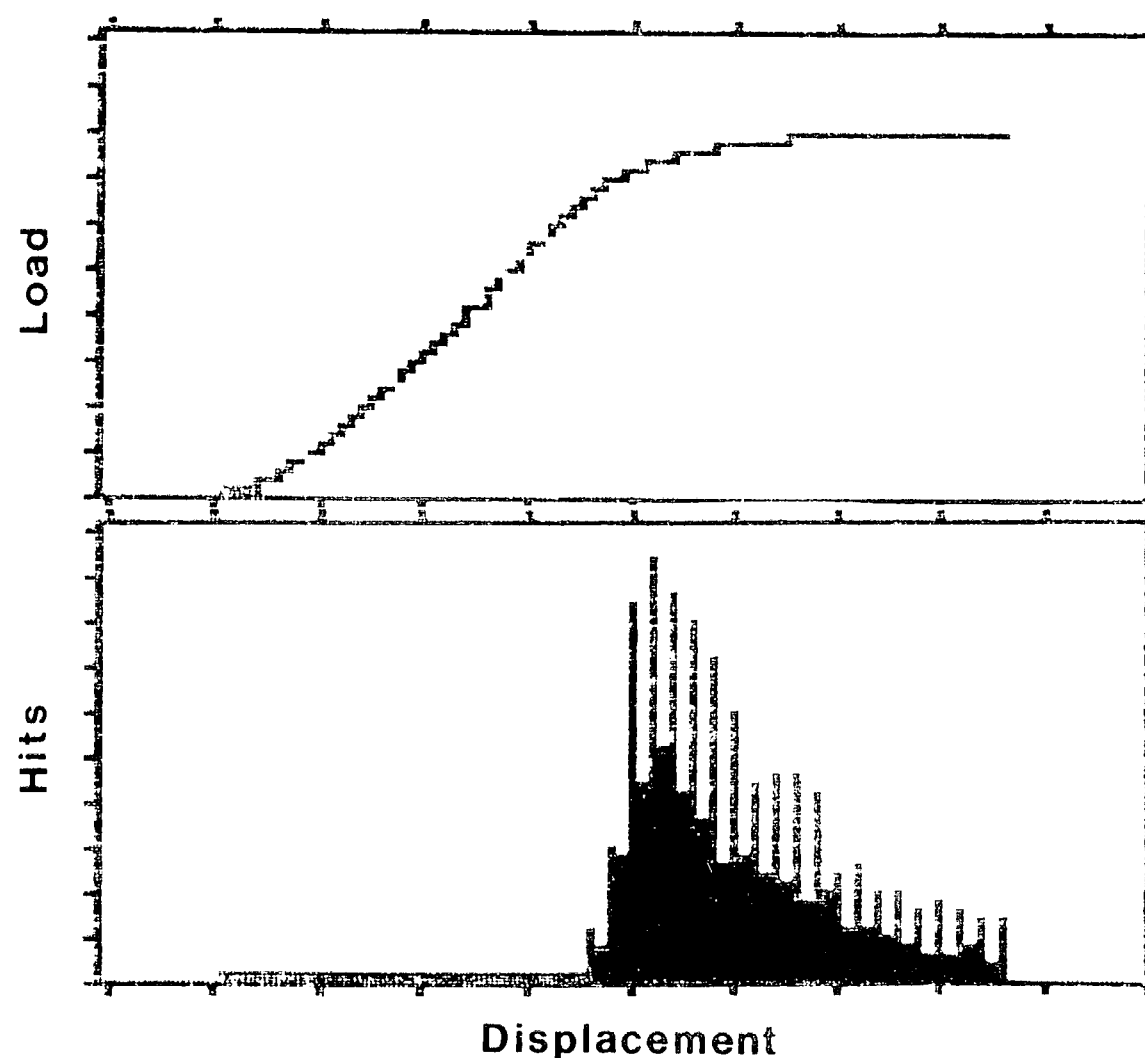


Figure 34. Four point Bend Data for A572 Steel with Mill Scale (Specimen F1). Note that the onset of yielding produced a significant increase in hits. (Sensitivity 38dB)

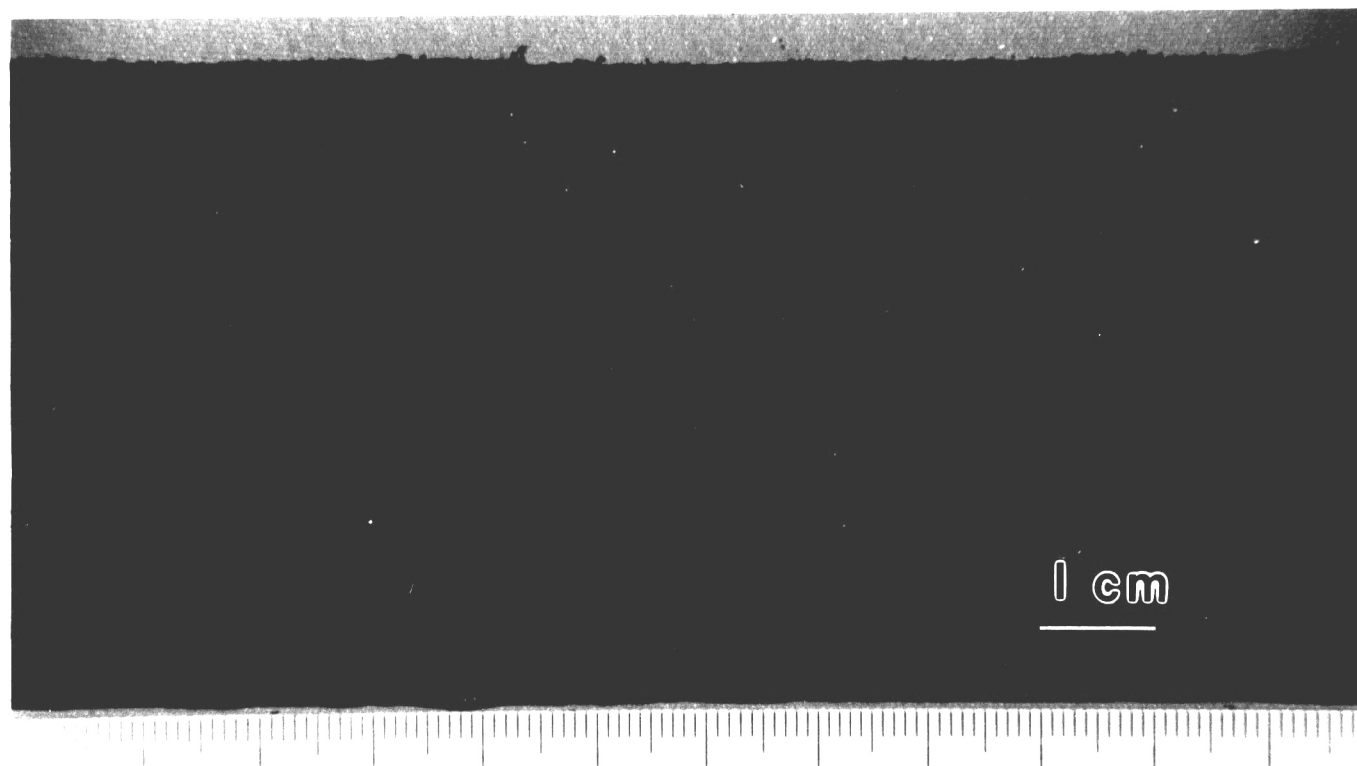


Figure 35. Surface Condition of ASTM 572 Steel Plate With Mill Scale And a 600 hr. Exposure To Salt Water. (Specimen FE1)

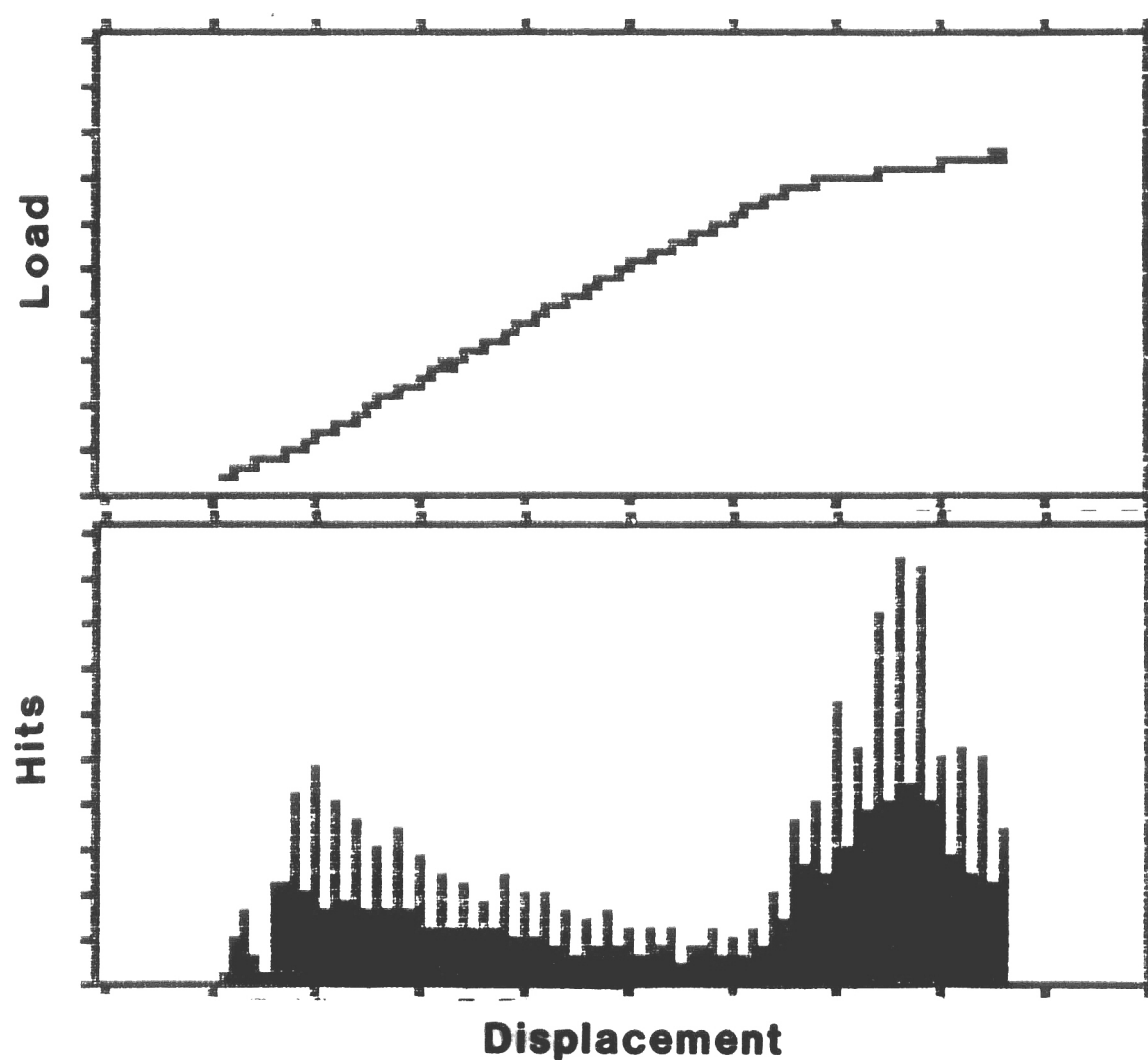


Figure 36. Four Point Bend Data For Specimen FE1. Note that the onset of yielding produced an increase in hits. (Sensitivity 38dB).

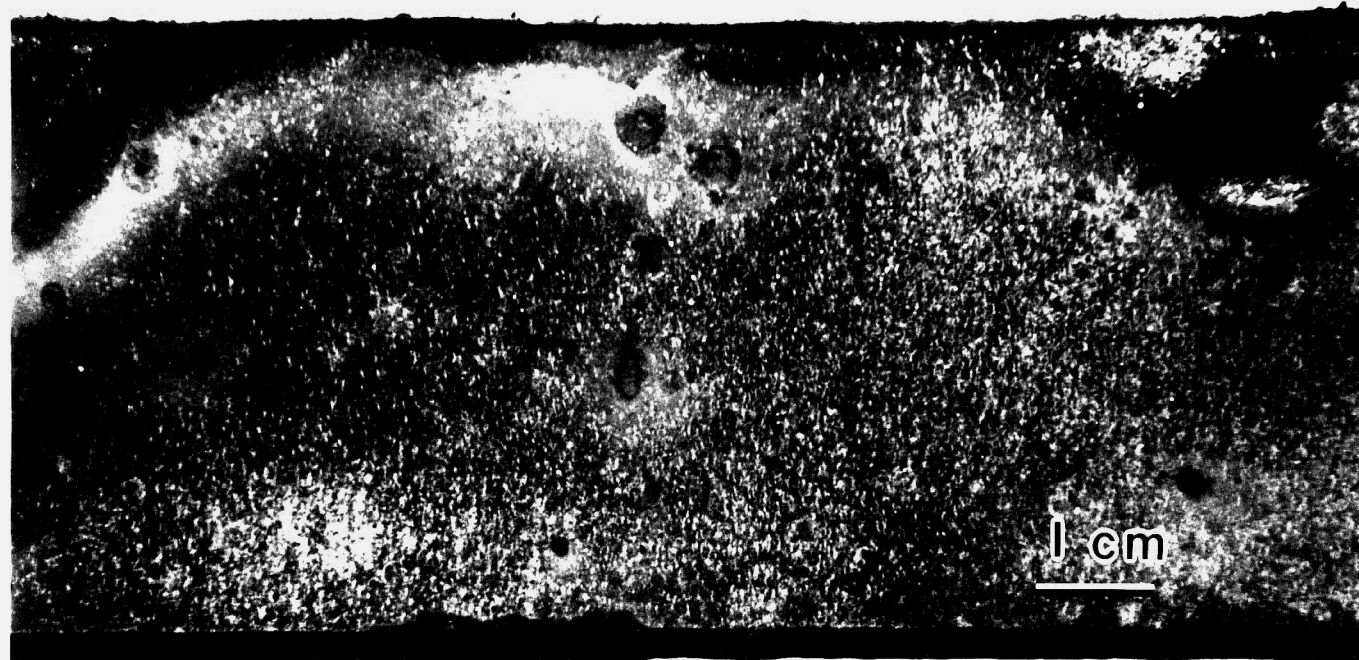


Figure 35. Surface Condition of ASTM 572 Steel Plate With Mill Scale And a 600 hr. Exposure To Salt Water. (Specimen FE1)

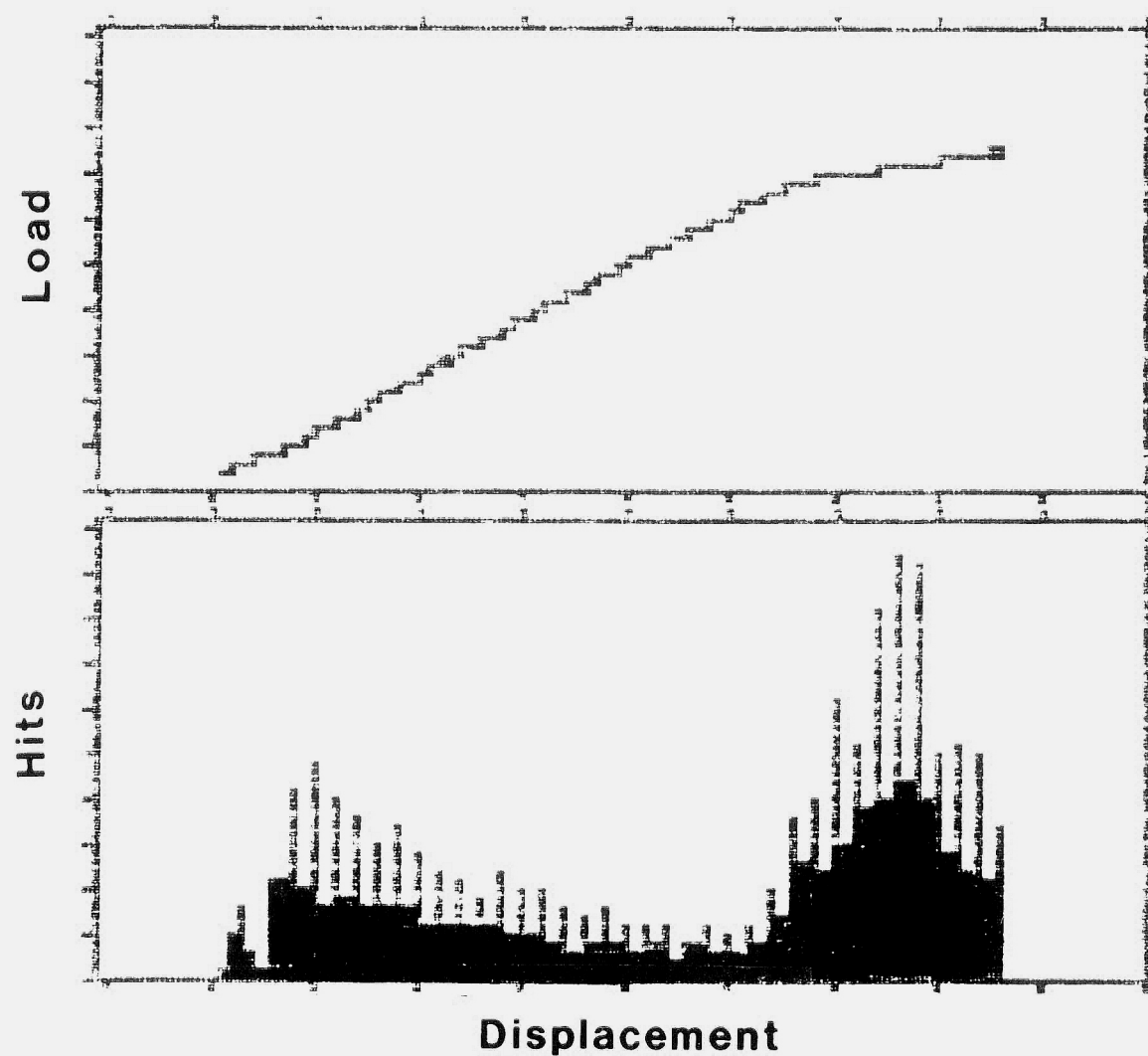


Figure 36. Four Point Bend Data For Specimen FE1. Note that the onset of yielding produced an increase in hits. (Sensitivity 38dB).

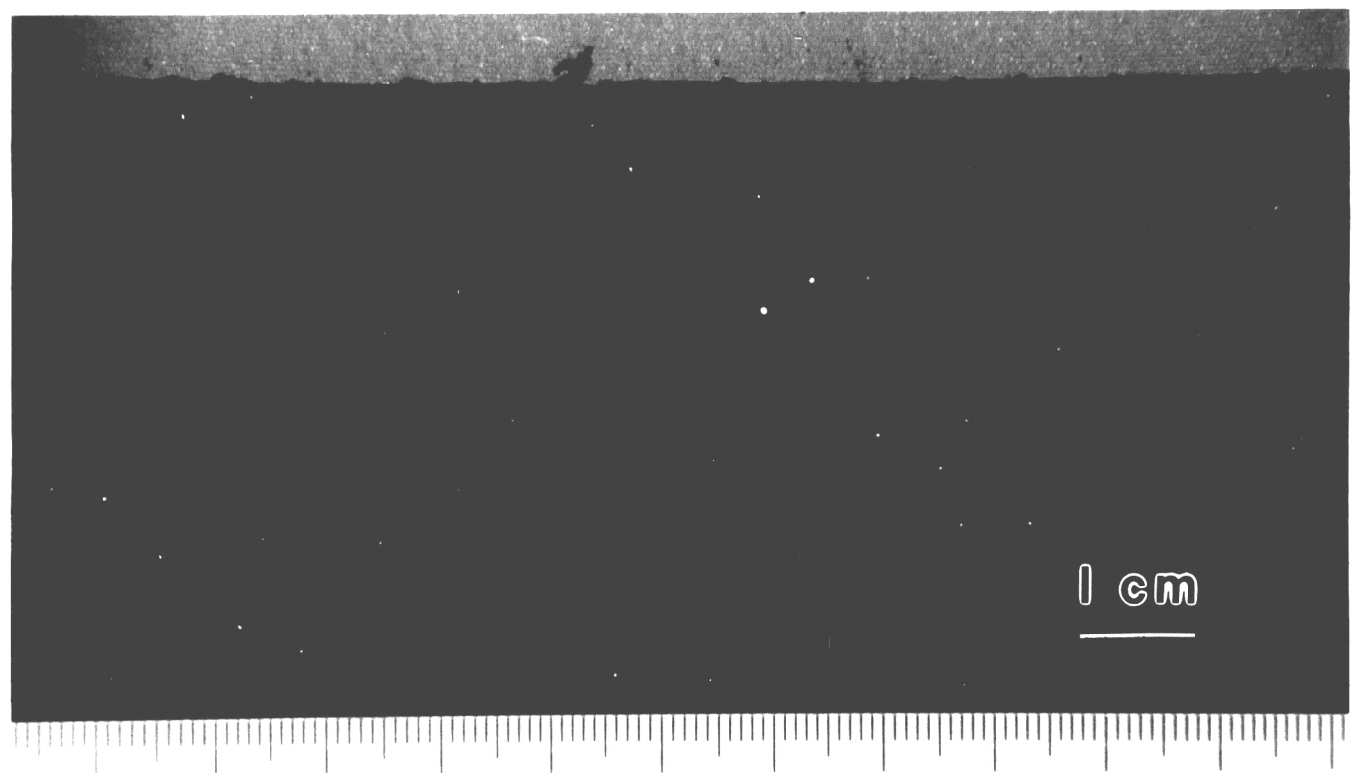


Figure 37. Surface Condition of ASTM A572 Steel Plate With Mill Scale And A 1200hr. Exposure To Salt Water. (Specimen FE2)

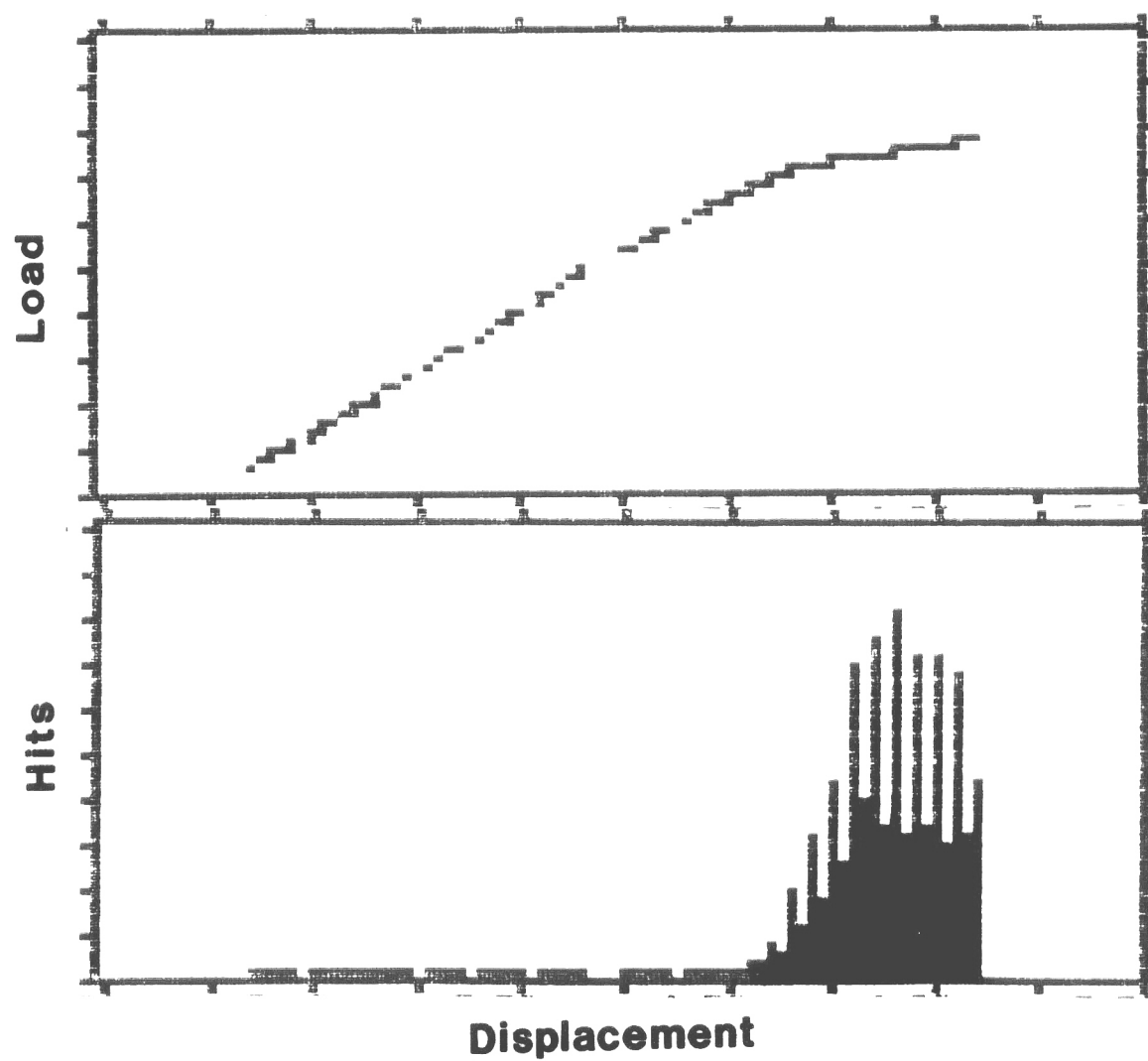


Figure 38. Four Point Bend Data For Specimen FE2. Note that the onset of yielding produced an increase in hits. (Sensitivity 38dB)

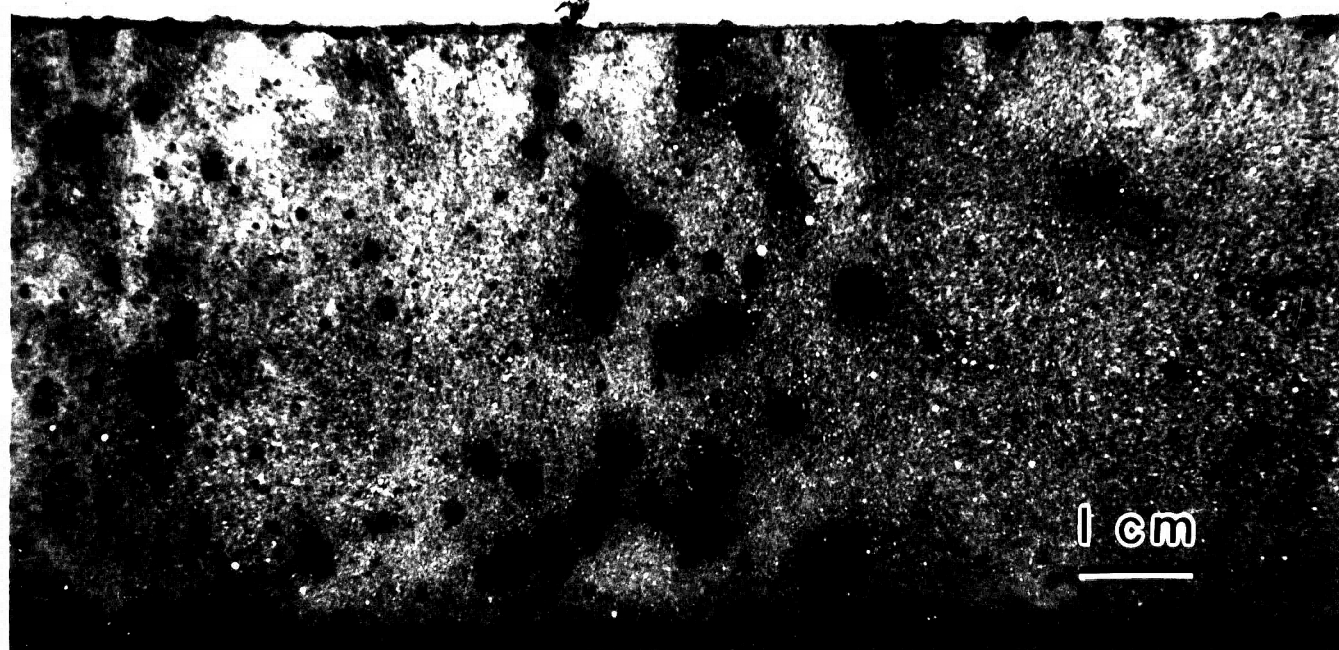


Figure 37. Surface Condition of ASTM A572 Steel Plate With Mill Scale And A 1200hr. Exposure To Salt Water. (Specimen FE2)

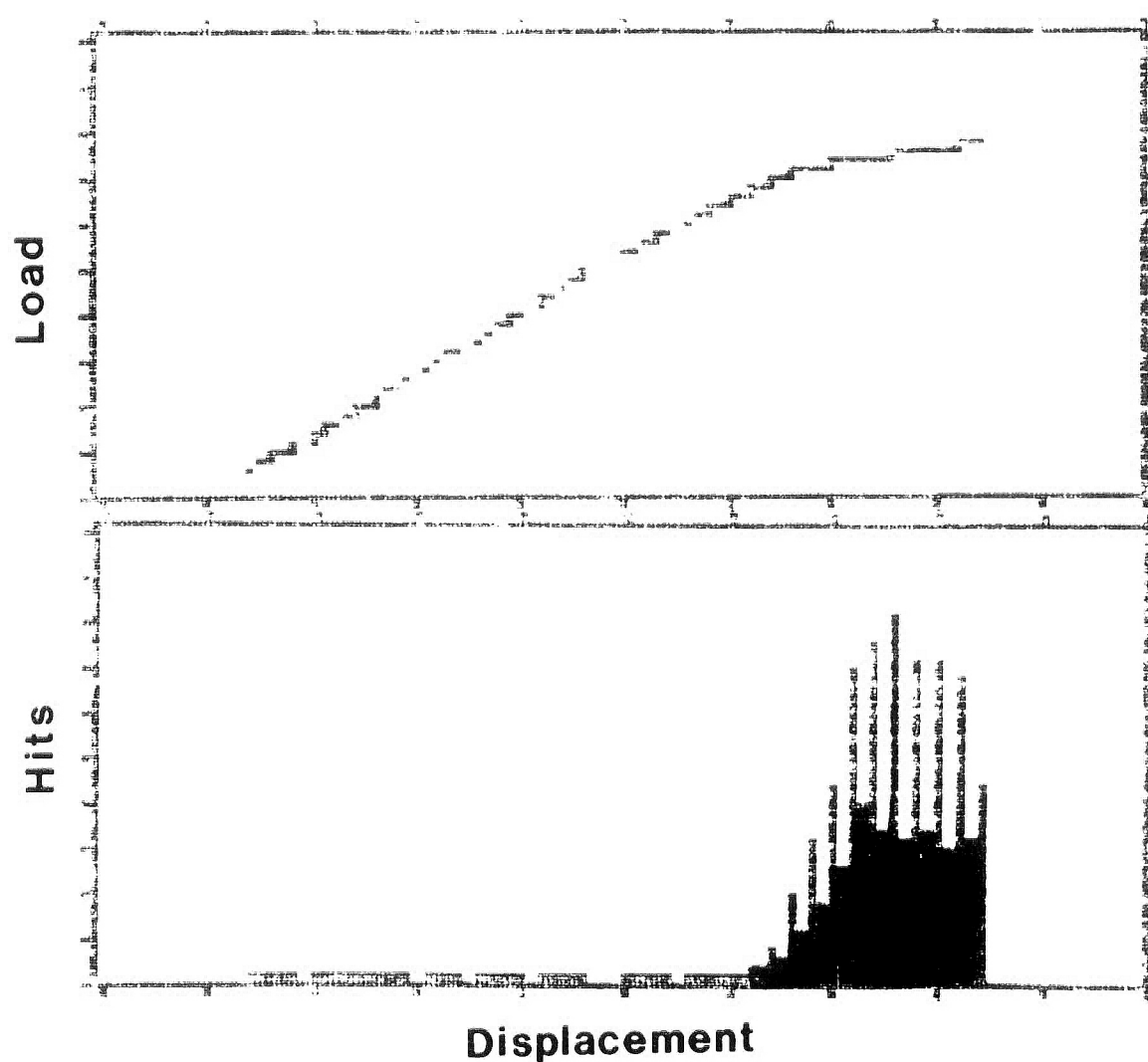


Figure 38. Four Point Bend Data For Specimen FE2. Note that the onset of yielding produced an increase in hits. (Sensitivity 38dB)



Figure 39. Surface Condition of ASTM A572 Steel Plate With Mill Scale and a 2400hr. Salt Water Exposure. (Specimen FE3).

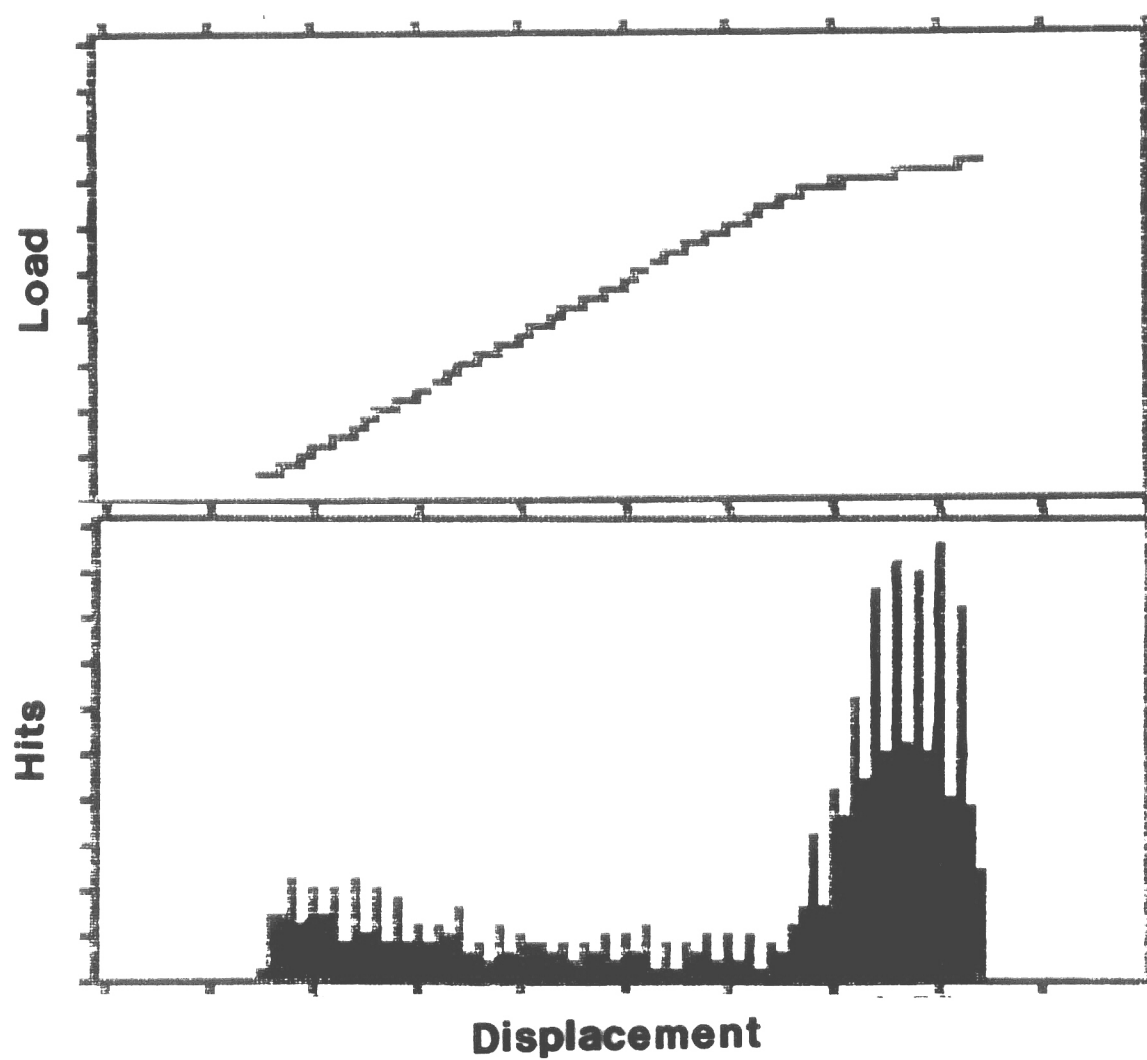


Figure 40. Four Point Bend Data for Specimen FE3. Note that the onset of yielding produced an increase in hits (Sensitivity 38dB)

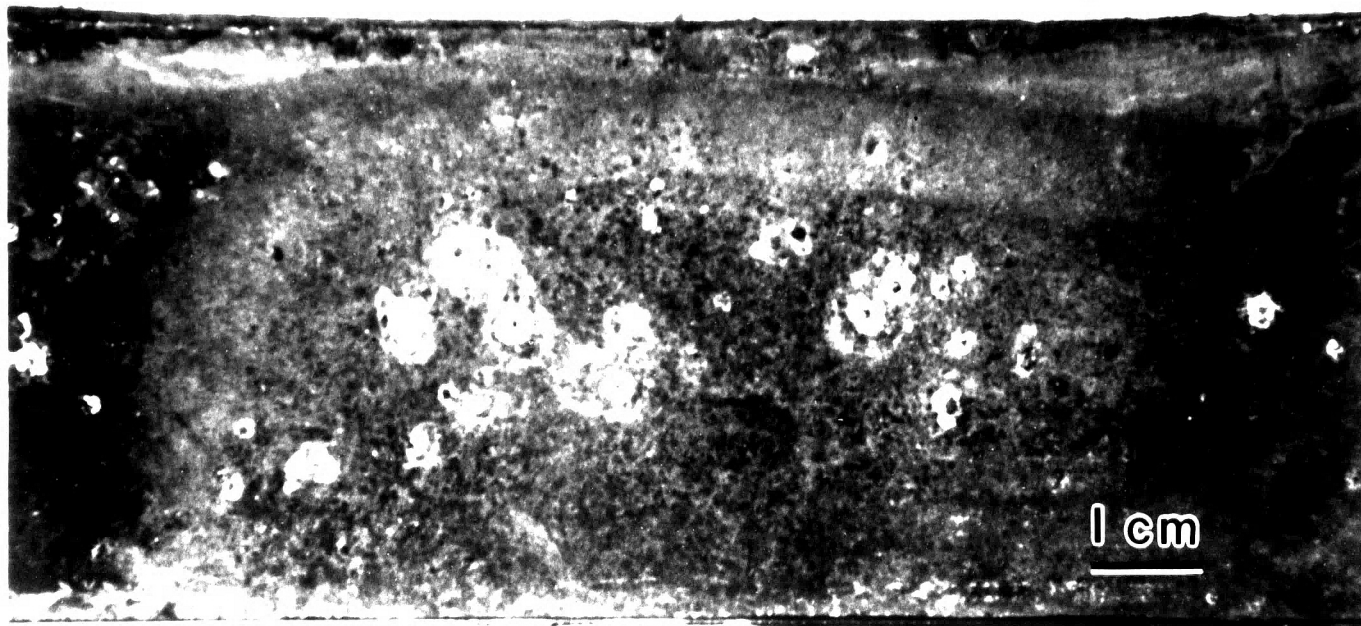


Figure 39. Surface Condition of ASTM A572 Steel Plate With Mill Scale and a 2400hr. Salt Water Exposure. (Specimen FE3).

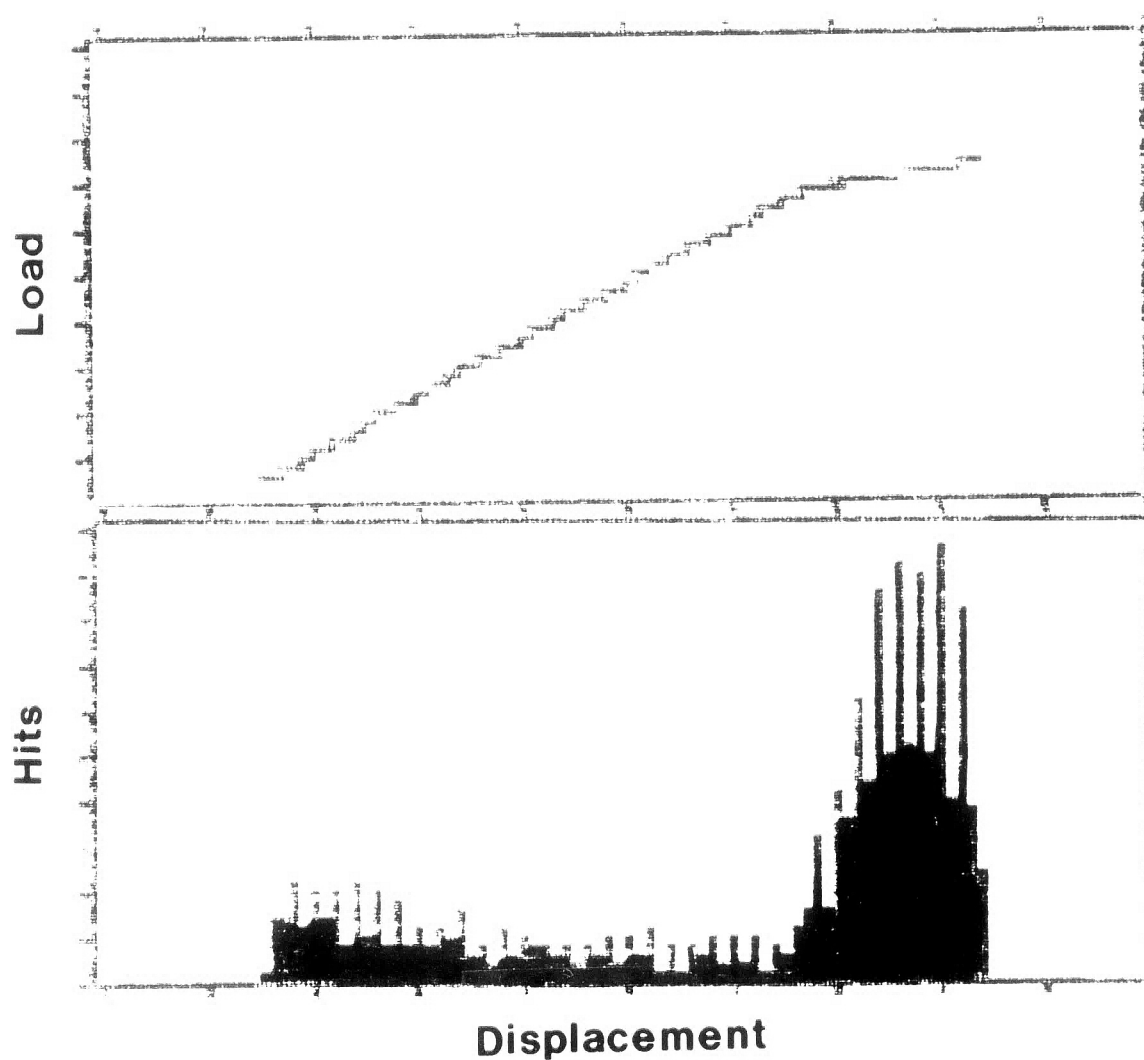


Figure 40. Four Point Bend Data for Specimen FE3. Note that the onset of yielding produced an increase in hits (Sensitivity 38dB)

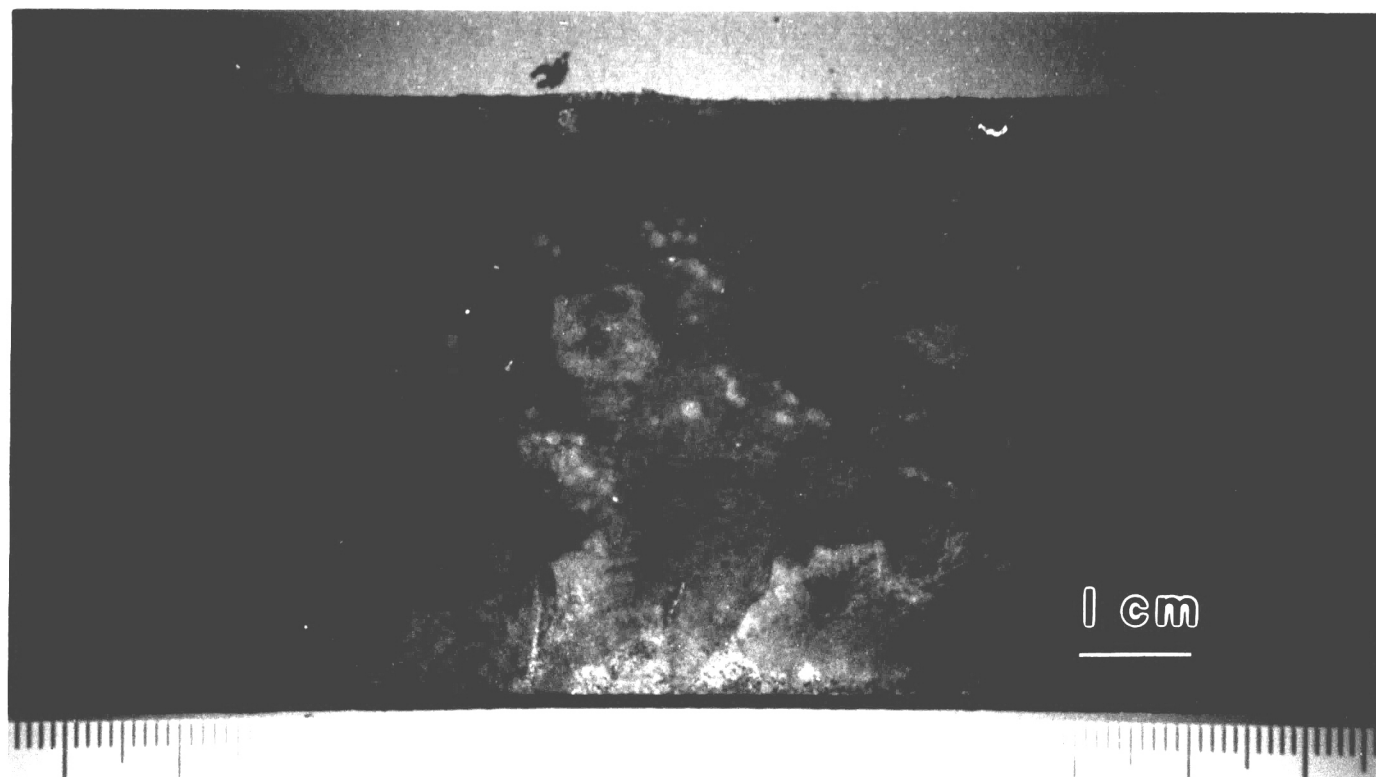


Figure 41. Surface Condition of a ASTM A572 Steel Plate Without Mill Scale and Exposed for 600hr. In a Salt Water Environment. (Specimen FNSE1)

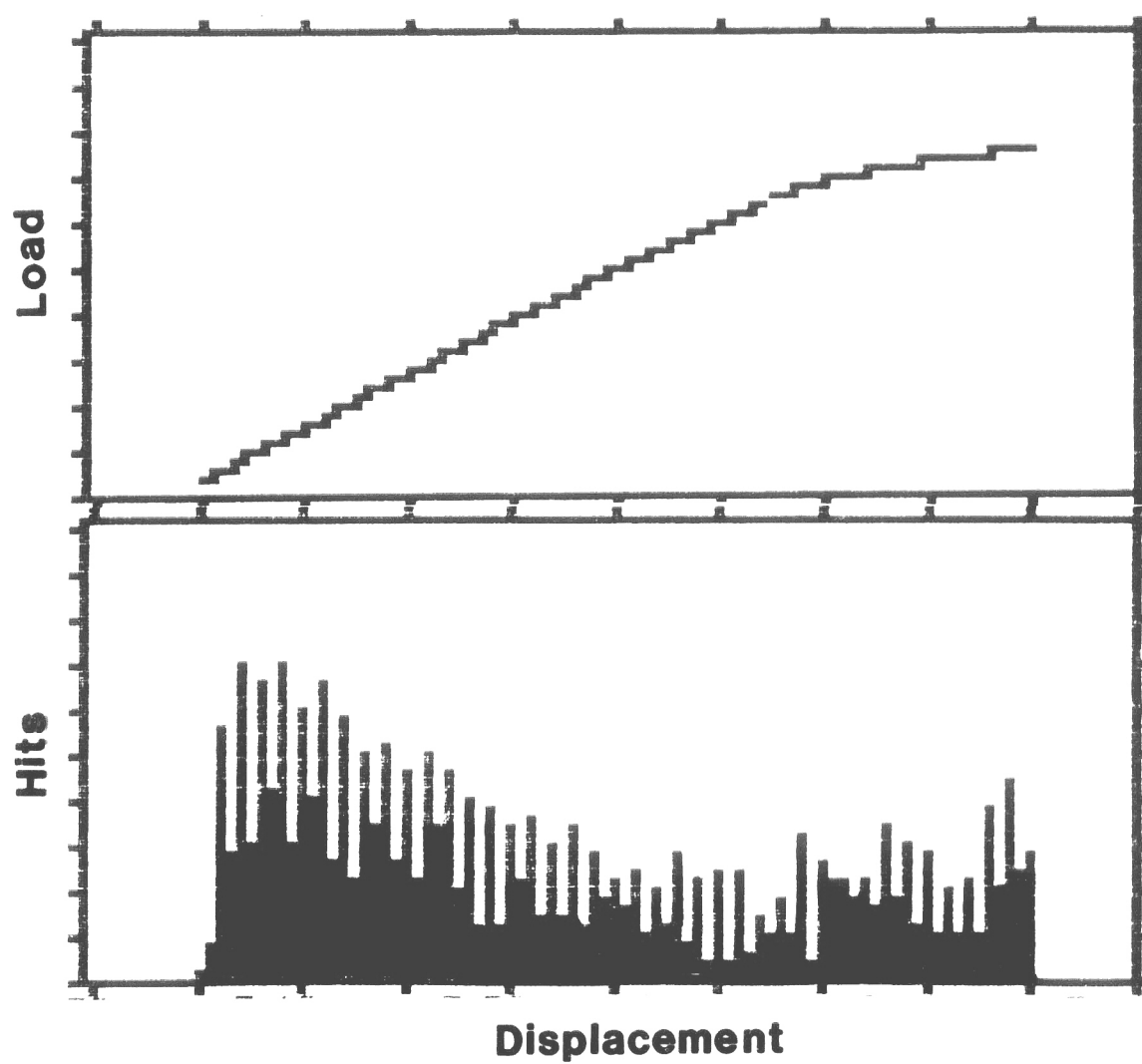


Figure 42. Four Point Bend Data for Specimen FNSE1. Note that the onset of yielding could not be determined by viewing the AE data. (Sensitivity 38dB)

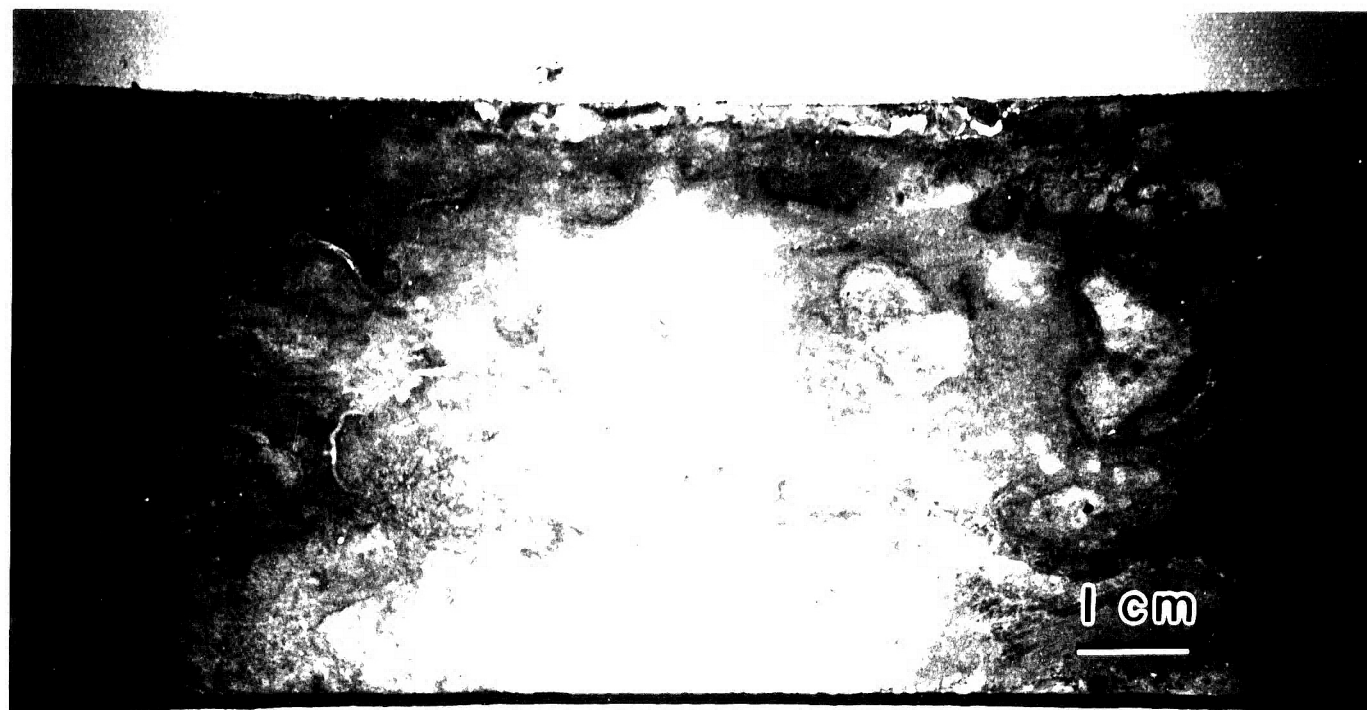


Figure 41. Surface Condition of a ASTM A572 Steel Plate Without Mill Scale and Exposed for 600hr. In a Salt Water Environment. (Specimen FNSE1)

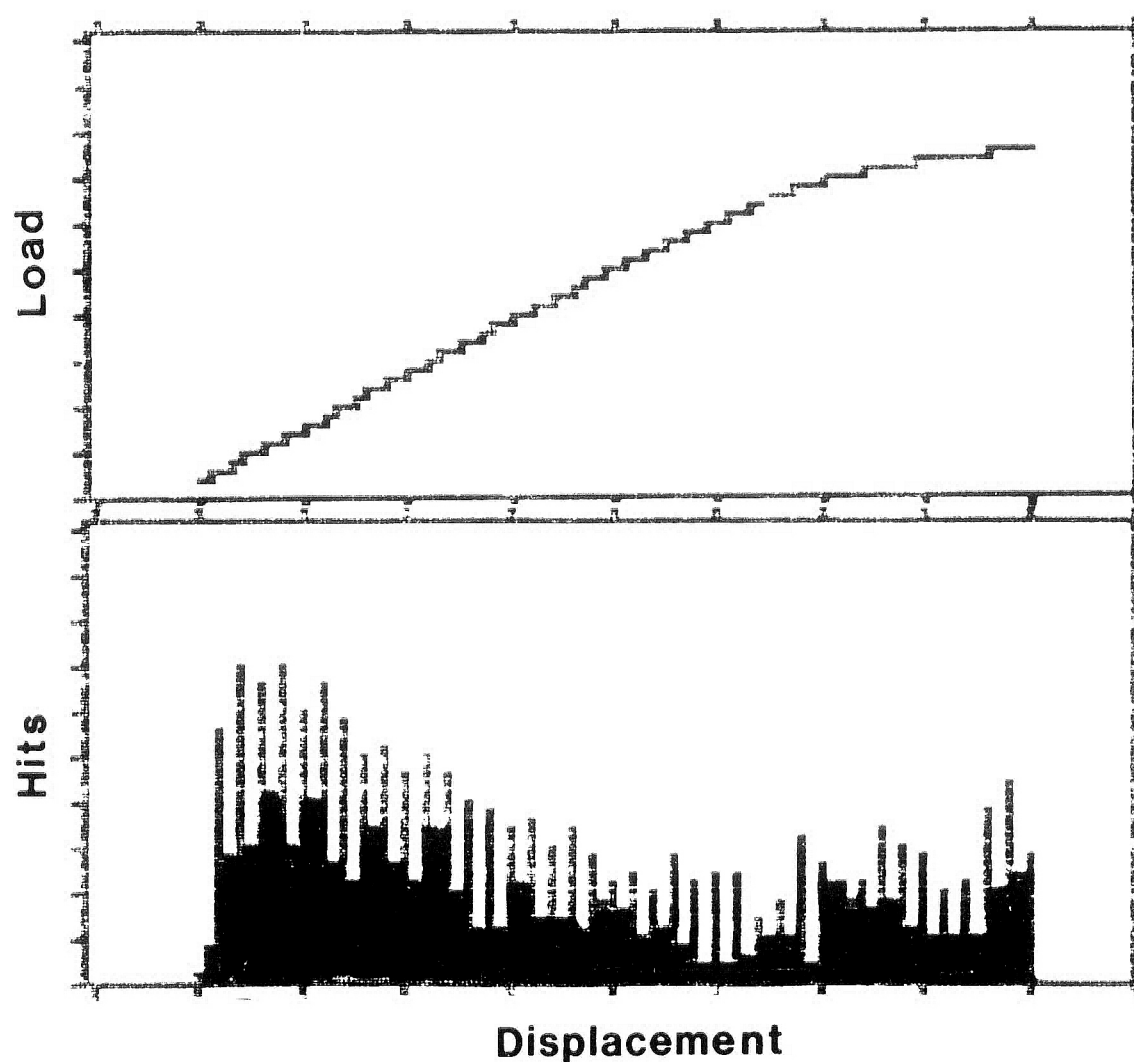


Figure 42. Four Point Bend Data for Specimen FNSE1. Note that the onset of yielding could not be determined by viewing the AE data. (Sensitivity 38dB)



Figure 43. Surface Condition of a ASTM A572 Steel Plate Without Mill Scale and Exposed for 1800hr. In A Salt Water Environment. (Specimen FNSE2)

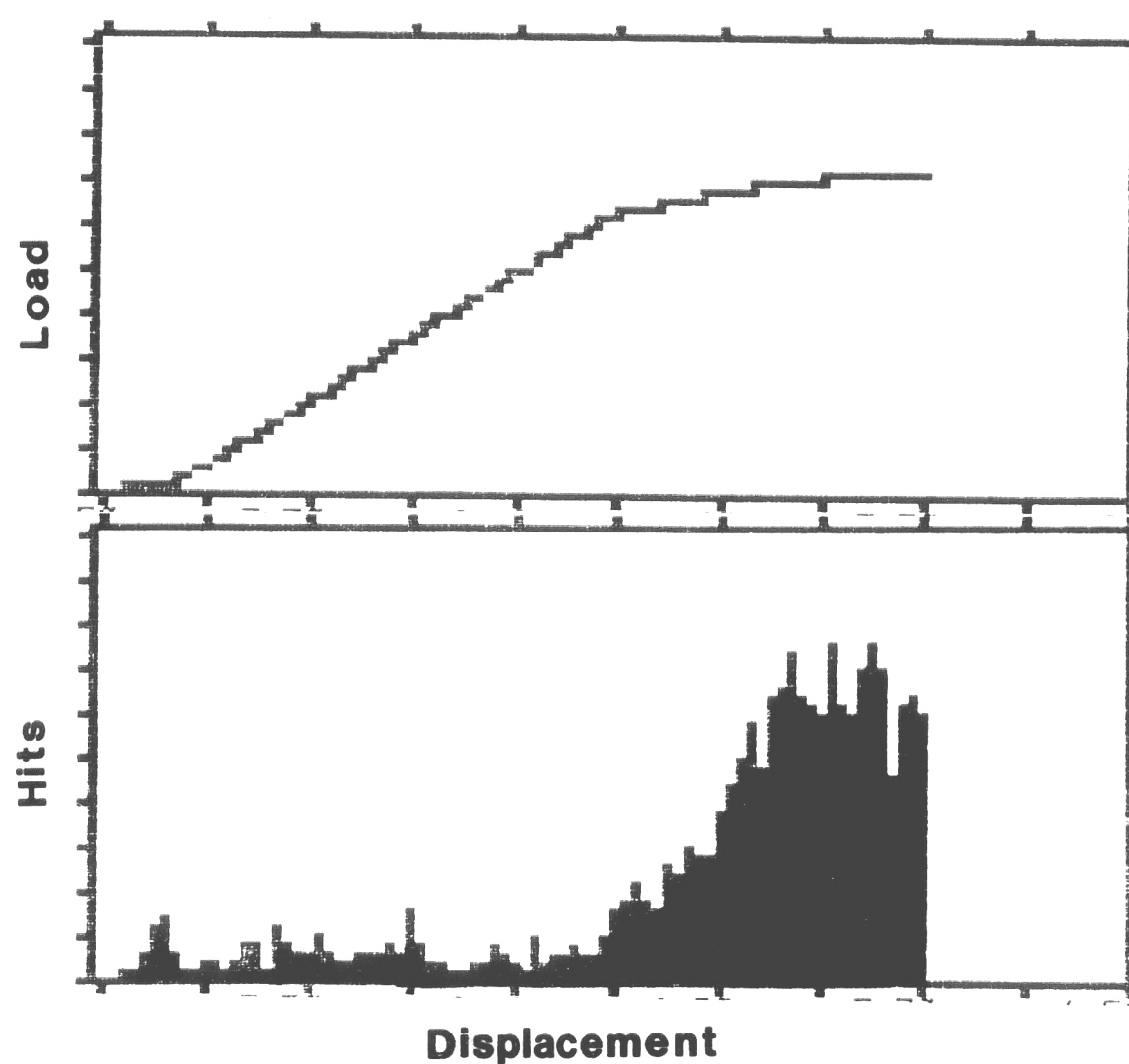


Figure 44. Four Point Bend Data for Specimen FENS2. Note that the onset of yielding produced an increase in hits. (Sensitivity 38dB)

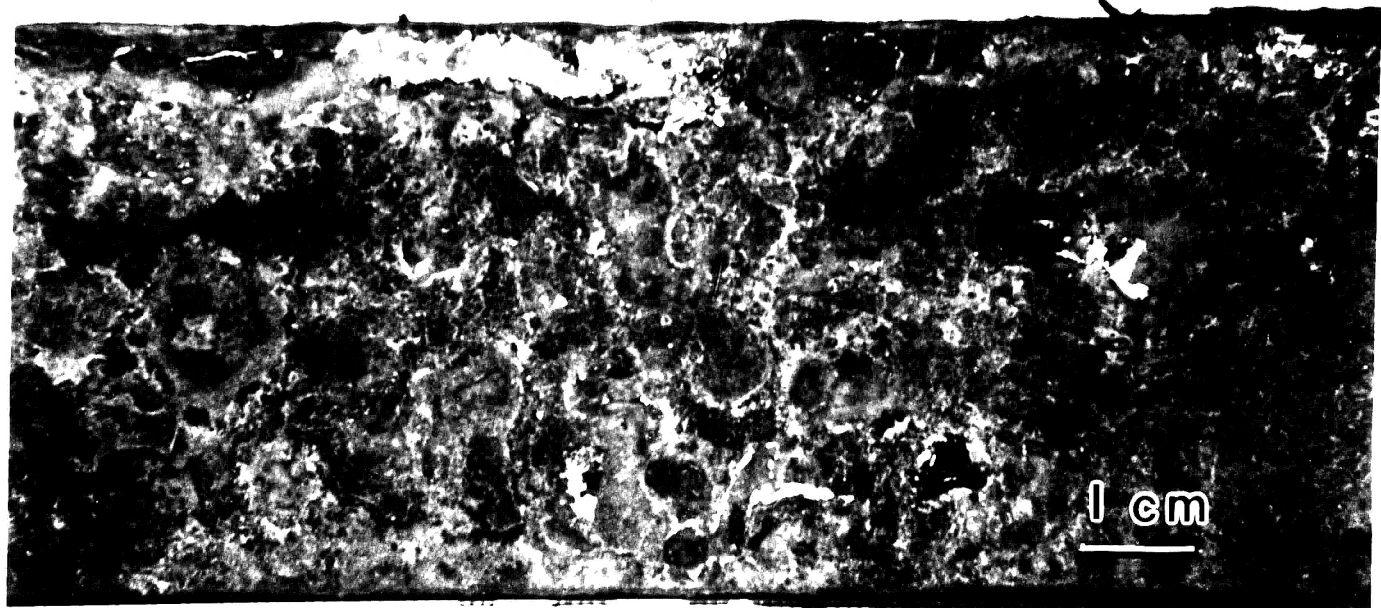


Figure 43. Surface Condition of a ASTM A572 Steel Plate Without Mill Scale and Exposed for 1800hr. In A Salt Water Environment. (Specimen FNSE2)

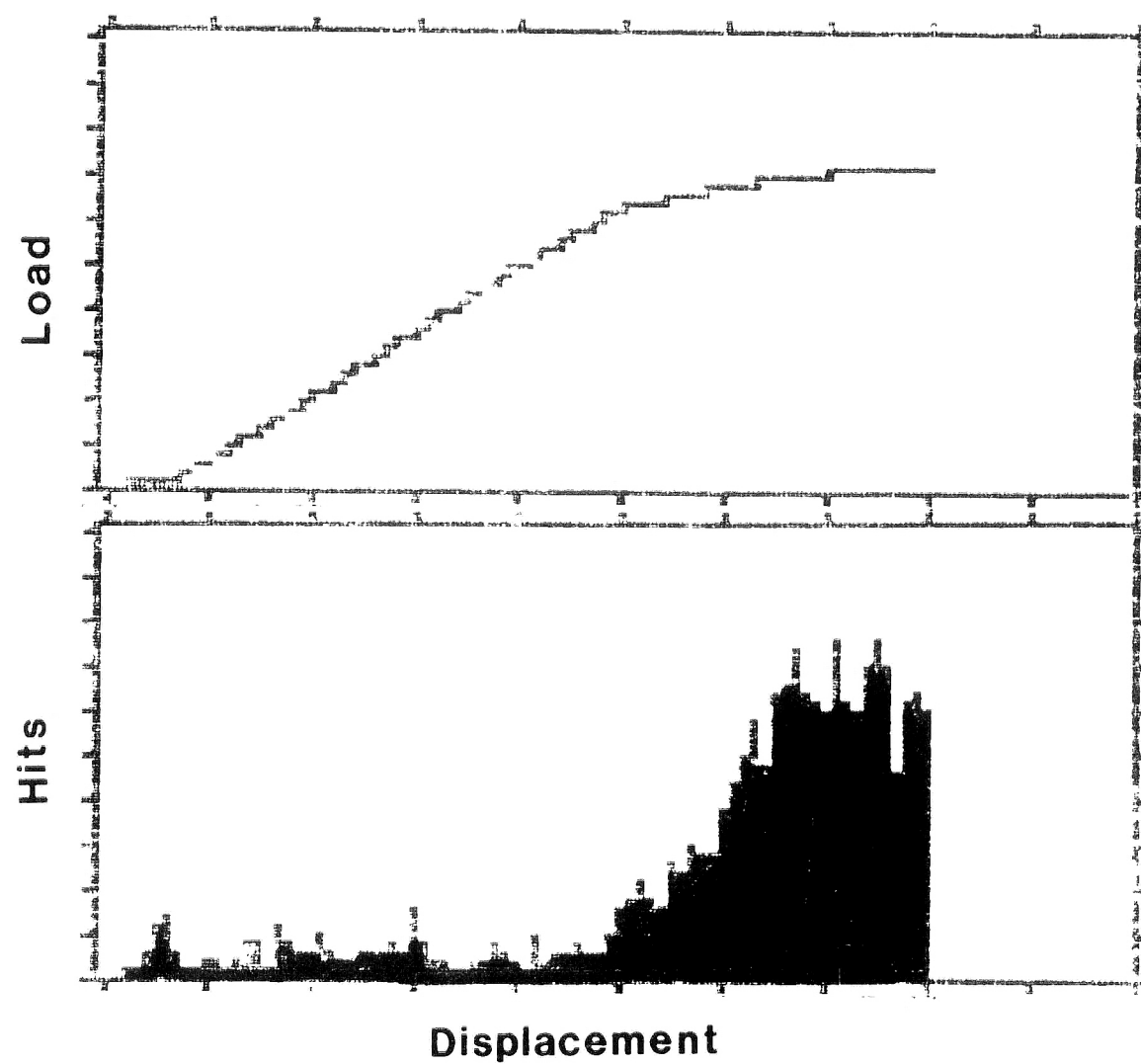


Figure 44. Four Point Bend Data for Specimen FENS2. Note that the onset of yielding produced an increase in hits. (Sensitivity 38dB)



Figure 45. Surface Condition of A ASTM Steel Plate Without Mill Scale and Thermally Oxidized for 100hr at 560°C (Specimen FS1).

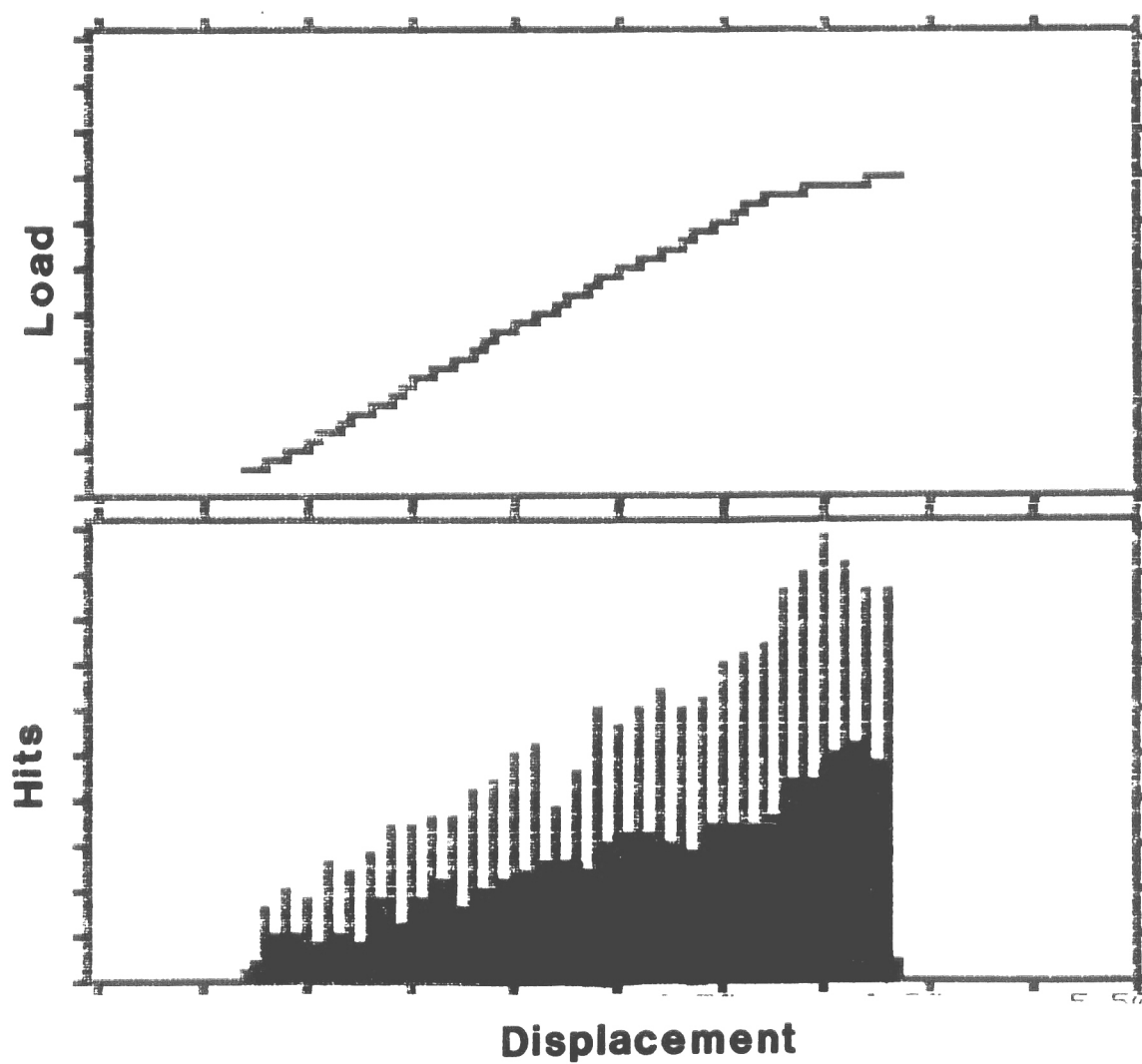


Figure 46. Four Point Bend Data for Specimen FS1. Note that the onset of yielding can not be determined by viewing the AE data. (Sensitivity 38)



Figure 45. Surface Condition of A ASTM Steel Plate Without Mill Scale and Thermally Oxidized for 100hr at 560°C (Specimen FS1).

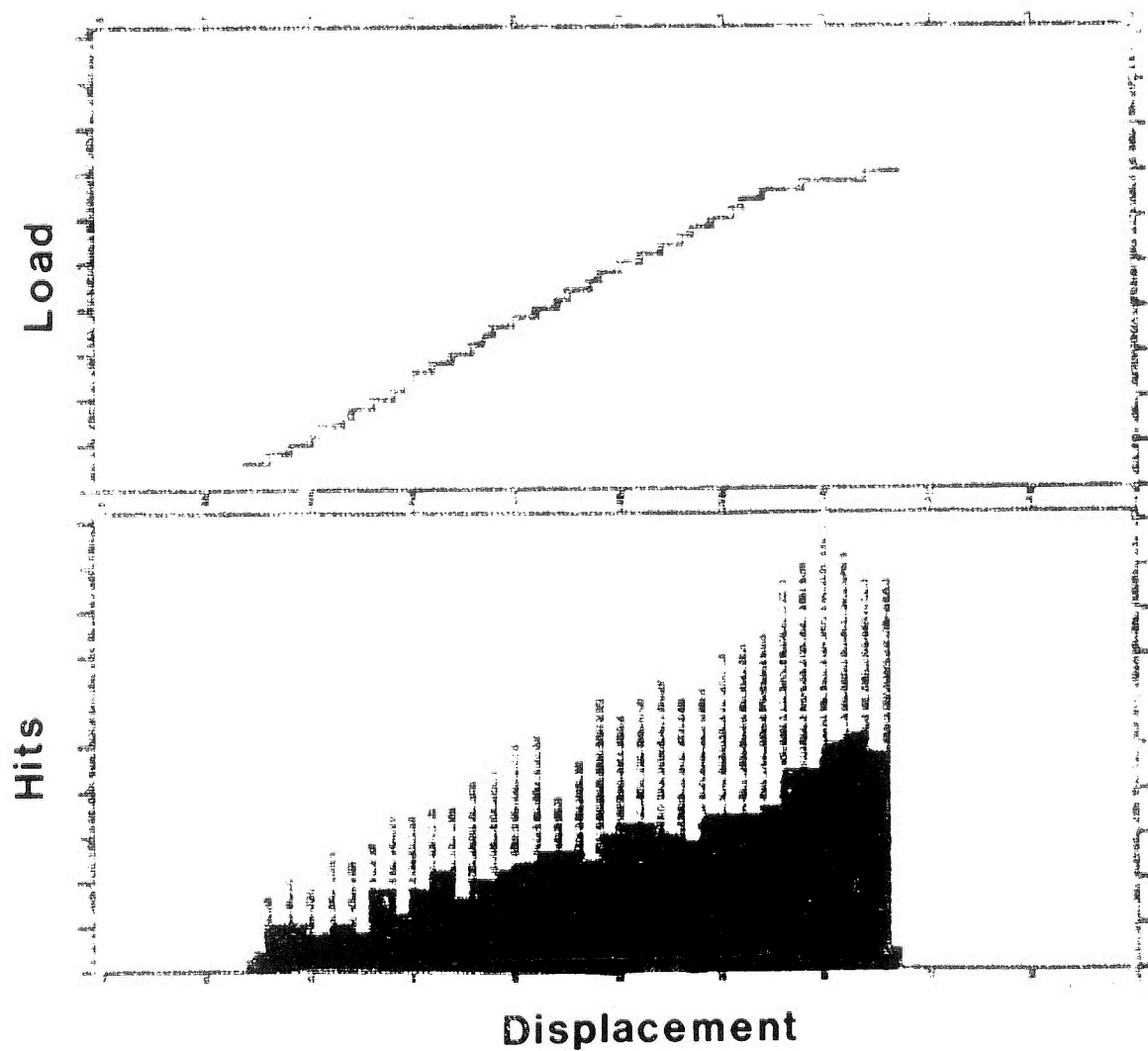


Figure 46. Four Point Bend Data for Specimen FS1. Note that the onset of yielding can not be determined by viewing the AE data. (Sensitivity 38)



Figure 47. Surface Condition of a ASTM A572 Steel Plate Without Mill Scale and Thermally Oxidized For 300 hrs. at 550°C (Specimen FS2)

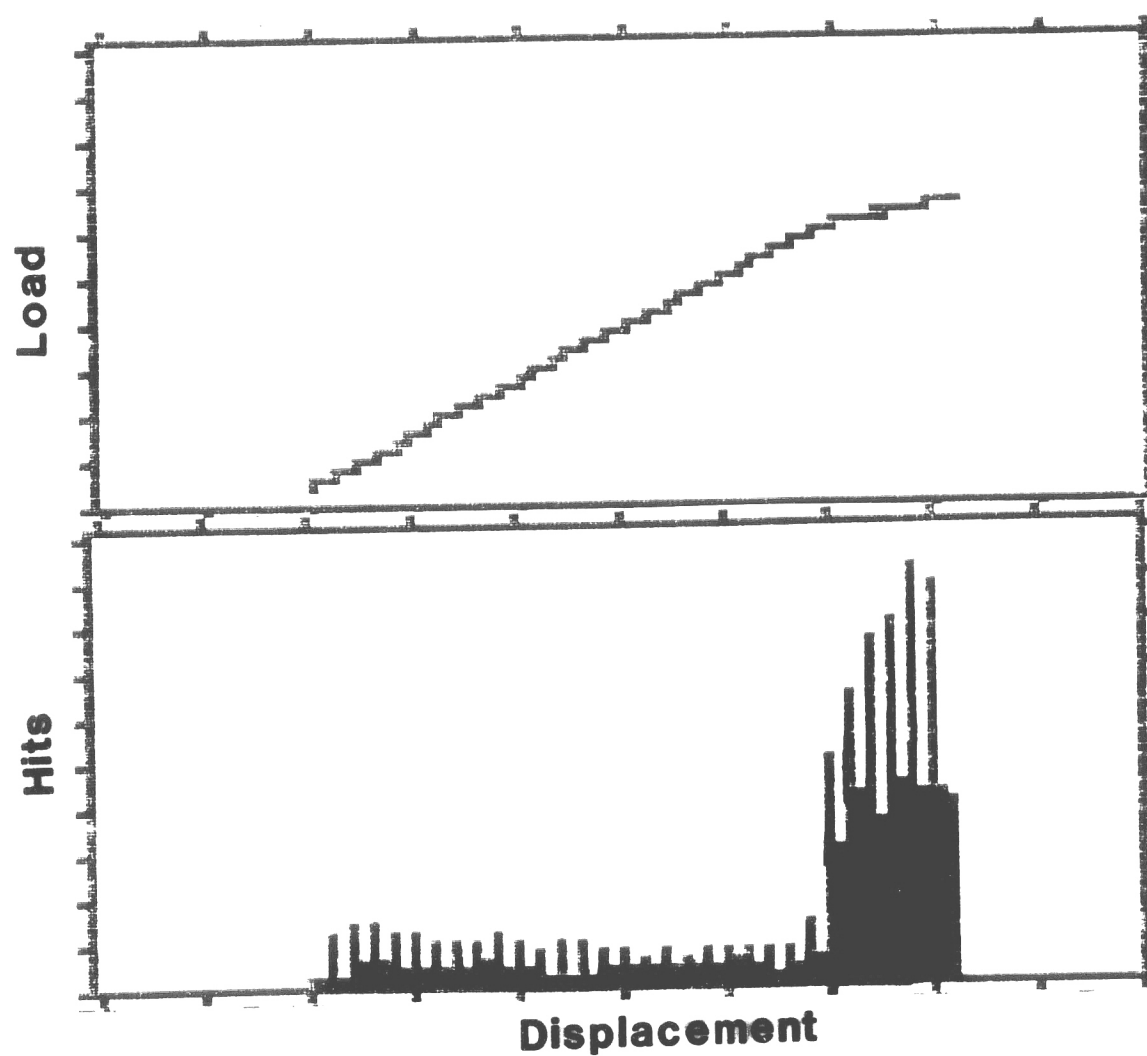


Figure 48. Four Point Bend Data for Specimen FS2. Note that the onset of yielding produced an increase in hits (Sensitivity 38dB)



Figure 47. Surface Condition of a ASTM A572 Steel Plate Without Mill Scale and Thermally Oxidized For 300 hrs. at 550°C (Specimen FS2)

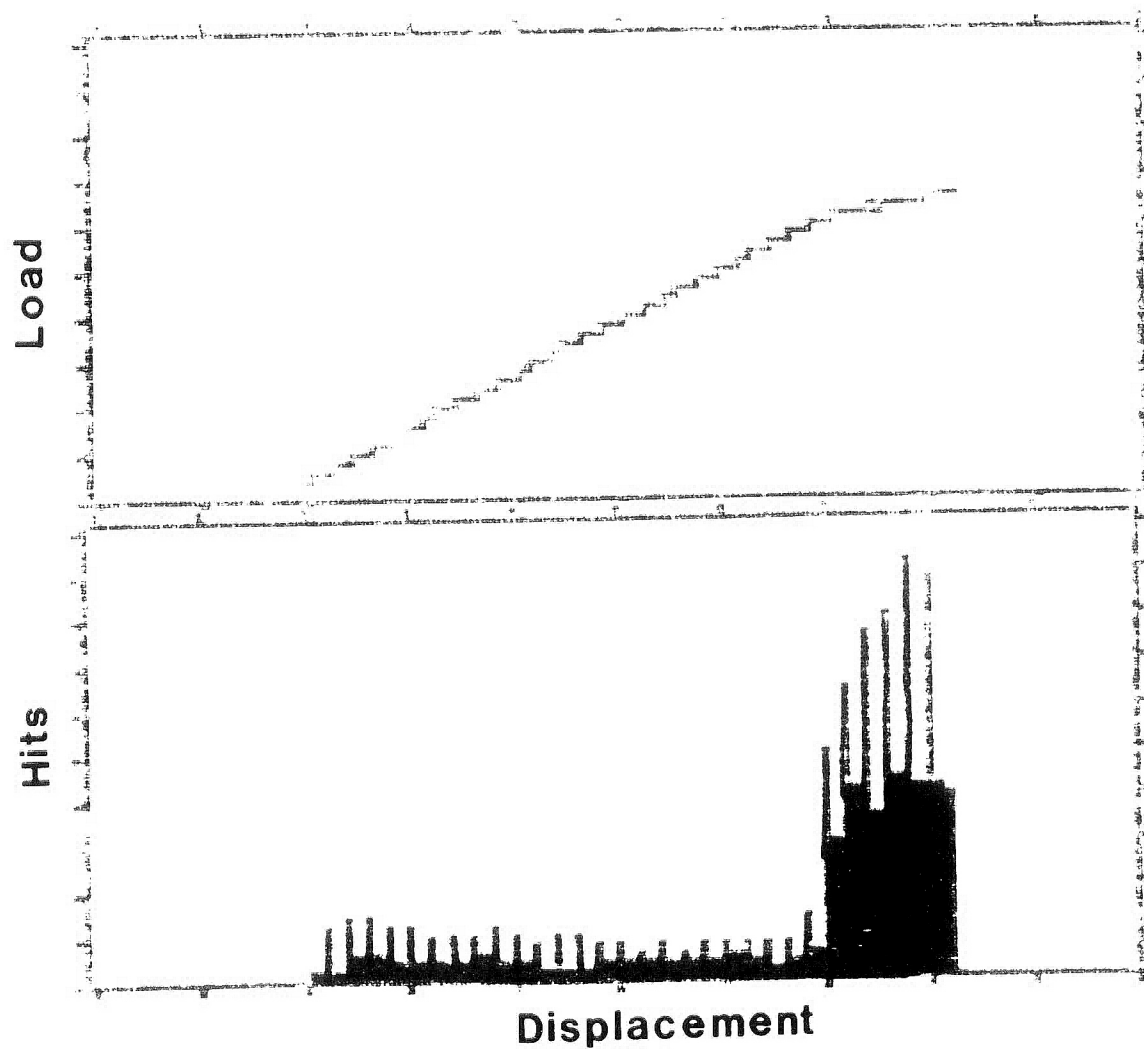


Figure 48. Four Point Bend Data for Specimen FS2. Note that the onset of yielding produced an increase in hits (Sensitivity 38dB)



Figure 49. Surface Condition of a ASTM A572 Steel Plate Without Mill Scale And Thermally Oxidized for 10 hrs. at 960°C (Specimen FS3) Note the various oxide layers. They grey oxide layer was very hard and brittle and was not bonded very well to the specimen.

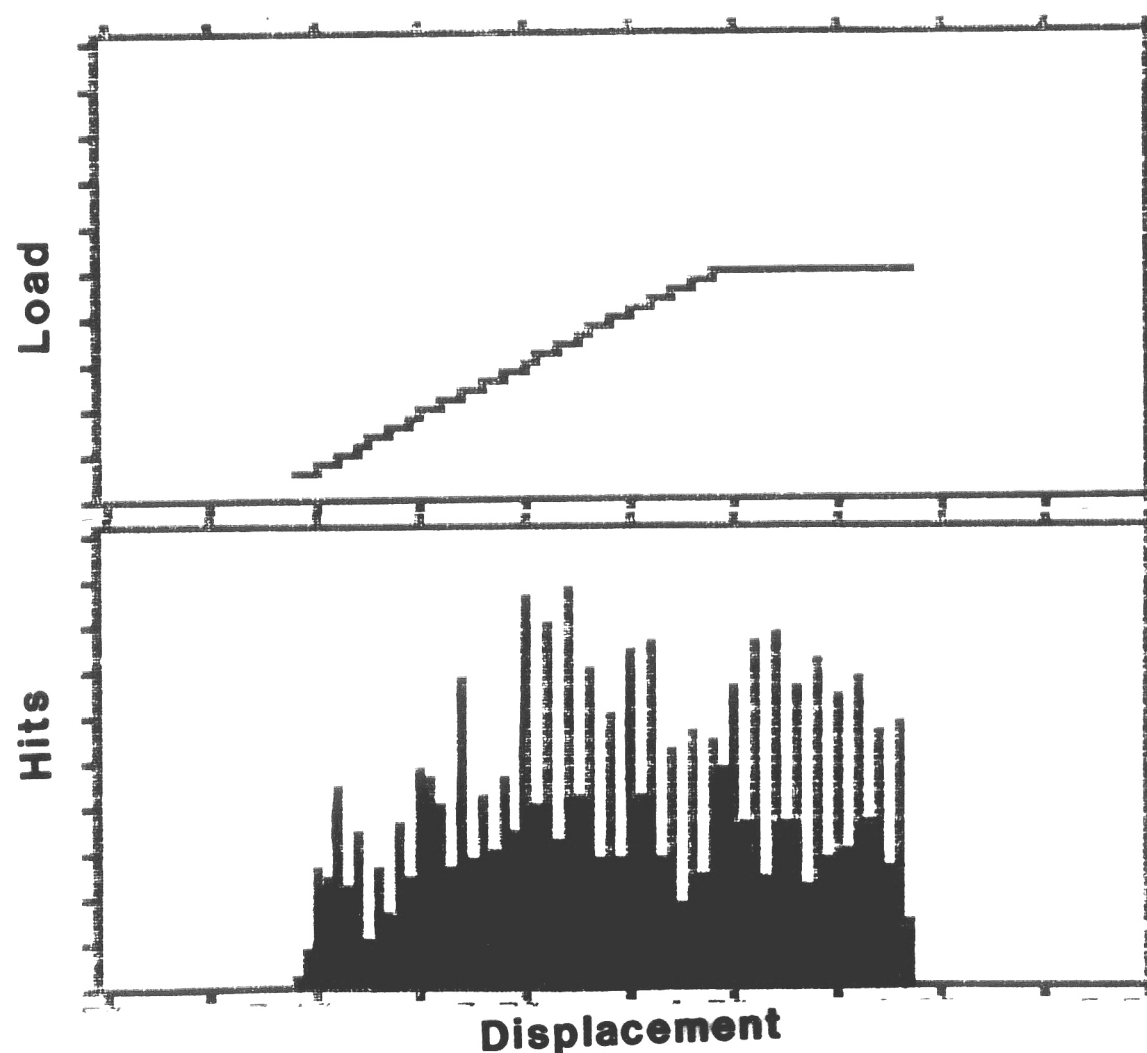


Figure 50. Four Point Bend Data for Specimen FS3. Note that the onset of yielding can not be determined by viewing the AE data. (Sensitivity 38dB)



Figure 49. Surface Condition of a ASTM A572 Steel Plate Without Mill Scale And Thermally Oxidized for 10 hrs. at 960°C (Specimen FS3) Note the various oxide layers. They grey oxide layer was very hard and brittle and was not bonded very well to the specimen.

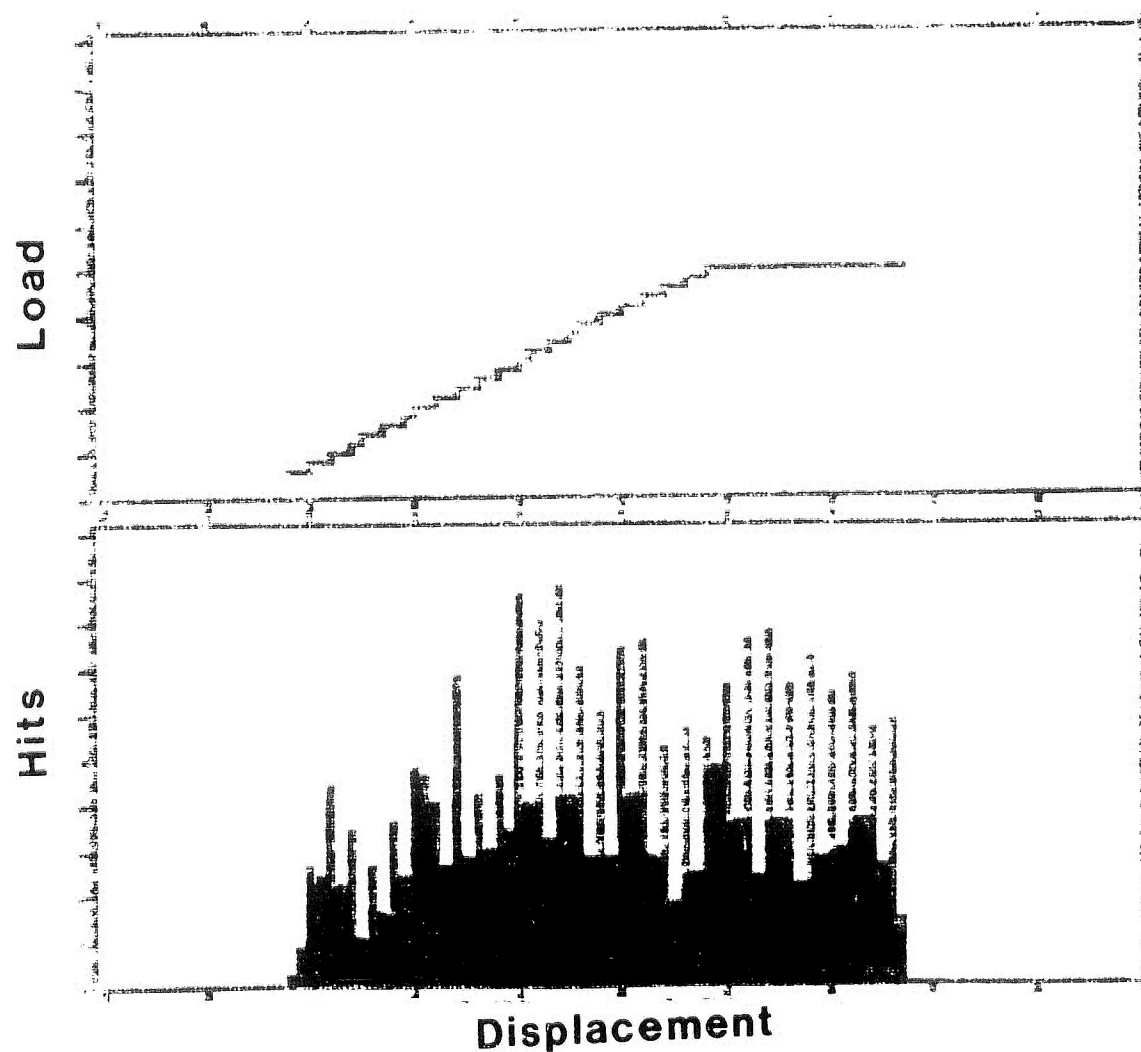


Figure 50. Four Point Bend Data for Specimen FS3. Note that the onset of yielding can not be determined by viewing the AE data. (Sensitivity 38dB)

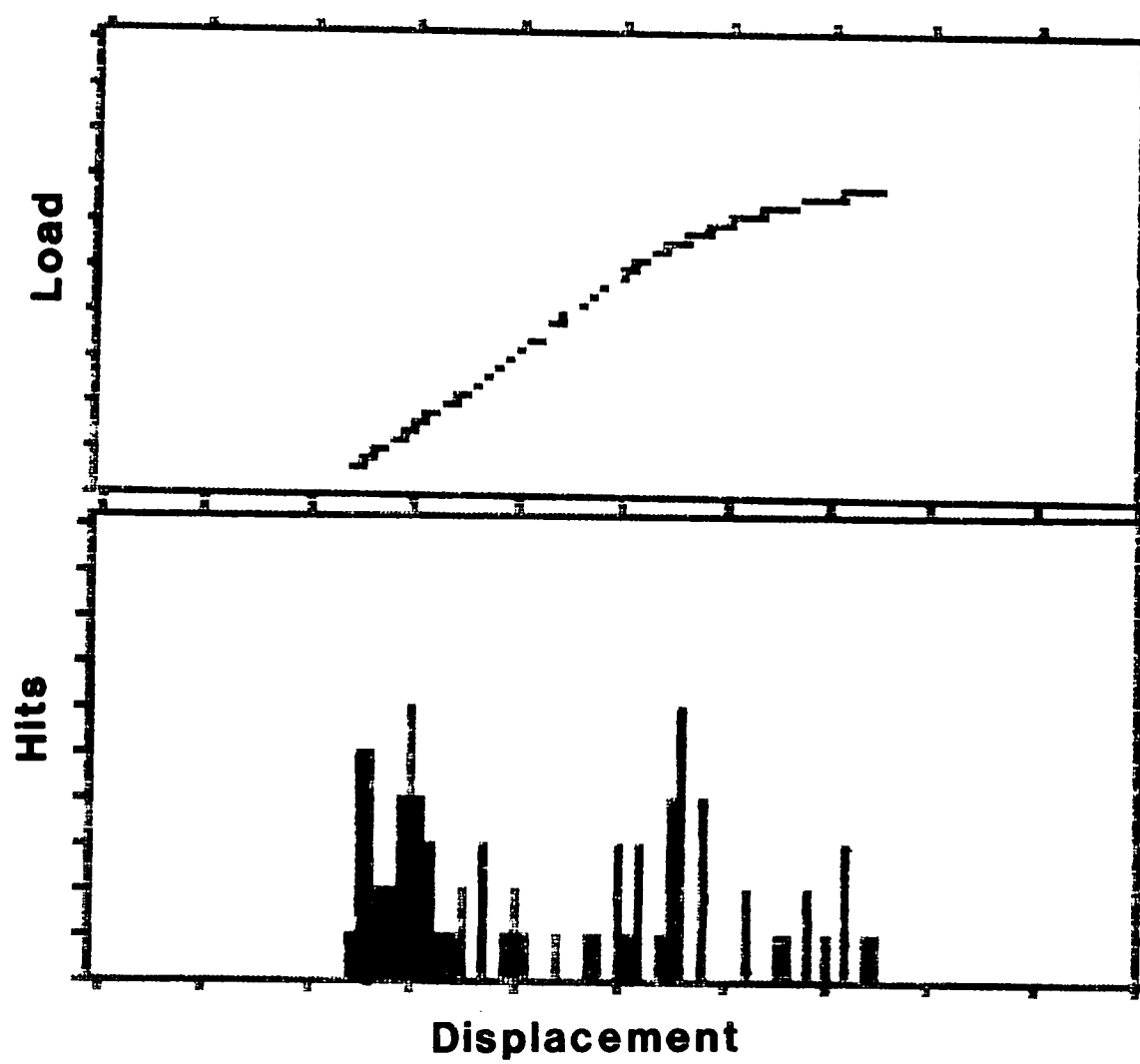


Figure 51. Four Point Bend Data for a Polished Specimen That Was Fabricated From Long Column E1-LC. Note that the onset of yielding can not be determined by viewing the AE data. (Sensitivity 38 dB)



Figure 52. Surface Condition of Four Point Bend Specimen That Was Fabricated From Salvaged Column E1-LC After All Oxides Were Removed, and Then Exposed To a Salt Water Environment For 600hr. (Specimen IE1).

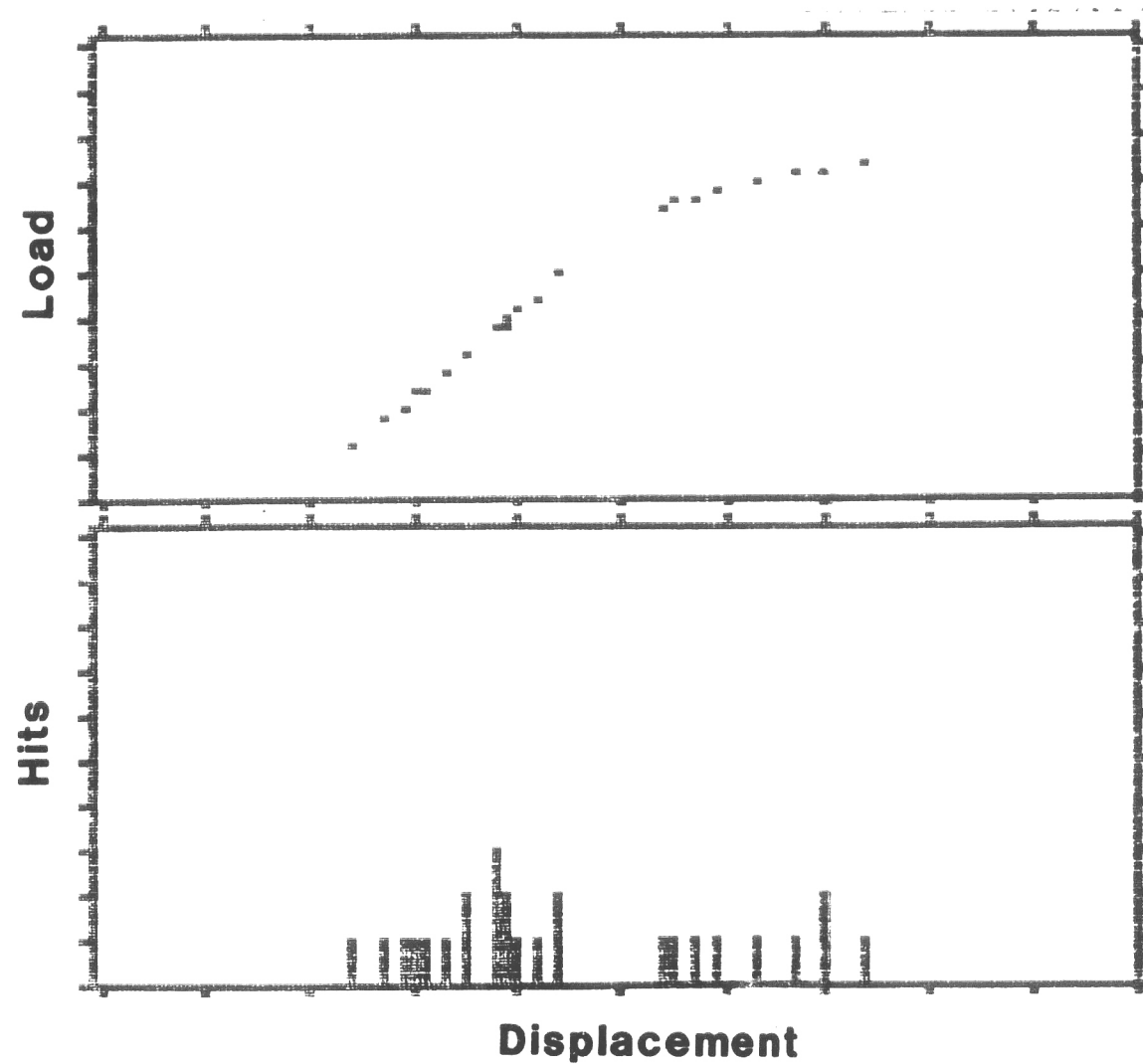


Figure 53. Four Point Bend Data For Specimen IE1. Note that the onset of yielding can not be determined by viewing the AE data. (Sensitivity 38dB)

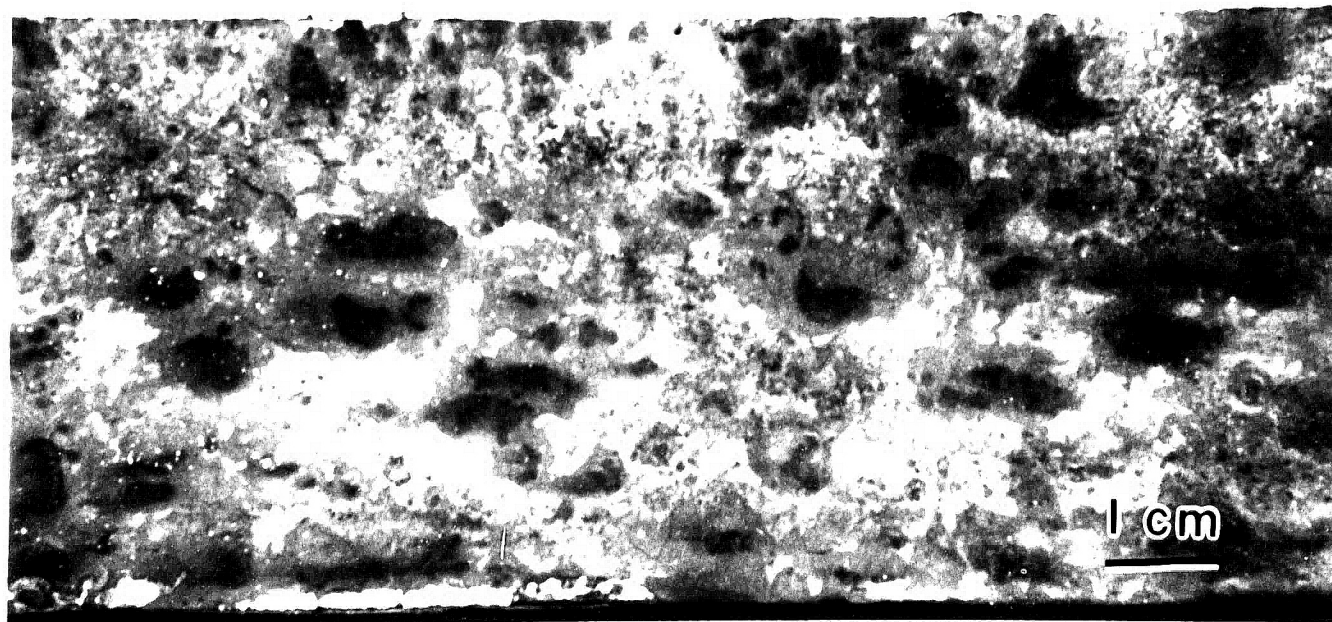


Figure 52. Surface Condition of Four Point Bend Specimen That Was Fabricated From Salvaged Column E1-LC After All Oxides Were Removed, and Then Exposed To a Salt Water Environment For 600hr. (Specimen IE1).

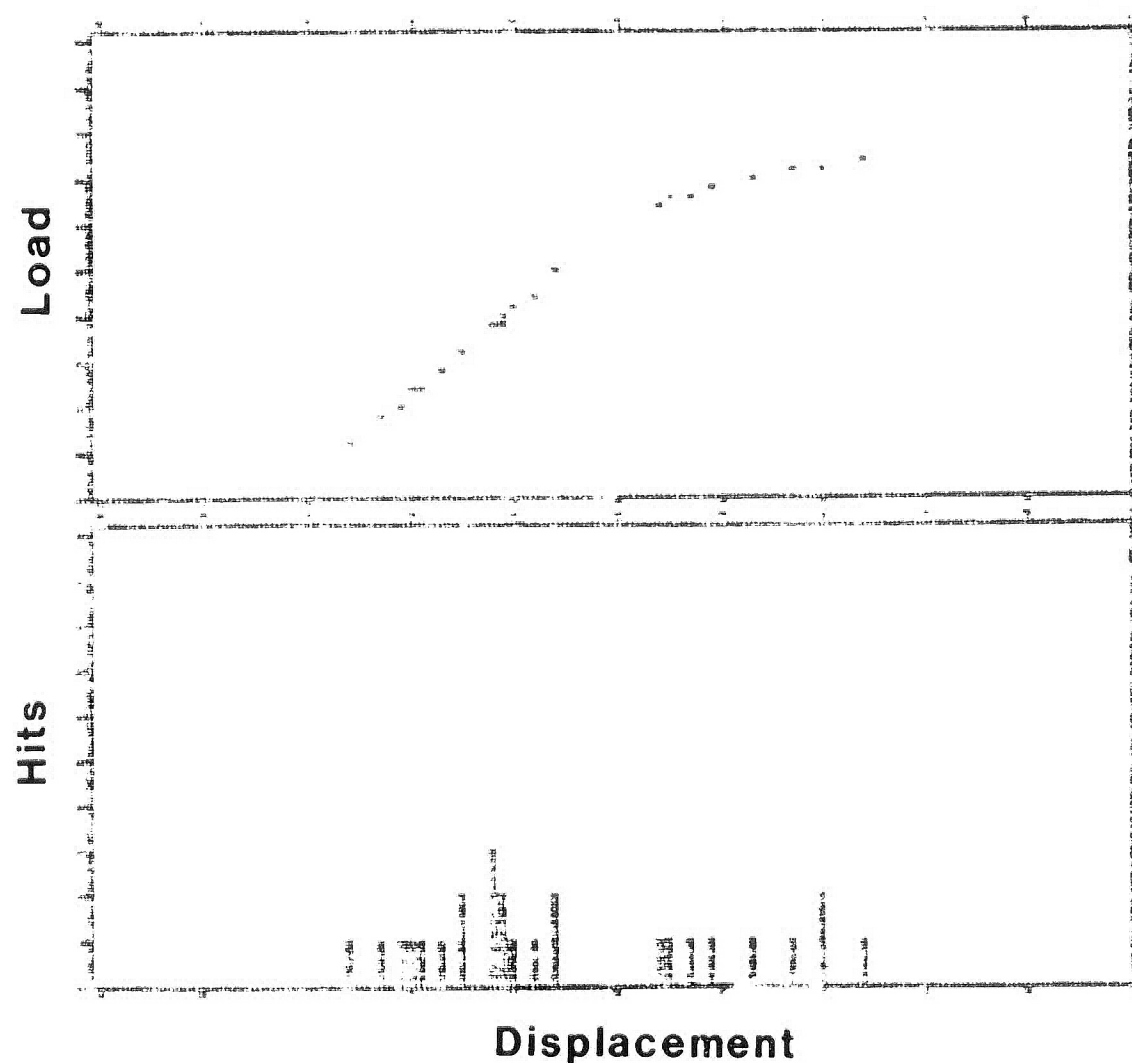


Figure 53. Four Point Bend Data For Specimen IE1. Note that the onset of yielding can not be determined by viewing the AE data. (Sensitivity 38dB)



Figure 54. Surface Condition of Four Point Bend Specimen Fabricated From a Salvaged Column E1-LC After Oxides Were Removed and Exposed To a Salt Water Environment for 1200hrs. (Specimen IE2).

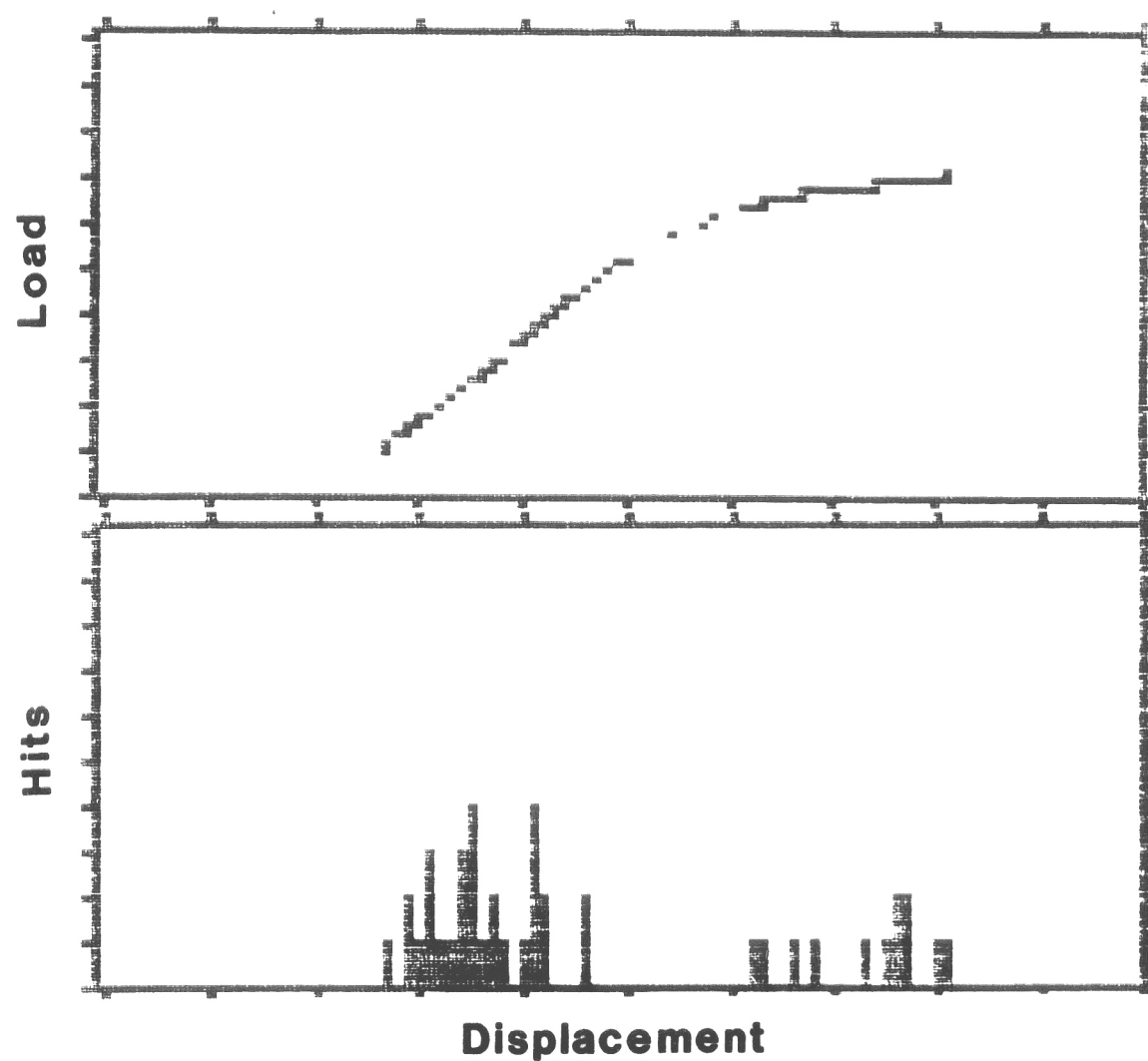


Figure 55. Four Point Bend Data for Specimen IE2. Note that the onset of yielding can not be determined by viewing the AE data. (Sensitivity 38)

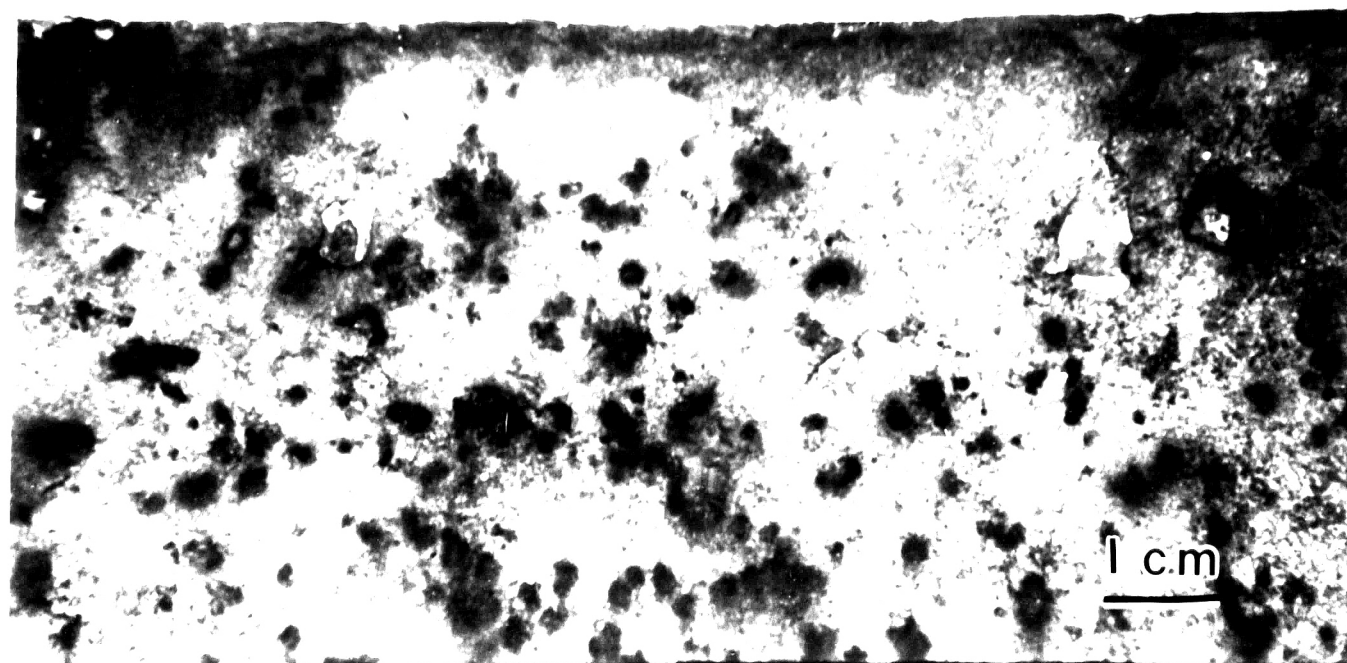


Figure 54. Surface Condition of Four Point Bend Specimen Fabricated From a Salvaged Column E1-LC After Oxides Were Removed and Exposed To a Salt Water Environment for 1200hrs. (Specimen IE2).

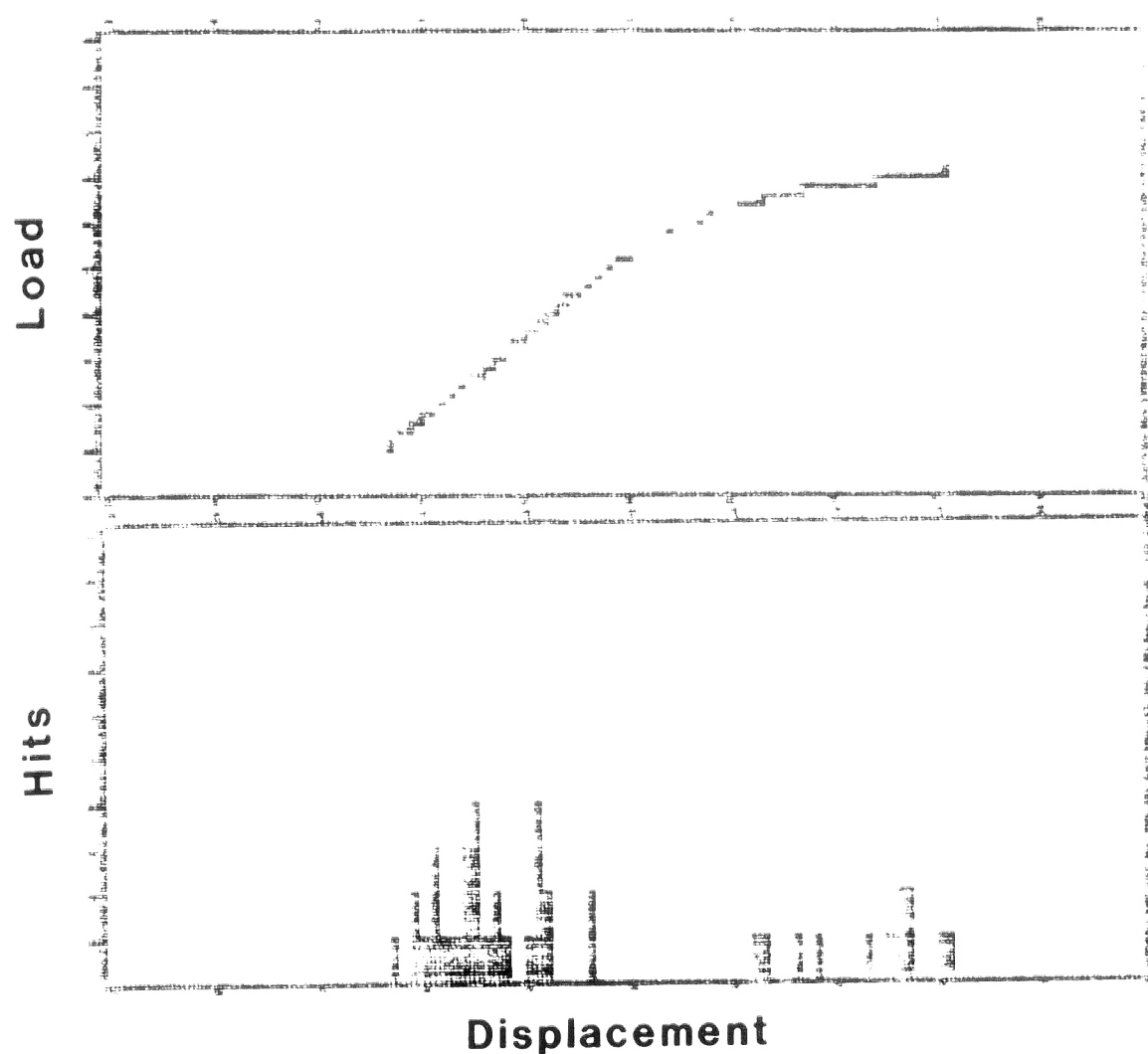


Figure 55. Four Point Bend Data for Specimen IE2. Note that the onset of yielding can not be determined by viewing the AE data. (Sensitivity 38)



Figure 56. Surface Condition of Four Point Bend Specimen Fabricated From a Salvaged Column E1-LC After All Oxides Were Removed and Then Exposed To a Salt Water Environment for 2400hrs. (Specimen IE3).

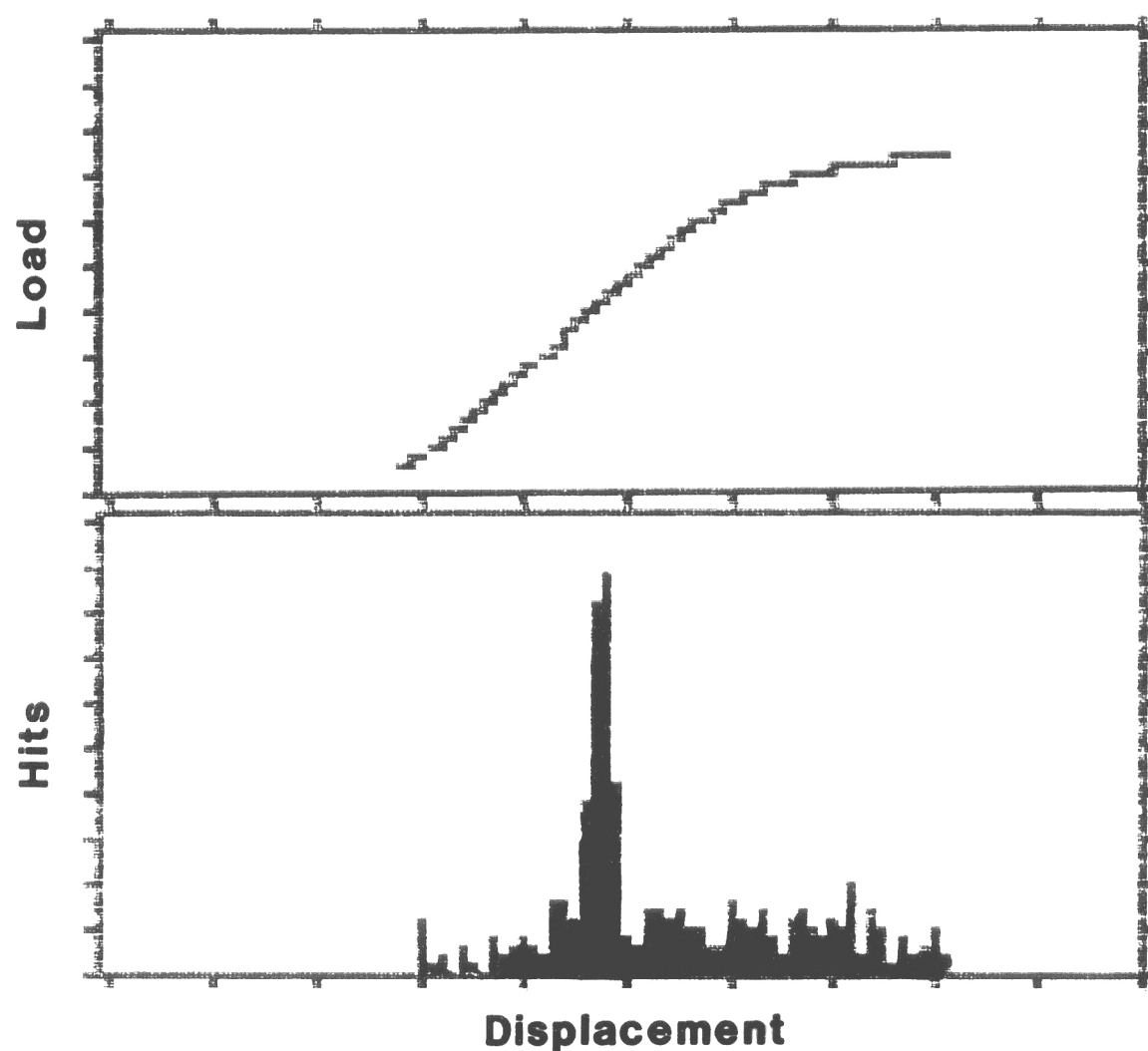


Figure 57. Four Point Bend Data for Specimen IE3. Not that the onset of yielding can not be determined by viewing the AE data. The burst of emissions that occurred during the elastic region was generated when the AE sensor began to slip on the specimen. (Sensitivity 38dB)

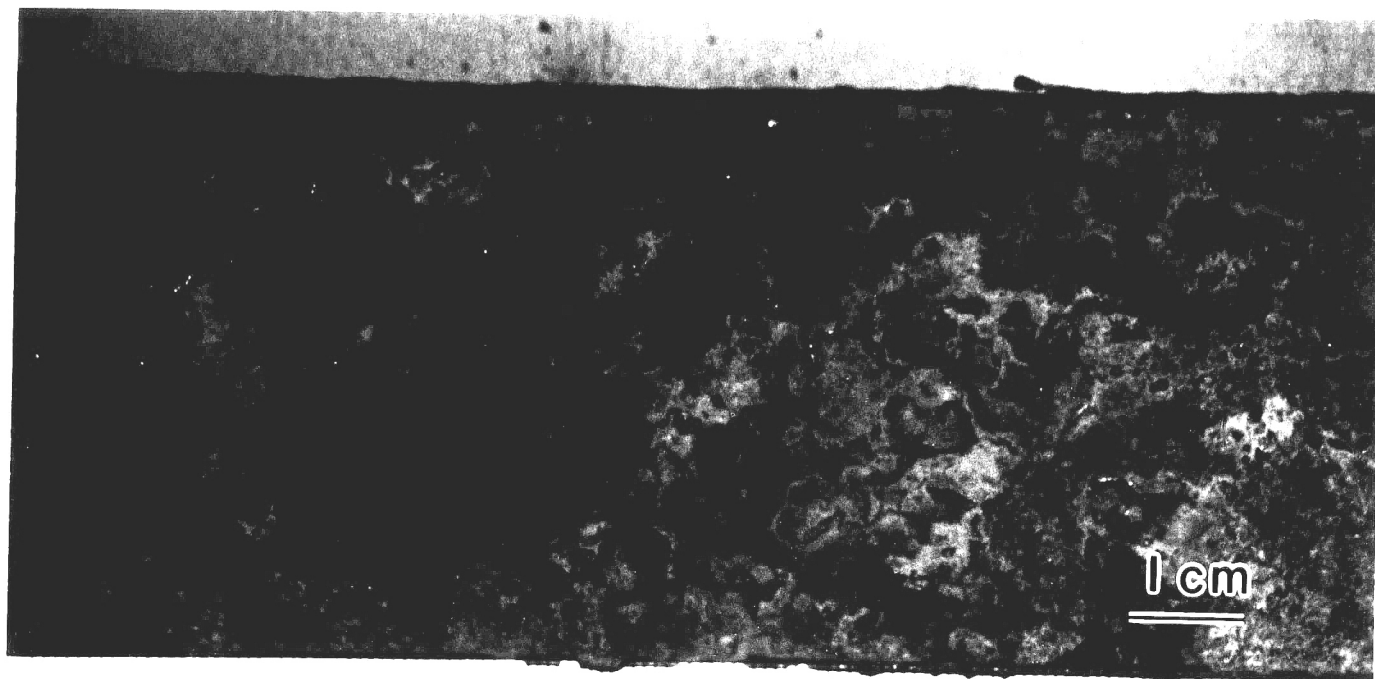


Figure 56. Surface Condition of Four Point Bend Specimen Fabricated From a Salvaged Column E1-LC After All Oxides Were Removed and Then Exposed To a Salt Water Environment for 2400hrs. (Specimen IE3).

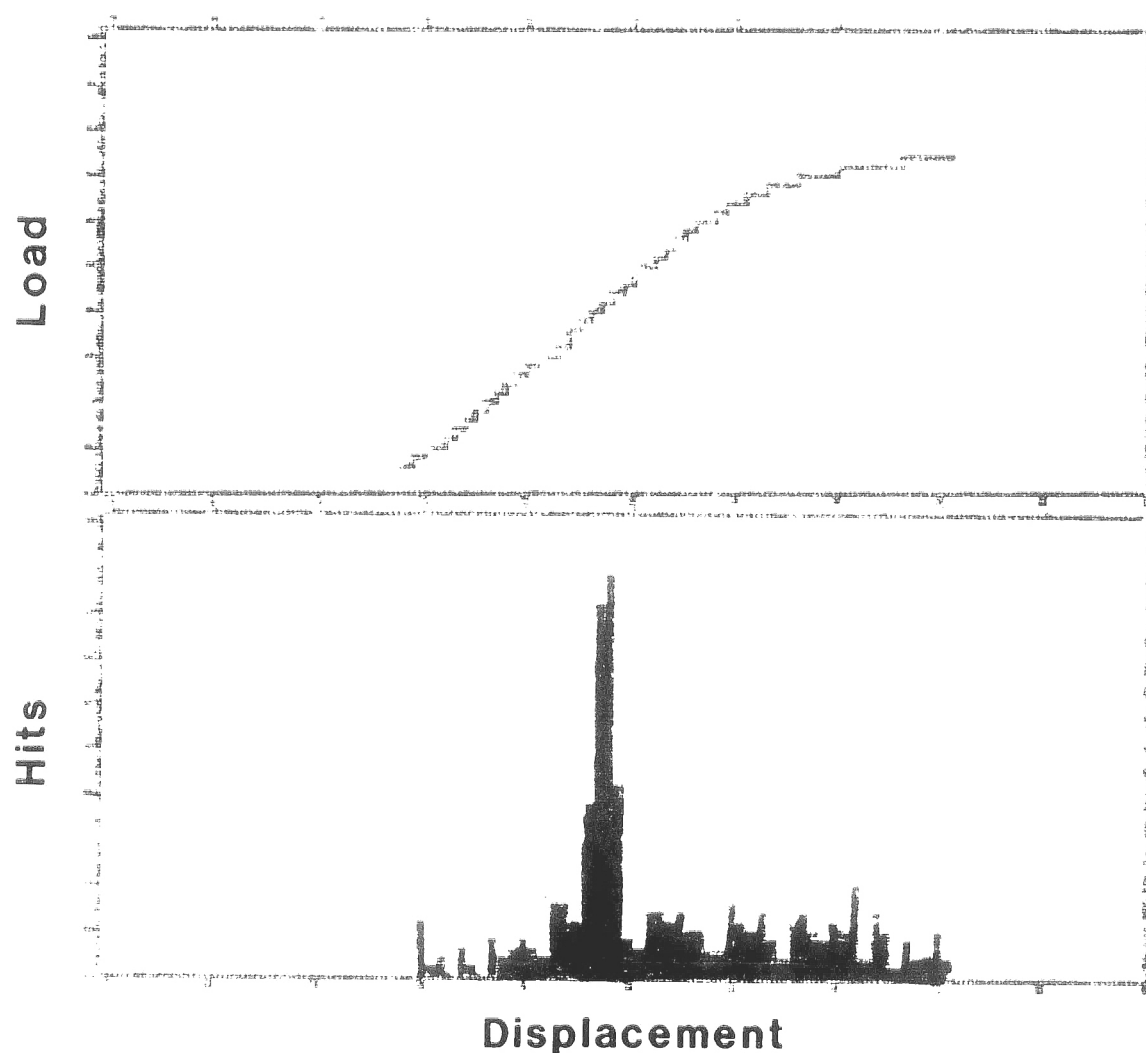


Figure 57. Four Point Bend Data for Specimen IE3. Not that the onset of yielding can not be determined by viewing the AE data. The burst of emissions that occurred during the elastic region was generated when the AE sensor began to slip on the specimen. (Sensitivity 38dB)

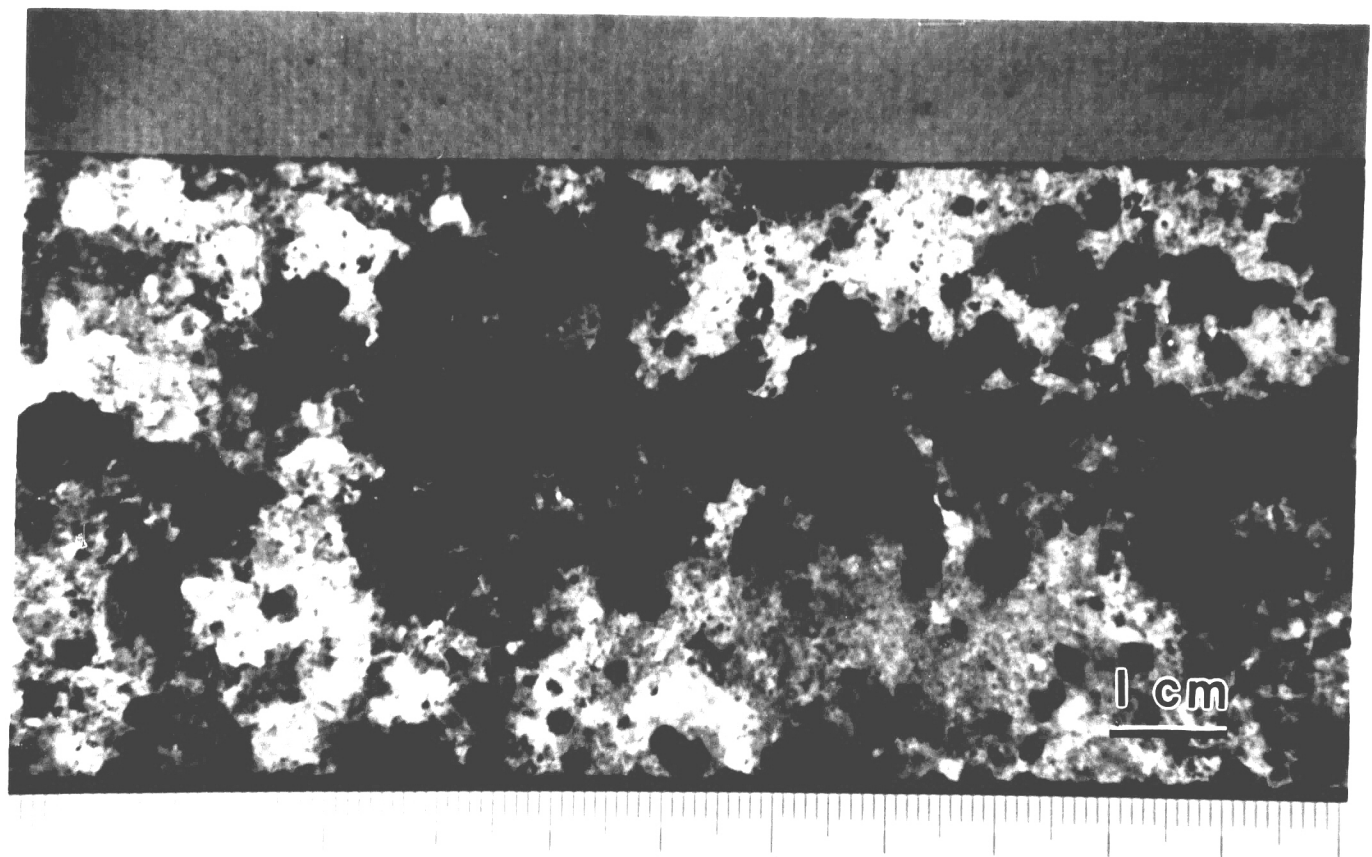


Figure 58. Surface Condition of Four Point Bend Specimen Fabricated From a Salvaged Column E1-LC. Note the presence of marine life (white area). (Specimen I1).

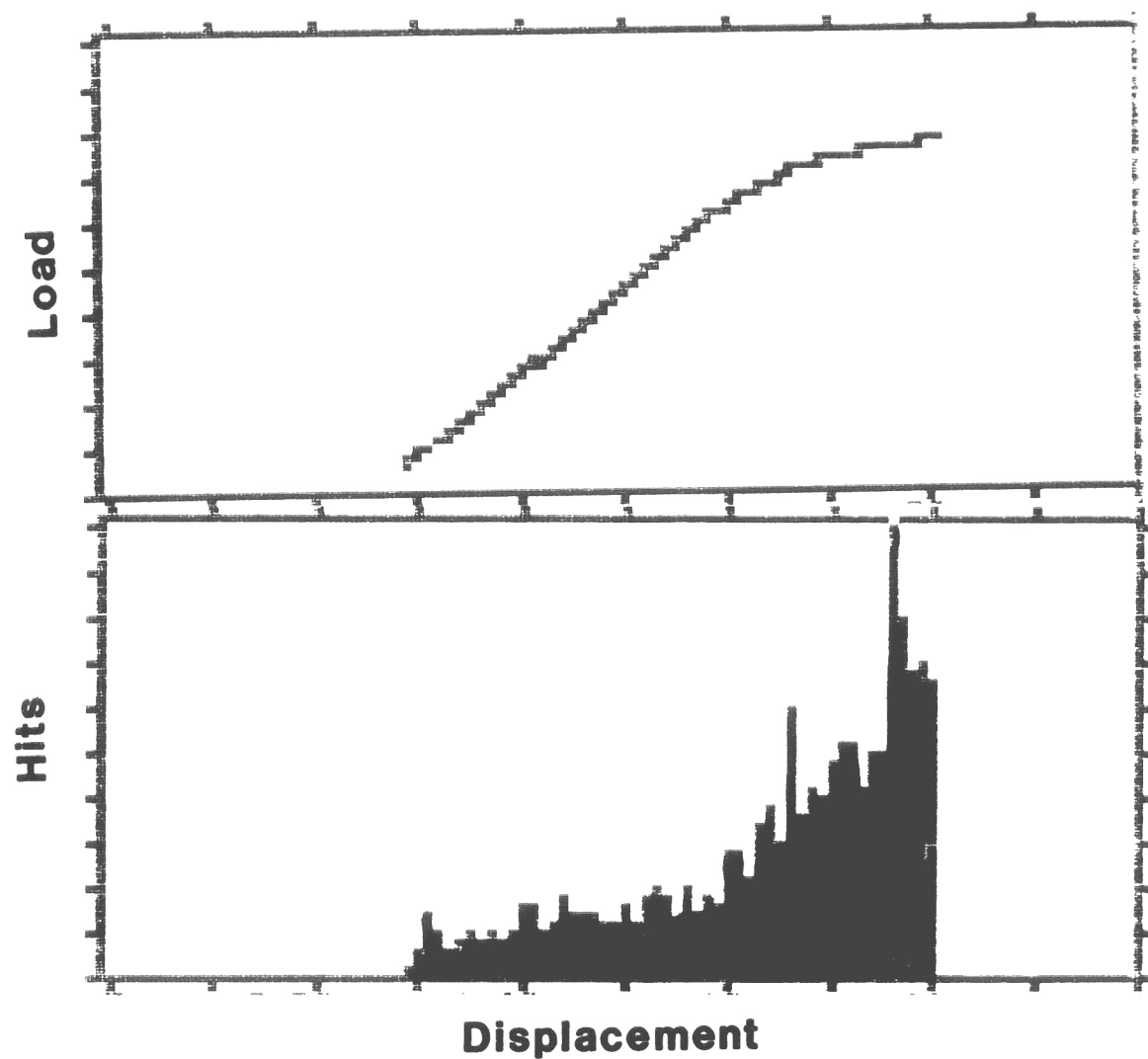


Figure 59. Four Point Bend Data for Specimen I1. Note that the onset of yielding produced an increase in hits. (Sensitivity 38dB)

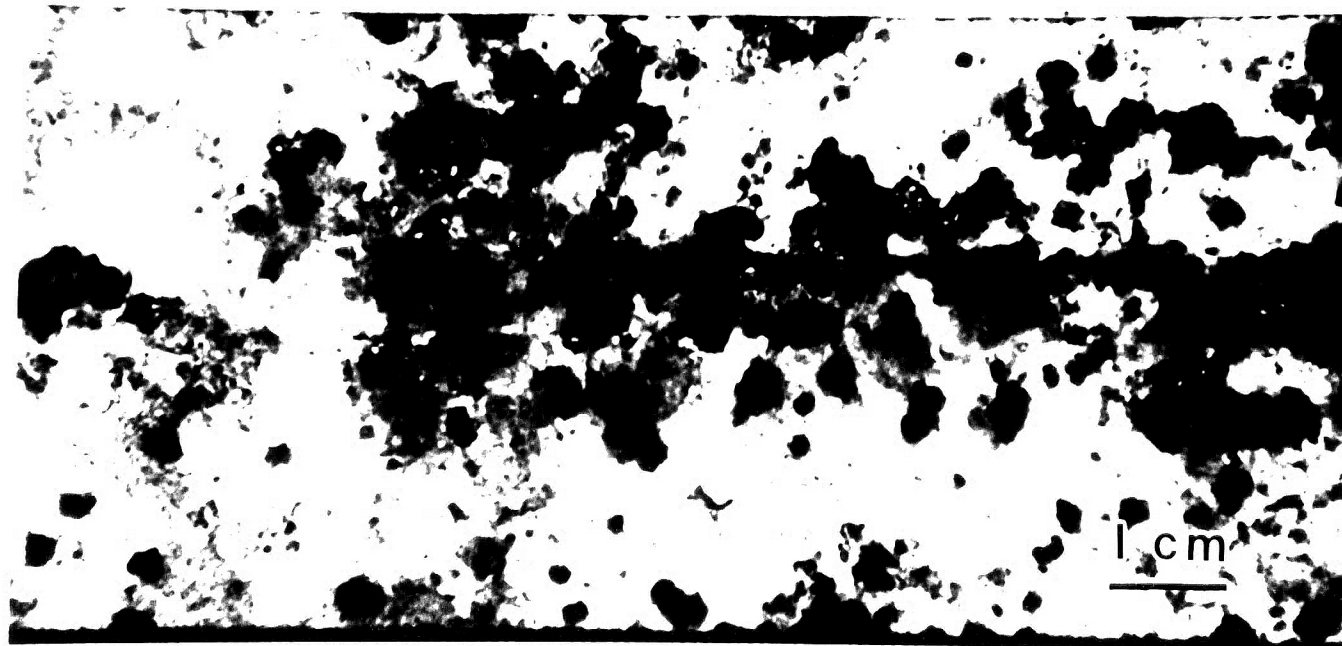


Figure 58. Surface Condition of Four Point Bend Specimen Fabricated From a Salvaged Column E1-LC. Note the presence of marine life (white area). (Specimen I1).

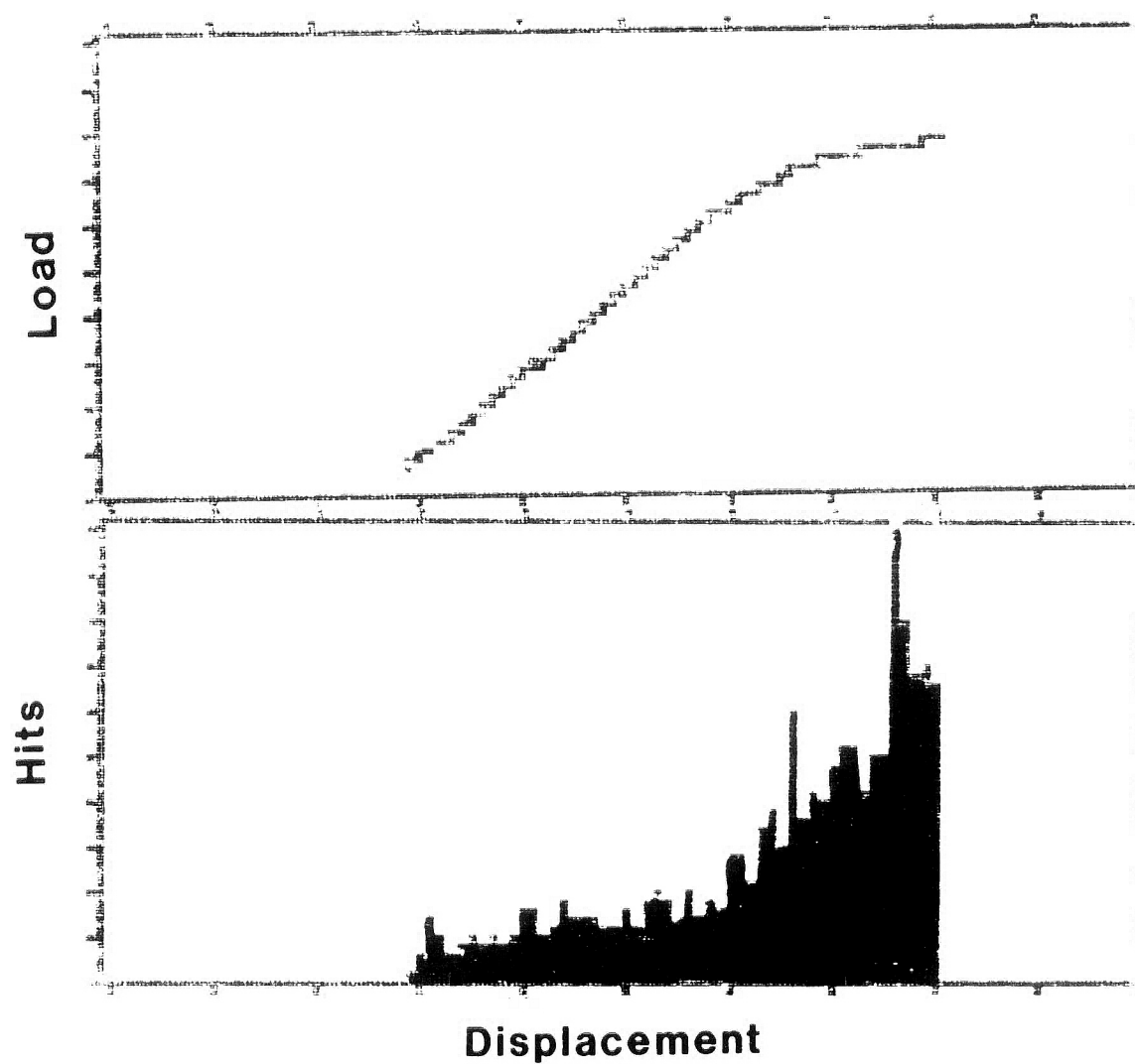


Figure 59. Four Point Bend Data for Specimen I1. Note that the onset of yielding produced an increase in hits. (Sensitivity 38dB)

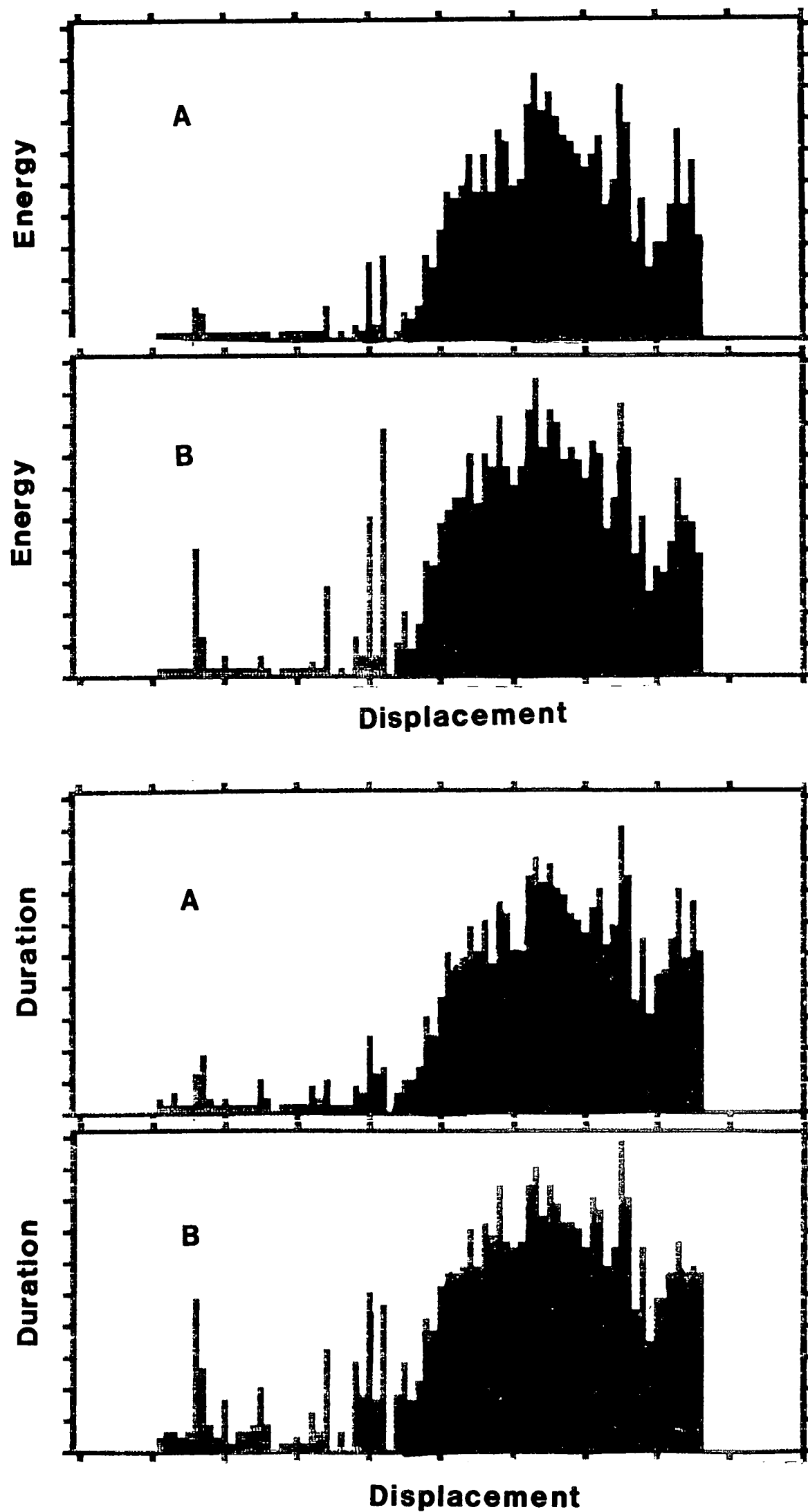


Figure 60. AE Data Showing The Effects Of Filtering. The first graph of each set (A) represents data that was not filtered while (B) was filtered.

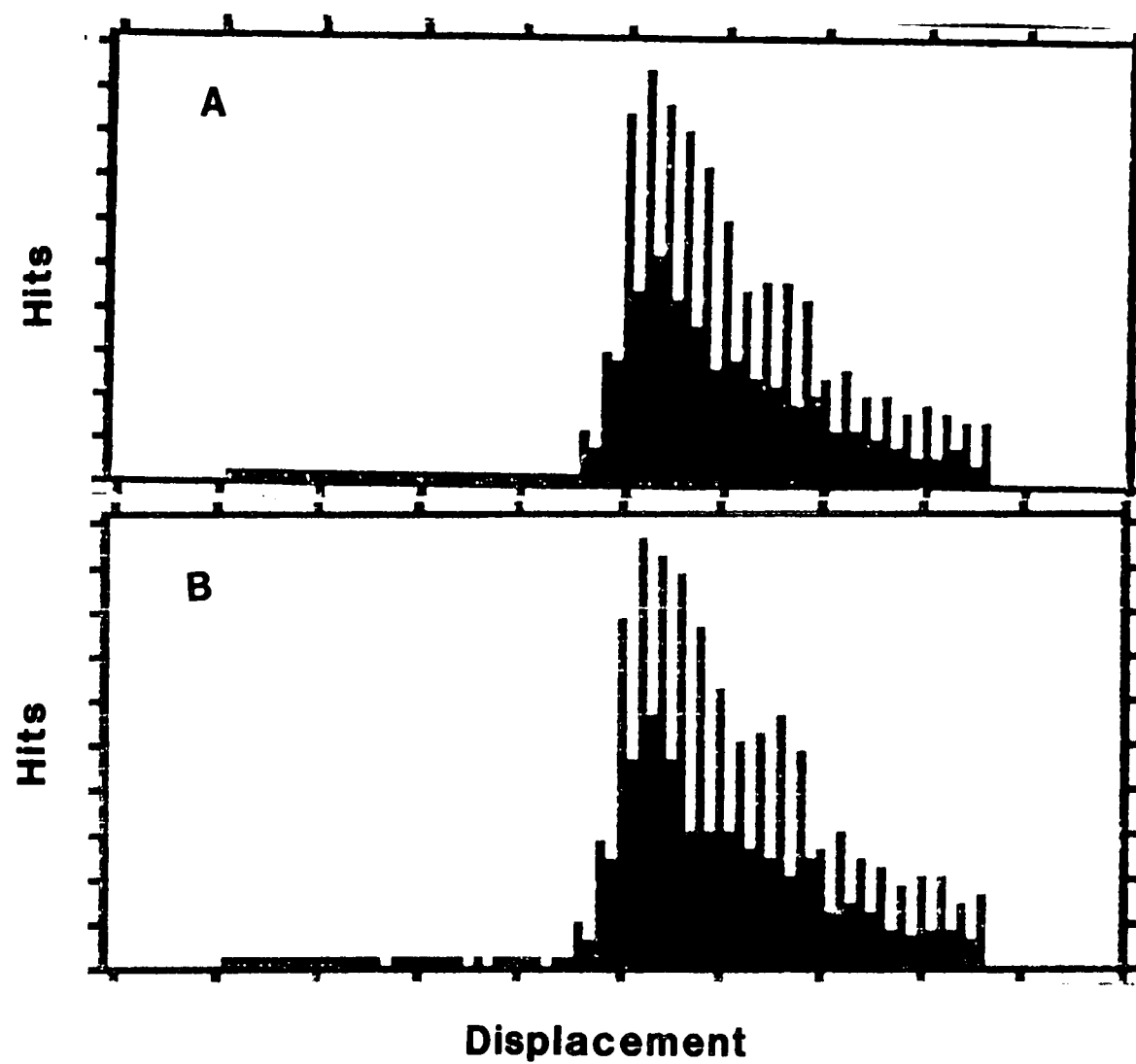


Figure 60 cont) Figure A Represents Data That Was Not Filtered While Figure B Had Erroneous Data Removed. Note that the figures appear very similar.

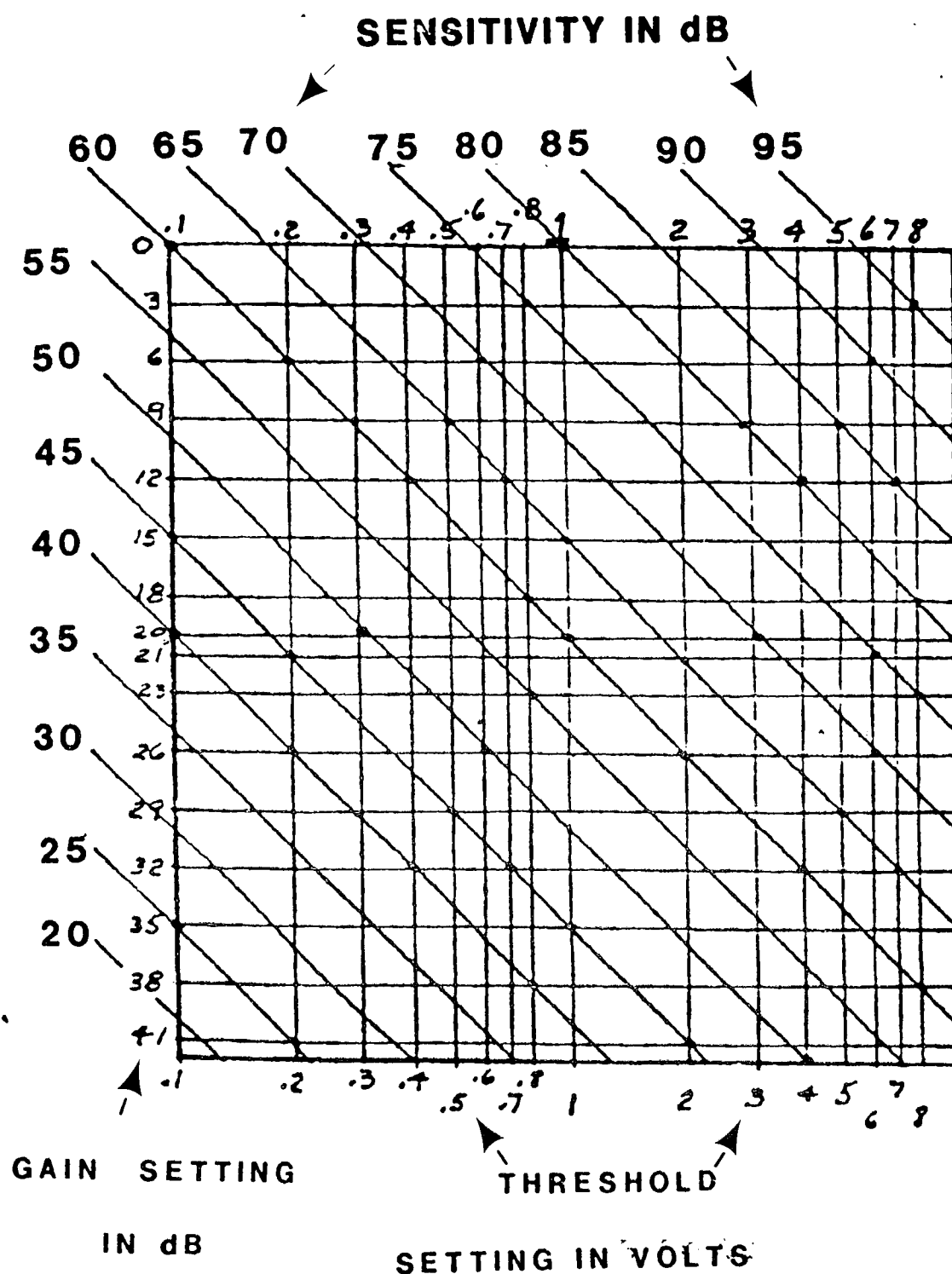
APPENDIX

EXPERIMENTAL SENSITIVITY DETERMINATION

The pressure wave, generated by an event, stimulates the piezoelectric crystal in the acoustic sensor. This in turn creates an electrical potential which is sent to the AE processor to be analyzed. Due to the weak electrical signal produced by the crystal, the signal has to be increased by a preamplifier before it can travel the long distances of the coaxial cable. This preamplification is generally a fixed 40dB gain. For example, a 40dB preamplifier is incorporated into the R6I sensor housing and the inspector can not change this gain setting.

The signal then travels to the main amplifier where the gain can be further increased and a threshold can be set. Manipulation of the gain and threshold settings on the amplifier can change the sensitivity of the equipment. Very weak signals such as generated from dislocation movements would have a low dB value while strong signals such as produced by a supply boat impacting a structure would have a very high dB value. The figure on the next page can help determine the sensitivity setting that is obtained for a particular gain and threshold setting. For example, a 1 volt threshold (read on the abscissa) and a 35dB gain (ordinate) gives a sensitivity of 45dB. In other words, any signal greater than 45dB will be recorded by the equipment. The

detection of weaker signals is possible either by lowering the threshold or by increasing the gain. For example a decrease in the threshold to 0.8 V allows a sensitivity of 40dB to be resolved. The same sensitivity (40dB) can be achieved by increasing the gain to 40dB at a threshold of 1V.



The data in the above figure is for a 40dB preamplified signal.

VITA

Robert William Kowalik was born to Chester and Cecelia Kowalik on November 1, 1965 in Philadelphia Pennsylvania. He received his secondary degree from Central High School in the spring of 1984. The fall of the same year he enrolled at Drexel University in Philadelphia and graduated in the spring of 1989 with a B.S. in Materials Science and Engineering.

Robert worked for the Naval Air Development Center in Warminster PA during his undergraduate studies. Upon graduation from Drexel, Robert enrolled at Lehigh University in the fall of 1989 and began work towards his M.S. in the Materials Science and Engineering Department.